76-14.1

Implementation Package

Volume I
Master

WAVE EQUATION ANALYSIS OF PILE DRIVING

WEAP PROGRAM

Volume I — Background

Updated March 1981

U.S. DEPARTMENT OF TRANSPORTATION
Federal Highway Administration
Offices of Research and Development
Implementation Division
Washington, D.C. 20590

ClibPDF - www.fastio.com

ClibPDF - www.fastio.com

NOTICE

This document is disseminated under the sponsorship of the Department of Transportation in the interest of information exchange. The United States Government assumes no liability for its contents or use.

The contents of this report reflect the views of Goble & Associates who are responsible for the facts and the accuracy of the data presented herein. The contents do not necessarily reflect the official views or policy of the Department of Transportation. This report does not constitute a standard, specification, or regulation.

The United States Government does not endorse products or manufacturers. Trade or manufacturers' names appear herein only because they are considered essential to the object of this document.

ClibPDF - www.fastio.com

ClibPDF - www.fastio.com

Wave Equation Analysis of Pile Driving

WEAP PROGRAM

Vol. 1: Background

by

Goble, G. G., and Rausche, Frank

Submitted to

U.S. Department of Transportation
Federal Highway Administration
Offices of Research and Development
Washington, D.C. 20590

Goble & Associates, Inc.
4423 Emery Industrial Parkway
Warrensville Hts., Ohio 44128

ClibPDF - www.fastio.com

ClibPDF - www.fastio.com

PREFACE

During the past 15 years wave equation computer programs have enjoyed a gradual but continual increase in use for the analysis of pile driving. The motivation for the preparation of the WEAP program (Wave Equation Analysis of Piles) came from problems which were experienced by the New York Department of Transportation when they attempted to implement routine wave equation analyses into their pile driving practice. They used a program prepared by the Texas Transportation Institute. In spite of the fact that this program is probably the most widely used wave equation program in the United States, serious difficulties were encountered in that unrealistic stresses were sometimes obtained for piles driven by diesel hammers.

The authors of this report have performed extensive research studies on pile driving emphasizing the measurement of force and acceleration during driving. These measurements involving piles driven by all types of hammers have been made for several states including New York. In order to take advantage of these measurements the Federal Highway Administration contracted with the authors to prepare a wave equation program which would accurately model the diesel hammer. Several years have passed since the TTI program was developed, so it could be expected that other general improvements could be introduced into the program for all types of hammers. Finally the large

ClibPDF - www.fastio.com

ClibPDF - www.fastio.com

volume of available measurements of force and acceleration at the pile top were used to test the program performance. No currently available program has been subjected to such a demanding and thorough testing.

This report is presented in four volumes. The first presents a general discussion of the use of the wave equation and how this particular program models the hammer-pile-soil system. Emphasis is placed on a discussion of the operation of diesel hammers and how that operation is modeled by WEAP. The second volume provides a description of program input and output and can serve as a user's manual for the program. It is strongly recommended that all users read Volume I prior to the User's Manual so that they will understand the assumptions contained in the program and how it is intended that it be used. The third volume was prepared to aid the computer operator during the initial stages of program and data file loading. It also contains a flow chart which may be of interest to those users who want to study the program in greater detail. The fourth volume contains the three parts of a lecture which is also available in the form of a tape/slide show. The contents of this narrative report deal with background, models and applications of the Wave Equation.

This "Background Report" together with program, "Manual" and "Documentation" was updated in 1980. As far as the Background Report is concerned, only typographical errors were eliminated. Manual and Documentation were more thoroughly reedited.

ClibPDF - www.fastio.com

ACKNOWLEDGEMENTS

The following agencies have given invaluable assistance toward the improvement of the program and its documentation by providing comments and suggestions:

Federal Highway Administration, Office of Development

New York Department of Transportation, Soil Mechanics Bureau

New York Department of Transportation, EDP Bureau

The following firms have contributed important data:

FMC Corporation - Cedar Rapids, Iowa

Foundation Equipment Corporation - Newcomerstown, Ohio

International Construction Equipment - Matthews, No. Carolina

L. B. Foster Corporation - Pittsburgh, Pennsylvania

MKT Corporation - Dover, New Jersey

Soil Exploration Company - St. Paul, Minnesota

Vulcan Iron Works, Inc. - West Palm Beach, Florida

Raymond International, Houston, Texas

Menck, Division of Koehring GmbH, West Germany

ClibPDF - www.fastio.com

LIST OF TABLES

NO.	TITLE	PAGE
1	DESCRIPTION OF TEST DATA	75
2	COMPARISON OF COMPUTED WITH OBSERVED QUANTITIES FOR TESTED DATA	77

ClibPDF - www.fastio.com

LIST OF FIGURES

NO.	TITLE
2-1	A BEARING GRAPH DERIVED FROM THE ENGINEERING NEWS FORMULA
2-2	(A) THE SYSTEM TO BE ANALYZED; (B) THE WAVE EQUATION MODEL AND (C) THE COMPONENTS OF THE SOIL RESISTANCE MODEL
3-1	WORKING PRINCIPLE OF THE OPEN END DIESEL HAMMER
3-2	(A) SCHEMATIC AND (B) MODEL OF OPEN END DIESEL HAMMER
3-3	(A) STIFFNESS VS. COMPRESSION RELATION (B) STIFFNESS VS. COMPRESSION VELOCITY RELATION; BOTH FOR DRIVING SYSTEM COMPONENTS
3-4	EXAMPLE OF FORCE VS. DEFORMATION RELATION FOR COMPONENTS OF DRIVING SYSTEM
3-5	THE FOUR PHASES OF THE THERMODYNAMIC MODEL
3-6	MEASURED COMBUSTION CHAMBER PRESSURE
3-7	SCHEMATICS OF CLOSED END DIESEL HAMMERS (A) UNIFORM (B) NON-UNIFORM RAM
3-8	SCHEMATIC OF A VACUUM CHAMBER DIESEL HAMMER
3-9	SIMPLE ACTING AIR/STEAM HAMMER (A) DURING FALL (B) AFTER IMPACT
3-10	DIFFERENTIAL ACTING AIR/STEAM HAMMER (A) AFTER IMPACT (B) DURING FALL
3-11	AIR/STEAM HAMMER (A) SCHEMATIC AND (B) WEAP MODEL
3-12	(A) SCHEMATIC REPRESENTATION OF PILE AND (B) PILE AND SOIL MODEL
4-1	THE REAL LOAD DEFLECTION CURVE AND ITS MODEL. IN A CORRECT ANALYSIS QUAKES SMALLER THAN REAL MUST BE USED.
5-1	BLOCK DIAGRAM OF PROGRAM FLOW

ClibPDF - www.fastio.com

LIST OF FIGURES (cont)

NO.	TITLE
6-1	COMPARISON OF PREDICTED WITH MEASURED PILE TOP FORCES AND COMBUSTION PRESSURES FOR PILE NO. 1
6-2	COMPARISON OF PREDICTED WITH MEASURED PILE TOP FORCE AND VELOCITY FOR (A) PILE NO. 2 AND (B) PILE NO. 3
6-3	FORCE AND VELOCITY MATCH FOR PILE NO. 4 (PURDUE)
6-4	FORCE AND VELOCITY MATCH FOR PILE NO. 5 (MIAMI DTP 3)
6-5	FORCE, VELOCITY AND PRESSURE MATCH FOR PILE NO. 6
6-6	FORCE AND VELOCITY MATCH FOR PILE NO. 7 (A) NORMAL PROGRAM PERFORMANCE, (B) USING PREIGNITION AND REDUCED FUEL SETTING
6-7	FORCE AND VELOCITY MATCH FOR PILE NO. 8 USING PREIGNITION AND REDUCED FUEL SETTING
6-8	FORCE AND VELOCITY MATCH FOR PILE NO. 9
6-9	FORCE AND VELOCITY MATCH FOR PILE NO. 10 (GEORGIA)
6-10	FORCE AND VELOCITY MATCH FOR PILE NO. 11
6-11	FORCE AND VELOCITY MATCH FOR PILE NO. 12 (CUYAHOGA RIVER)
6-12	FORCE AND VELOCITY MATCH FOR PILE NO. 13
6-13	FORCE AND VELOCITY MATCH FOR PILE NO. 14 (PHILADELPHIA)
6-14	FORCE AND VELOCITY MATCH FOR PILE NO. 15
6-15	FORCE AND VELOCITY MATCH FOR PILE NO. 16
6-16	FORCE MATCH AND THREE DIMENSIONAL FORCE PLOT FOR PILE NO. 17
A1	COMPARISON OF COMPUTED WITH MEASURED COMBUSTION AND EXPANSION CYCLE

ClibPDF - www.fastio.com

WAVE EQUATION ANALYSIS FOR PILES
RESEARCH REPORT

TABLE OF CONTENTS

		Page No.
PREFACE		ii
ACKNOWLEDGEMENTS		iv
LIST OF TABLES		v
LIST OF FIGURES		vi
TABLE OF CONTENTS		viii
CHAPTER 1	INTRODUCTION	1
CHAPTER 2	BASIC OPERATION AND USE OF THE WAVE EQUATION	4
CHAPTER 3	MATHEMATICAL MODELS	13
	3.1 Indroduction	13
	3.2 Hammer	13
	3.2.1 Working Principle of the Open End Hammer	13
	3.2.2 The Mechanical Model of the Open End Diesel Hammer	16
	3.2.3 The Thermodynamic Model of the OED Hammer	22
	3.2.4 Working Principle of the Closed End Diesel Hammer	29

ClibPDF - www.fastio.com

TABLE OF CONTENTS (Continued)

		Page
	3.2.4.1 Hammers with Uniform Rams	31
	3.2.4.2 Hammers with Non-uniform Rams and Compression Tanks	33
	3.2.5 The Vacuum Chamber Hammer	35
	3.2.6 The Air/Steam Hammer Model	36
	3.3 Pile	42
	3.4 Soil	45
	3.5 Numerical Treatment	47
CHAPTER 4	PROGRAM INPUT INFORMATION	51
	4.1 Introduction	51
	4.2 Open End Diesel Hammer	51
	4.3 Closed End Diesel Hammers	53
	4.4 Air Steam Hammers	53
	4.5 Other Hammer Related Input Information	54
	* 4.6 Driving Accessories	57
	* 4.7 Pile	58
Running * -	* 4.8 Soil	62
	* 4.9 Other Program Options	64
* CHAPTER 5	PROGRAM FLOW	67
CHAPTER 6	PROGRAM PERFORMANCE	72
	6.1 Introduction	72

ClibPDF - www.fastio.com

TABLE OF CONTENTS (Continued)

6.2 Data Selection

6.3 Representation of Results

6.4 Results

CHAPTER 7 CONCLUSIONS AND RECOMMENDATIONS

APPENDIX A COMBUSTION CALCULATIONS USING COMBUSTION CHARTS

A.1 General Remarks

A.2 Sample Calculation

A.3 Discussion

REFERENCES

METRIC CONVERSION FACTORS

ClibPDF - www.fastio.com

CHAPTER 1

INTRODUCTION

The purpose of this report is to describe the development, modeling and basic ideas behind a computer program called WEAP (Wave Equation Analysis of Pile Driving) which was developed under contract with the Federal Highway Administration. The study was conducted to serve the following purposes:

(a) To produce a program for analyzing a pile driven by a diesel hammer using a thorough model of both the thermodynamic and mechanical hammer operation.

(b) To improve and refine existing techniques for wave analysis of piles driven by air-steam hammers.

(c) To study the performance of the program by comparing computed values of pile top force and velocity with those measured previously by the Case project (1)+.

(d) To provide a program that requires minimal effort for the preparation of input data for "typical" cases and puts the volume of output information in the control of the user.

The wave equation concept is not new. Smith (2,3) first proposed the use of this discrete method for modeling the hammer-pile-soil system. Among the researchers that have further contributed to the advancement of the art are Forehand and Reese (4) and Samson et al (5). Probably the largest research efforts were made by the Texas Transportation Institute of Texas A&M University (6,7)* (TTI). The program versions that they created were pub-

+ Numbers in paranthesis pertain to references listed at end of text.
* Only two of the large number of their reports are referenced here.

ClibPDF - www.fastio.com

lished and made generally available in the United States.

When the TTI program was written, air-steam hammer operation was of primary interest and concern. Therefore, it is not surprising that results were much less satisfactory when diesel hammer systems were analyzed. Particularly the prediction of driving stresses for these cases has been found to be unsatisfactory by many program users.

Prior to the development of the WEAP program the performance of wave equation programs was tested either by analysis of simple cases where closed form solutions giving force-time relationships were available, or for real cases where the predicted capacity was compared so that measured in a static load test. Since only a few cases with oversimplified hammer systems can be solved in closed form, the primary testing was against load test results. Such a comparison involves only one parameter in a domain where more than twenty are unknown and must be found. To make matters worse, the system is non-linear and simplifying assumptions, interpolations and extrapolations do not always hold. Other problems such as time - dependent characteristics of the soil, numerical defects of the discrete model and inadequate soil modeling can also yield erroneous results. While large volumes of measurements have been published by the Case Research Project, apparently this data was not used to any substantial degree in checking the performance of other programs. One of the tasks of the project reported here was to subject the program to extensive testing by comparing measured and calculated force and velocity records at the pile tope for a wide variety of hammer and pile types.

ClibPDF - www.fastio.com

As indicated above, the principal goal of this work was to improve analysis capabilities for diesel hammers. The WEAP program differs from the TTI program for diesel hammers in that, first, WEAP includes the determination of the gas pressure in the combustion chamber using a thermodynamic analysis rather than a constant, specified pressure and, secondly, the hammer stroke is calculated in the dynamic analysis rather than being specified in advance. Diesel hammers can operate at a wide variety of strokes that cannot be estimated in advance by intuitive means. Moreover, the hammer's effectiveness is strongly dependent on the stroke.

In Chapter 2 of this report the basic use of the wave equation is discussed. Real hammer performance is discussed in Chapter 3 and the model for hammer operation is described with emphasis placed on diesel hammers. The soil model is also described and an alternate approach to that used by Smith is presented. Some further elaboration on diesel hammer operation is contained in Appendix A.

The information necessary for the preparation of the program input data is described in Chapter 4 (and also in the User's Manual). Chapter 5 gives a general description of the program organization and flow. The extensive study of program performance which compares calculated and measured values of force and velocity for 17 different test piles is reported in Chapter 6. Chapter 7 gives some conclusions and recommendations.

ClibPDF - www.fastio.com

CHAPTER 2

BASIC OPERATION AND USE OF THE WAVE EQUATION

For over 100 years foundation engineers have used dynamic formulas to estimate pile bearing capacity (or the inverse, to estimate the required blow count for a specified capacity). The use of these formulas has been severely criticized since all of them have been proven grossly inaccurate and unreliable. Their use persists in spite of the criticism because of their simplicity and the lack of something better. Also, some dynamic means of capacity prediction will continue to be required since pile design loads have tended to increase making static load tests increasingly difficult to perform.

In order to place the wave equation in context it is appropriate to review the use of a dynamic formula. Consider a typical example (EN-formula)

$$R = \frac{2\,Wh}{S+C} \qquad (2.1)$$

where R is the design load, W is the ram weight, h is the ram stroke, S is the permanent set of the pile per hammer blow and C is a term which represents the energy losses and carries the same units as set. Contained in the constant of equation 2.1 is a theoretical factor of safety of 6 plus the quantities necessary to make the units correct. The product Wh usually is used to represent the rated hammer energy. This formula can be represented by the curve shown in Figure 2.1. The design pile capacity is given as a function of blow count and is known as a bearing graph. A number of applications can be visualized. When a particular blow count is observed and the rated hammer

ClibPDF - www.fastio.com

commonly arise are: Is the bearing capacity sufficient? Would further driving produce pile damage? Is the hammer performing properly? Is the driving system of the correct size?

However, the observation of blow count is a very convenient way to gage the quality of the pile installation. Therefore, the wave equation approach was developed. The one dimensional wave equation can be derived by applying Newton's Second Law to a rod element of infinitesimal length. It is written

$$\rho \frac{\partial^2 u}{\partial t^2} = E \frac{\partial^2 u}{\partial x^2} \qquad (2.2)$$

where ρ is the material mass density, E is the modulus of elasticity of the material and u is the axial displacement of a point on the rod at location x and time t. Thus, $\partial^2 u/\partial t^2$ is the acceleration and $\partial^2 u/\partial x^2$ is the strain gradient at x and t.

Using this continuous form of the wave equation for pile analysis is usually not practical for the real boundary conditions which must be handled. However, a similar equation can be derived if elements of finite length, ΔL, are chosen having mass, $m = \rho A \Delta L$ and spring stiffness, $K = EA/\Delta L$. Here A is the pile cross sectional area. Newton's Second Law leads to

$$ma = K(\Delta u_t - \Delta u_b) \qquad (2.3)$$

where a is the acceleration of the mass and Δu_t and Δu_b are the compression of the springs at the top and bottom, respectively, of the mass

ClibPDF - www.fastio.com

under consideration.

The Wave Equation (the term Wave Equation is the name that has been attached to computer programs for discrete dynamic pile analysis. In the remainder of this report, this usuage will be adopted) makes use of the concept of equation 2.3 by representing the pile and driving system (Figure 2.2a) by a series of masses and springs as shown in Figure 2.2b. The soil is modeled by a spring (R, Static) and a dashpot (R, Dynamic) attached to each mass. The soil resistances so represented are shown in Figure 2.2c and are linear elastic plastic for the spring where the maximum force, R_u, is reached at a displacement q, called the quake, and linearly proportional to the element velocity for the dashpot (commonly known as the damping force).

The analysis proceeds by giving the ram an initial velocity. At each element the displacement can be calculated for a small time increment with element velocities determined from the previous time increment. With these displacements and velocities the forces acting on each mass can be determined. They arise from the pile spring deformations, from the soil spring deformation and from the dashpot force. Using Newton's Second Law in the form represented in Equation 2.3 the mass accelerations can be calculated and by integration also the velocity. The computation then proceeds to the next time increment.

In application a set of soil forces R_u and damping forces are assigned at each element. Then the ram is given it's rated impact velocity and the dynamic computation outlined above is continued through successive time

ClibPDF - www.fastio.com

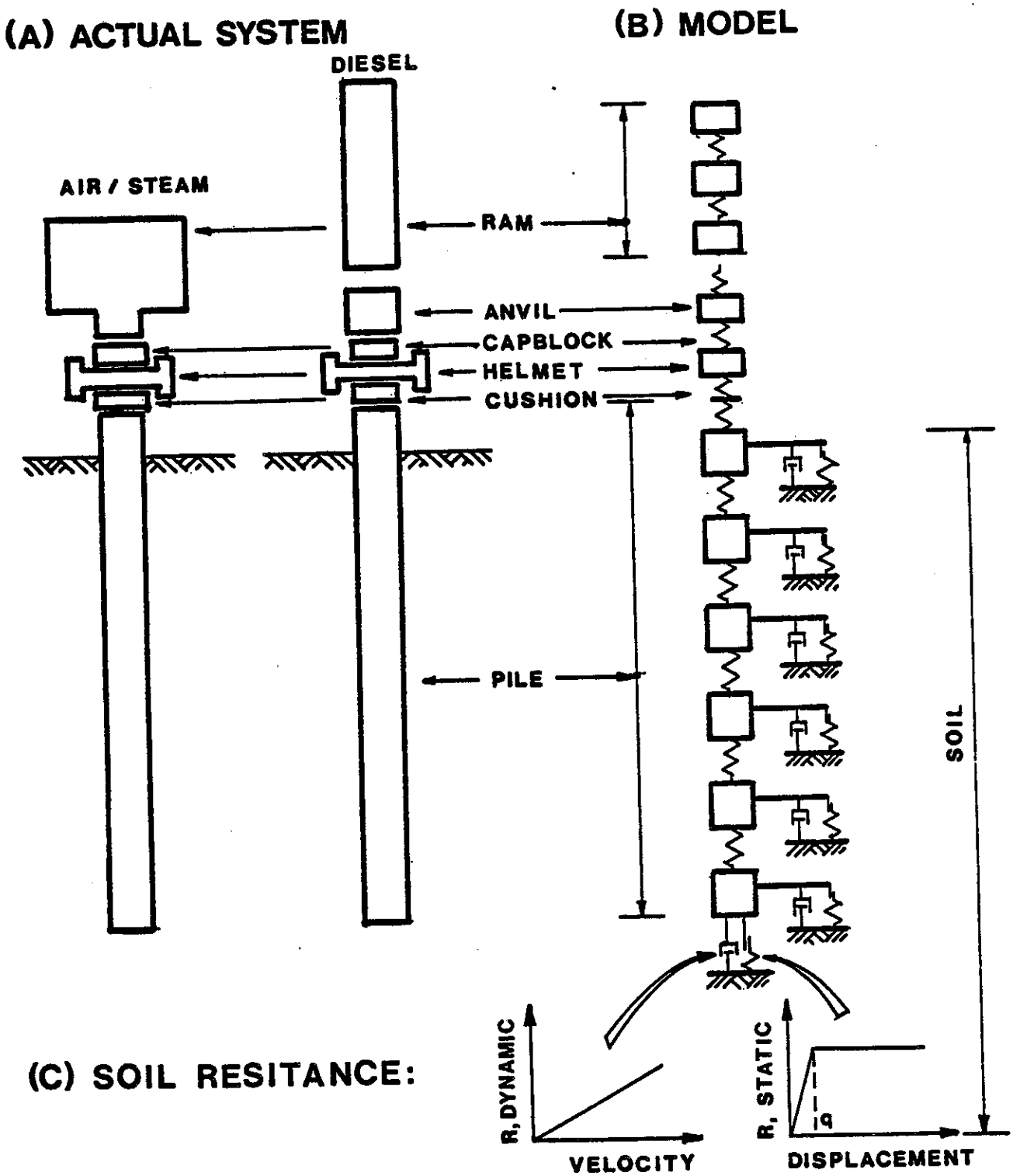

FIGURE 2-2: (A) THE SYSTEM TO BE ANALYZED;
(B) THE WAVE EQUATION MODEL AND
(C) THE COMPONENTS OF THE SOIL RESISTANCE MODEL

ClibPDF - www.fastio.com

increments until all soil forces are less than R_u. The total permanent displacement will have then been calculated and a point on the bearing graph is known. The capacity value is known as R_{ut} and is equal to the sum of the R_u values at each element. The blow count is obtained from the calculated permanent set. In this procedure the permanent set (or blow count) is determined for a set of assigned resistances. However, the bearing graph is plotted, by tradition, with the blow count as the independent variable. A variety of R_{ut} values can be used to calculate the total shape of the bearing graph.

In addition to the bearing graph the wave equation also gives stresses in the pile and they can also be shown as a function of blow count.

In practice, the wave equation bearing graph can be used in a manner quite similar to the dynamic formula bearing graph. In addition, driving stresses can be rationally limited. While the shape of the two curves are quite similar the differences are substantial. A particular wave equation bearing graph is associated with a single driving system pile type, soil profile and a particular pile penetration. If any one of the above items are changed, the bearing graph changes.

The above description summarizes very briefly the operation of traditional wave equation programs such as the TTI program. The system model will be described in greater detail in Chapter 3. The operation of the WEAP program will also be described emphasizing those aspects which are different.

ClibPDF - www.fastio.com

Usually, the stroke of a diesel hammer cannot be prescribed as was done in the above description since it is not known. Thus, the WEAP program's mathematical model is constructed like that shown in Figure 2.2 except that a combustion chamber force is introduced between the ram and the anvil. The program operation begins by dropping the ram from some initial preassigned height. The ram velocity at the exhaust ports can be calculated directly from the free fall distance. When the exhaust ports are closed by the ram it continues to fall against the confined gas in the combustion chamber. In this stage the gas pressure and ram velocity are calculated incrementally. The gas pressure can be determined from the gas law since the volume is known as the ram falls. When impact occurs, and the velocity at impact has been calculated, a dynamic analysis of the general type described above is performed. Shortly after impact ignition occurs in the combustion chamber and the pressure and temperature are given an appropriate increase. At some stage in the calculation separation occurs between the ram and the anvil. The computation now continues until the exhaust port is passed at a known velocity. From this velocity the rebound stroke can be calculated. If the initial stroke is not the same as the rebound, the computation is repeated using the rebound stroke as the initial stroke in the next cycle. Convergence usually occurs in two or three cycles.

A bearing graph similar to that previously described is obtained except that stroke and pile stresses are also included. An example is shown in Figure 6 of the User's Manual.

ClibPDF - www.fastio.com

A variation of this concept is necessary for hammers which do not have a definite fuel setting and for which the combustion pressure is not known a priori. In such cases, the stroke is usually kept as desired by adjusting the fuel amount. (In easy driving the stroke is probably always limited by the maximum combustion energy available). To model this process the stroke has to be specified and maximum combustion pressure is adjusted until the rebound stroke equals the specified one.

Now consider the three problems with the dynamic formula as they relate to the wave equation:

1. The driving system can be represented with considerable realism. The various dynamic parameters used to describe the system must be available. Of course, the wave equation cannot be expected to recognize a poorly performing hammer.

2. The pile is well represented.

3. The soil model is a substantial improvement over that used in the dynamic formula. However, it is still extremely simple and crude. Even for this simple model it is very difficult to obtain soil constants. Therefore, greater complexity hardly seems justified.

The use of either dynamic formula or the wave equation requires the accurate determination of blow count. Particular care must be used if the driving resistance is changing rapidly. Often when time dependent strength changes occur, it is desirable to restrike the pile. Here the blow count at the very beginning of restrike must be determined since it can be expected to change with driving.

ClibPDF - www.fastio.com

CHAPTER 3

MATHEMATICAL MODELS

3.1 Introduction

In this chapter the construction and operation of pile driving hammers will be discussed. After the hammer operation, the mathematical models which have been developed to represent the hammers will be described. Since the most important contribution of this report is probably the diesel hammer portion, it will be presented first.

The model used to represent the other parts of the driving system, the pile and the soil will also be described in considerable detail.

In general, the variables used to describe the system will be the same as those used in the program. While this approach is somewhat unwieldly—here it has substantial advantages for those readers who need to become deeply involved with the program.

3.2 Hammer

3.2.1 Working Principle of the Open End Diesel Hammer

The Open End Diesel hammer (OED) operates on a two stroke diesel cycle. The hammer is started by raising the ram with a lifting mechanism. At the upper end of its travel the lifting mechanism is tripped, the ram is released and descends by gravity. At the time the ram bottom passes the exhaust ports a certain volume of air, VIN, is trapped and is compressed (Figure 3-1a). Usually before the time of exhaust port closure, a certain amount of fuel is squirted into the cylinder. Some hammers inject an atomized

ClibPDF - www.fastio.com

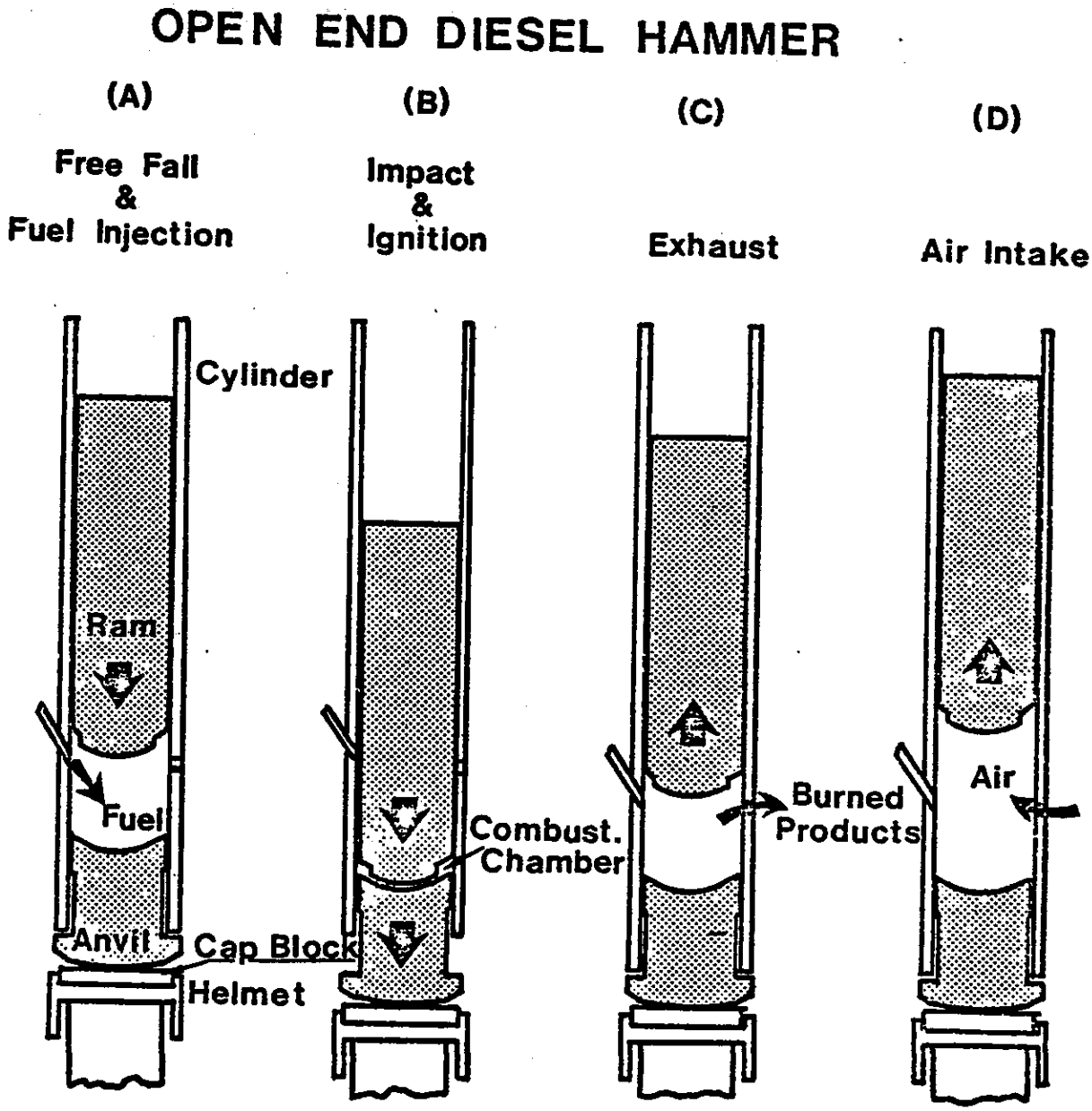

FIGURE 3-1: WORKING PRINCIPLE OF THE OPEN END DIESEL HAMMER

ClibPDF - www.fastio.com

fuel later in the cycle when the combustion chamber pressure is higher.

When the ram impacts against the anvil the air is compressed to a final volume (VFIN). The fuel is splattered by the impact into this final volume (if fuel atomization was not used) and combustion starts at some time after impact (combustion delay). This delay is due to the time that is required for the fuel to mix with the (hot) air and to ignite. More volatile fuels might have a shorter combustion delay than heavier ones. Combustion occurring before impact is called preignition and can be caused by the wrong fuel type or an overheated hammer. In hard driving, preignition is usually considered to be undesirable.

During impact, anvil, capblock and pile top are rapidly driven downward (Figure 3-1b) leaving the cylinder with no support. Thus, it starts to descend by gravity.

Pile rebound and combustion pressure push the ram upwards. When the exhaust ports are cleared some of the combustion products are exhausted leaving in the cylinder a volume of burned gases at ambient pressure that is equal to VIN (Figure 3-1c). As the ram continues upward fresh air, which is drawn in through the exhaust ports, mixes with the remaining burned gases (Figure 3-1d).

Depending on the reaction of the pile and the energy provided by combustion the ram will rise to some height (stroke). It then descends again by gravity to start a new cycle.

ClibPDF - www.fastio.com

3.2.2 The Mechanical Model of the Open End Diesel Hammer

In order to properly model the mechanics of the OED hammer the following characteristic properties must be considered in addition to those described above:

(a) The ram is relatively long and flexible.

(b) Metal to metal impact occurs between ram and impact block.

(c) Energy losses occur on all interfaces of hammer components which transmit the impact.

The capblock, helmet and, if present, the cushion will be considered as a part of the hammer. The helmet is usually a rather heavy steel form that adapts to the pile top. The capblock is cushioning material between anvil and helmet while a cushion is sometimes inserted between helmet and pile top.

Figure 3-2 shows both an actual pile driving hammer (a) and its model (b). The ram was divided into M elements to account for its flexibility. Anvil and cap were represented by one mass each. The spring stiffness above the anvil was determined by the lowest ram element stiffness combined with that of the anvil. Thus, if HM(I) denotes the mass of the I-th hammer segment the following relations hold:

$$HM(I) = \frac{W_R}{M\,g} \quad \text{for } I \leq M \qquad (3\text{-}1)$$

where W_R is the weight of the ram (assumed to be uniform) and g is 32.2 ft/s^2 (9.81 m/s^2).

ClibPDF - www.fastio.com

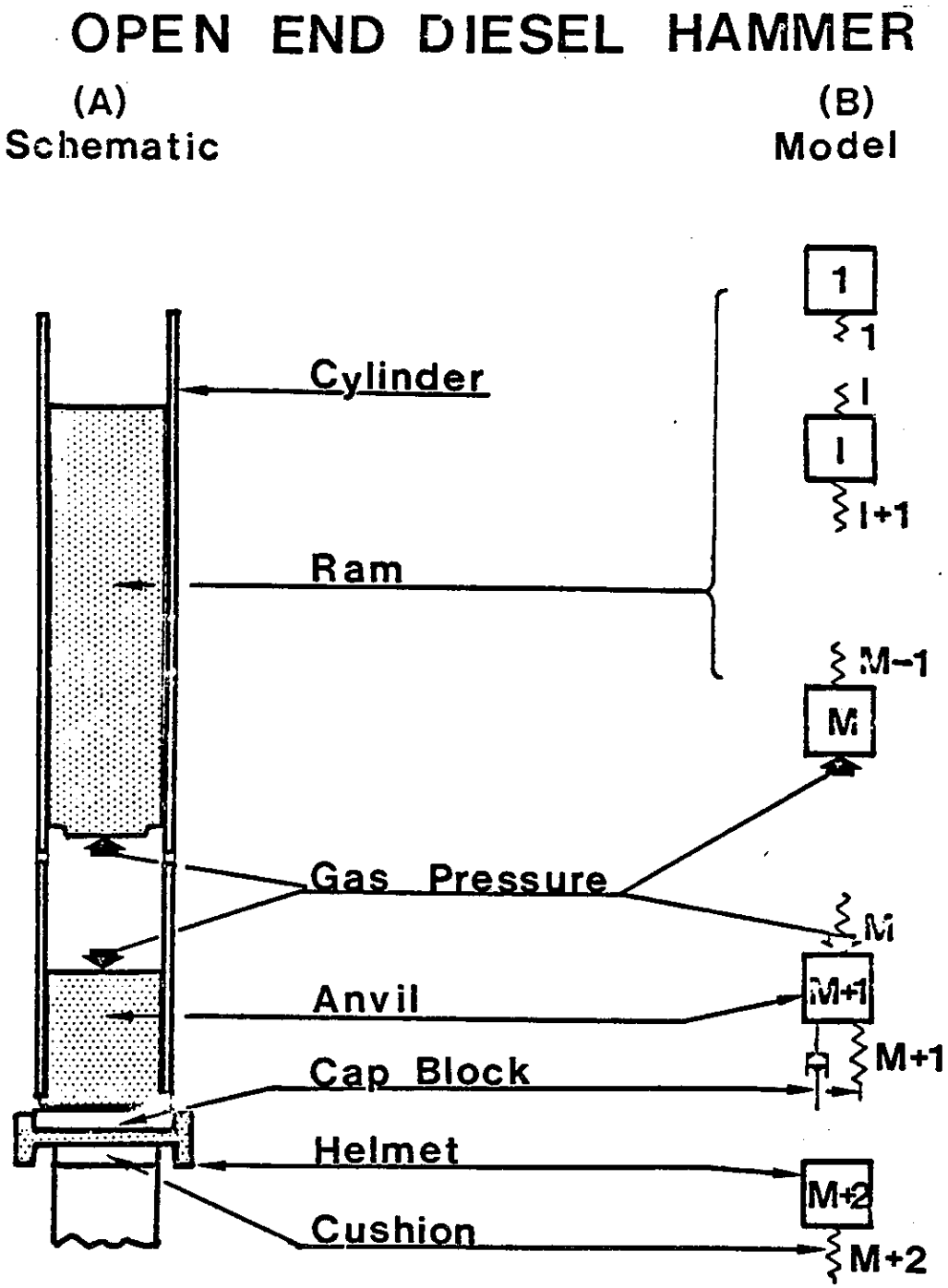

FIGURE 3-2: (A) SCHEMATIC AND (B) MODEL OF OPEN END DIESEL HAMMER

ClibPDF - www.fastio.com

Similarly one obtains

$$HM(M+1) = \frac{W_A}{g} \tag{3-2}$$

and

$$HM(M+2) = \frac{W_c}{g} \tag{3-3}$$

with W_A and W_c being the weight of the anvil and capblock, respectively. Thus, the hammer model always consists of M+2 elements. M depends on the length of the ram. Initial studies showed that ram segments of two to three feet in length yield sufficient accuracy.

The springs connecting the hammer masses have the following stiffnesses (if the ram is uniform):

$$STH(I) = \frac{A_R E}{L_R} M \qquad I \leq M \tag{3-4}$$

with A_R, L_R and E being the cross sectional area, length and elastic modulus of the ram, respectively. Furthermore,

$$STH(M) = \frac{\left(\frac{A_R M}{L_R}\right)\left(\frac{A_A}{L_A}\right)}{\frac{A_R}{L_R} M + \frac{A_A}{L_A}} E \tag{3-5}$$

with A_A and L_A being cross sectional area and length of the anvil, respectively. Note that STH(M) is the spring against which the ram impacts.

Since energy losses are usually associated with such an impact, the

ClibPDF - www.fastio.com

unloading stiffness of the anvil spring is:

$$\overline{STH(M)} = \frac{STH(M)}{EANV^2} \tag{3-6}$$

where EANV is the coefficient of restitution of the anvil. Similarly, if ECAP is the coefficient of restitution of the capblock the unloading stiffness of the capblock spring is:

$$\overline{STH(M+1)} = \frac{STH(M+1)}{ECAP^2} \tag{3-6a}$$

STH(M+1) depends solely on the cushion properties in the capblock. If there is a cushion at the pile top with ECUS as a coefficient of restitution and stiffness STC then

$$\overline{STC} = \frac{STC}{ECUS^2} \tag{3-6b}$$

This stiffness must be combined with that of the pile top element for which

$$\overline{STP(1)} = \frac{STP(1)}{ETOP^2} \tag{3-6c}$$

(the definition of STP(1) will be given below). In this way a combined pile top and cushion stiffness is obtained:

$$STH(M+2) = \frac{(STC)(STP(1))}{STC + STP(1)} \tag{3-7}$$

ClibPDF - www.fastio.com

For unloading the corresponding expressions can be found when the values of Equations (3-6b) and (3-6c) are used.

As a deviation from the usual approach the loading stiffness, say STH was always calculated as $(EA/L)(e^2)$, e being the coefficient of restitution. Then the unloading slope, $\overline{STH}$, becomes EA/L. In other words, if k = EA/L is the stiffness of a segment or component as determined in a compression test, then k is used as the unloading stiffness in the dynamic application. The effect is a lower stiffness during loading. This approach is justified if the tangent rather than the secant modulus is used for E in computing k. The program uses this approach for all springs where coefficient of restitution is less than 1.

Special consideration was given to the fact that the slope of a stress-strain curve of cushioning material usually is gradually increasing and does not - at zero stress - start with its maximum value. Similarly, the force deformation curve of two colliding bodies such as the ram impacting against the anvil cannot show an ideal elastic behavior.

It is neither possible nor necessary to provide a quantitatively exact model. Qualitatively, though, the curves can be rounded and the result can be judged by comparison with measurements.

For this reason three displacement values, DS, were assumed for anvil, cap and cushion. For a deformation less than or equal to DS the stiffness, ST, was assumed to be linearly increasing with the deformation (Figure 3-3a). Thus the modified stiffness is:

$$ST = STH(I) \frac{DNH(I-1) - DNH(I)}{DS}, \quad I = M, M+1, M+2 \qquad (3\text{-}8)$$

ClibPDF - www.fastio.com

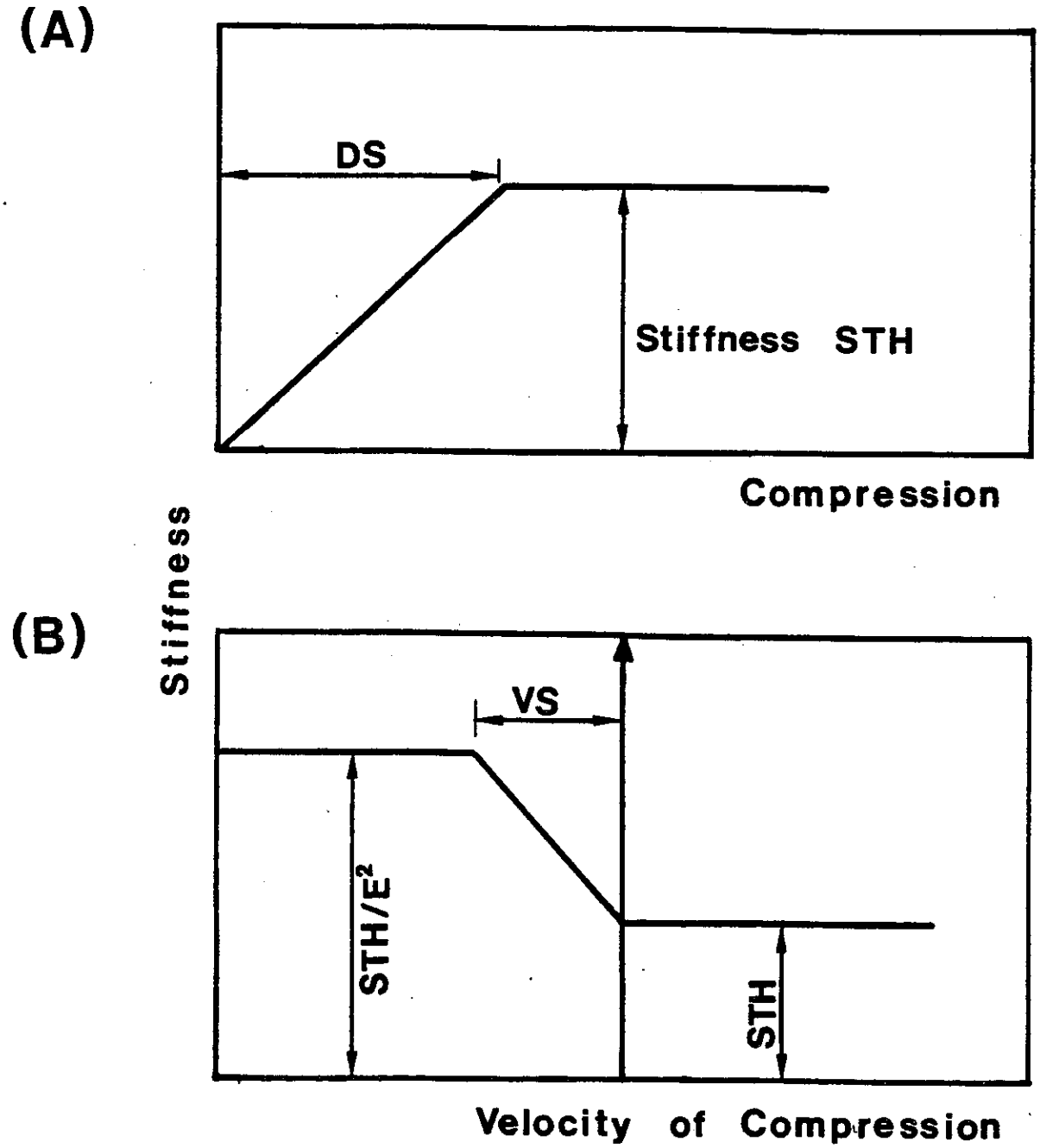

FIGURE 3-3: (A) STIFFNESS VS. COMPRESSION RELATION (B) STIFFNESS VS. COMPRESSION VELOCITY RELATION; BOTH FOR DRIVING SYSTEM COMPONENTS

ClibPDF - www.fastio.com

which is valid for DS > DNH(I-1) - DNH(I), with DNH(I) being the displacement of a hammer element, I, at a certain time. Modifications of this formula have to be made where the deformation becomes small during unloading. A load deformation curve obtained by going through several cycles of loading, unloading and separation is shown in Figure 3-4.

Another point of concern was the change of slope of the load deformation curve when the velocity changes sign. This change was programmed such that the stiffness of hammer springs M, M+1 and M+2 was changing linearly from the low to the high value between 0 and a negative compression velocity, VS (see Figure 3-3b), which was set at -0.5 ft/sec (0.15 m/sec).

In addition to the bilinear spring a dashpot was added to model the cap block. The dashpot constant was set at 2% of the ram's critical damping value ($2\sqrt{STH(1)(HM(1))}$). This damper is present more to improve the discrete model's accuracy than for physical reasons. It was found that agreement with measured data improved when using such a dashpot. An additional dashpot was not used with the cushion since the pile top already contains one in it's model (see 3.3).

3.2.3 The Thermodynamic Model of the OED Hammer

The thermodynamic model is divided into four parts: (a) compression, (b) combustion delay, (c) ignition and (d) expansion. These four phases are illustrated in Figure 3-5.

Compression begins when the ram has fallen to the level of the exhaust ports. The ram velocity is then:

ClibPDF - www.fastio.com

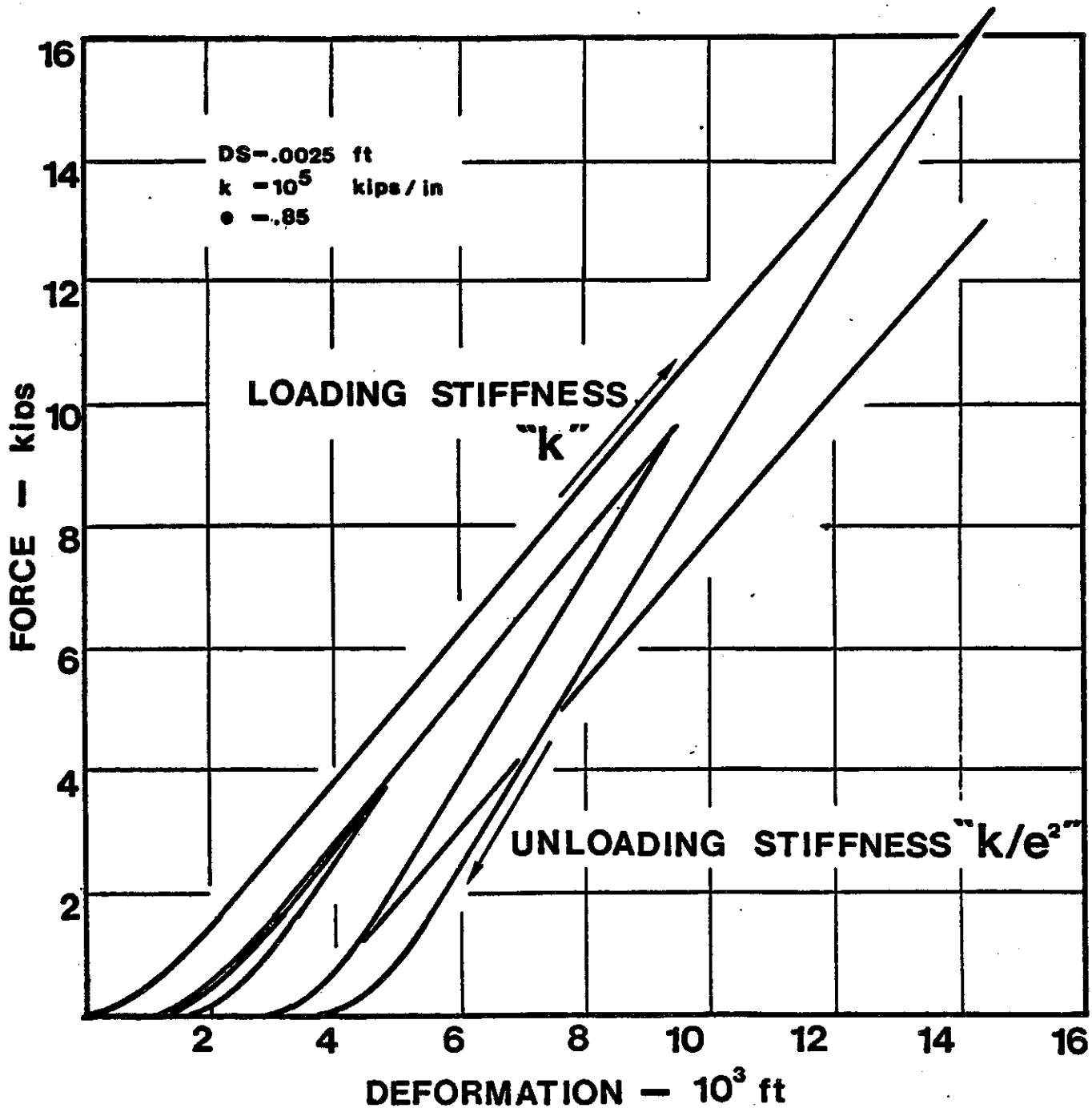

FIGURE 3-4: EXAMPLE OF FORCE VS. DEFORMATION RELATION FOR COMPONENTS OF DRIVING SYSTEM

ClibPDF - www.fastio.com

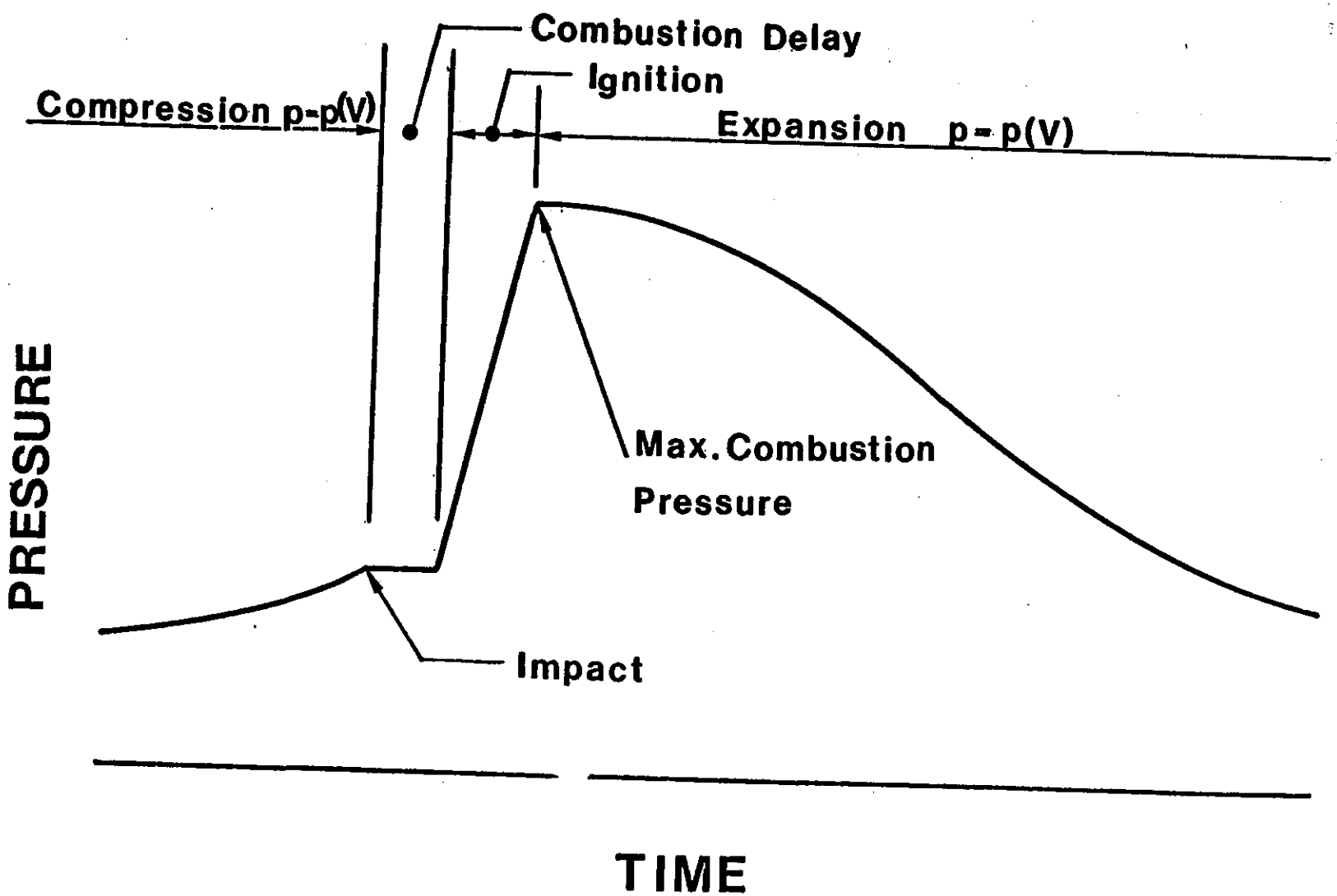

FIGURE 3-3: THE FOUR PHASES OF THE THERMODYNAMIC MODEL

ClibPDF - www.fastio.com

(3-9)

$$V_{R,E} = \sqrt{2g(\text{STROKE} - \text{DEPIB})*\text{EFFICY}}$$

is the ram fall height, DEPIB is the distance between the
ts and the impact block (or anvil) and EFFICY is an efficiency
). The initial volume of air is (3-10)

$$\text{VIN} = \text{DEPIB (ARAM)} + \text{VCHAM}$$

ARAM is the cross sectional area of the cylinder and VCHAM is the
volume at impact. If during compression the position of the ram
(measured from the anvil) then the pressure below the ram is (3-11)

$$P = \left(\frac{\text{VIN}}{(\text{DPOS})\ (\text{ARAM})}\right)^{\text{EXPP}} (\text{PATM})$$

, EXPP is a parameter dependent on the specific heats of the gas in the
inder and PATM is the atmospheric pressure (14.7 psi or 1.01 bar). For
adiabatic compression of air EXPP is 1.4. Since the process is not completely
adiabatic EXPP should be chosen less than 1.4. Results of actual measure-
ments were used to determine the correct value (see Appendix A).

With regard to the ignition phase either analytical, experimental or
combined approaches can be chosen. The truly analytical approach can only
be as good as the available information on many hammer parameters. Actually,
there are limits as to the accuracy of the analytical approach since effects
of cooling, scavenging, fuel atomization and others can only be estimated. It
should be added that efforts were actually made to predict combustion pressures.
Appendix A contains a sample calculation and a discussion of such results.

ClibPDF - www.fastio.com

The truly experimental approach can only be as good as are. In particular it is important to obtain representative other hand, limitations on the number of independent variabl will always have to be imposed. For the present program the limitations on the independent variables are:

(a) Normal ambient temperature (approximately 68°F (

(b) Normal atmospheric pressure (14.7 psi (1.01 bar)).

(c) Normal hammer performance and condition (compress temperature, lubrication, fuel injection etc.)

(d) Normal fuel type.

A hammer tested under these conditions, i.e. measurements of stroke and pile top force and acceleration, provides sufficient inf The parameters to be extracted would be time of ignition and magnitude pressure. Effects of variable stroke on the pressure behavior should studied. The records should be obtained under normal conditions.

Since it is too difficult to obtain pressure-volume data for most hammers the pressure must be computed in the program after ignition using appropriate model. An expansion modeled according to Equation (3-11) was found to be sufficiently accurate. This model can be considered a combined experimental and analytical approach.

The validity of the model of Figure 3-5 is shown in Figure 3-6. The solid curve in Figure 3-6 is a pressure record* obtained on a DELMAG D-12 hammer under "normal" conditions. The record exhibits first a gradual increase

*Courtesy of the Foundation Equipment Corporation, Newcomerstown, Ohio.

ClibPDF - www.fastio.com

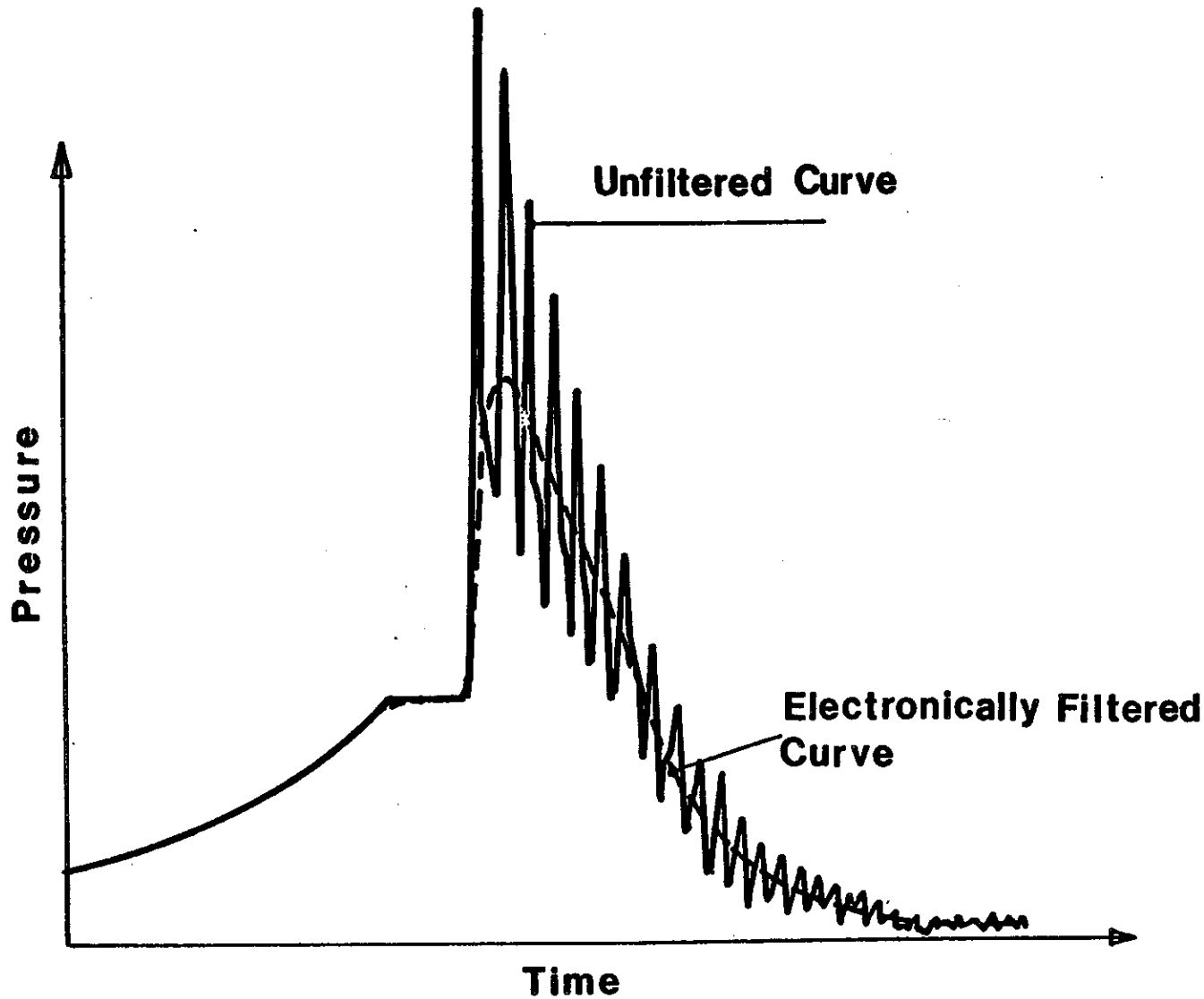

FIGURE 3-6: MEASURED COMBUSTION CHAMBER PRESSURE

ClibPDF - www.fastio.com

during precompression; then it stays constant for a short time period which is the time between impact and combustion and is called the combustion delay; next, it displays a very rapid increase (ignition) and very high magnitude, high frequency variations which gradually decay.

While the timing information on this record is accurate, it is very hard to determine the average or effective maximum pressure. For this reason a low pass, 1 kHz filter was employed which produced the dashed curve of Figure 3-6. The rise of pressure is slower in the filtered than in the unfiltered curve, the maximum pressure value, however, can easily be determined.

Further conclusions for the pressure record are:

(a) The high frequency components of the record are caused by pressure waves in the chamber and are of little significance to the hammer behavior. This phenomenon has also been reported in measurements made on internal combustion engines.

(b) The expansion process can only be judged in connection with actual pressure-volume data. It was found by simulation and comparison with measured data that the records represented Otto rather than Diesel cycles and that the expansion model can be rather simple.

In summary, the following values are used in the model:

(a) The expansion coefficient, EXPP, for the compression phase was set at 1.35.

(b) The duration of the combustion delay can vary but was never found to be greater than .002 seconds.

(c) The maximum combustion pressure depends on measurements.

(d) The duration of the ignition phase was set to 0.5 milliseconds.

ClibPDF - www.fastio.com

(e) The expansion coefficient, EXPP, for the expansion phase was set to 1.30.

Certain modifications of this model are necessary when a hammer using atomized fuel injection is considered. In this case the combustion delay has to be computed from the start of the fuel injection and the duration of the ignition should be increased to cover the duration of the injection.

For cases where manufacturer's data were not available, both a delay and duration of 10 milliseconds was used with the restriction that ignition occurs at least at impact. It should be mentioned that accurate timing information for atomized injection may be very important.

3.2.4 Working Principle of the Closed End Diesel Hammer

The closed end hammer works very much like the open ended one. In principle the main change consists of a closed cylinder top. Figure 3-7 shows two of these hammer types. When the ram moves upward, air is being compressed at the top of the ram which causes a shorter stroke and, therefore, higher blow rate.

The bounce chamber has ports such that atmospheric pressure exists as long as the ram top is below these ports. As the ram moves toward the cylinder top it creates a pressure which increases until it is just in balance with the weight of the cylinder itself. Further compression is not possible and if the ram still has an upwards velocity uplift of the cylinder will result. This uplifting cannot be tolerated as it can lead both to an unstable driving condition and to the destruction of the hammer. For this reason the fuel amount and, hence maximum combustion chamber pressure, has

ClibPDF - www.fastio.com

ClibPDF - www.fastio.com

CLOSED END DIESEL HAMMERS

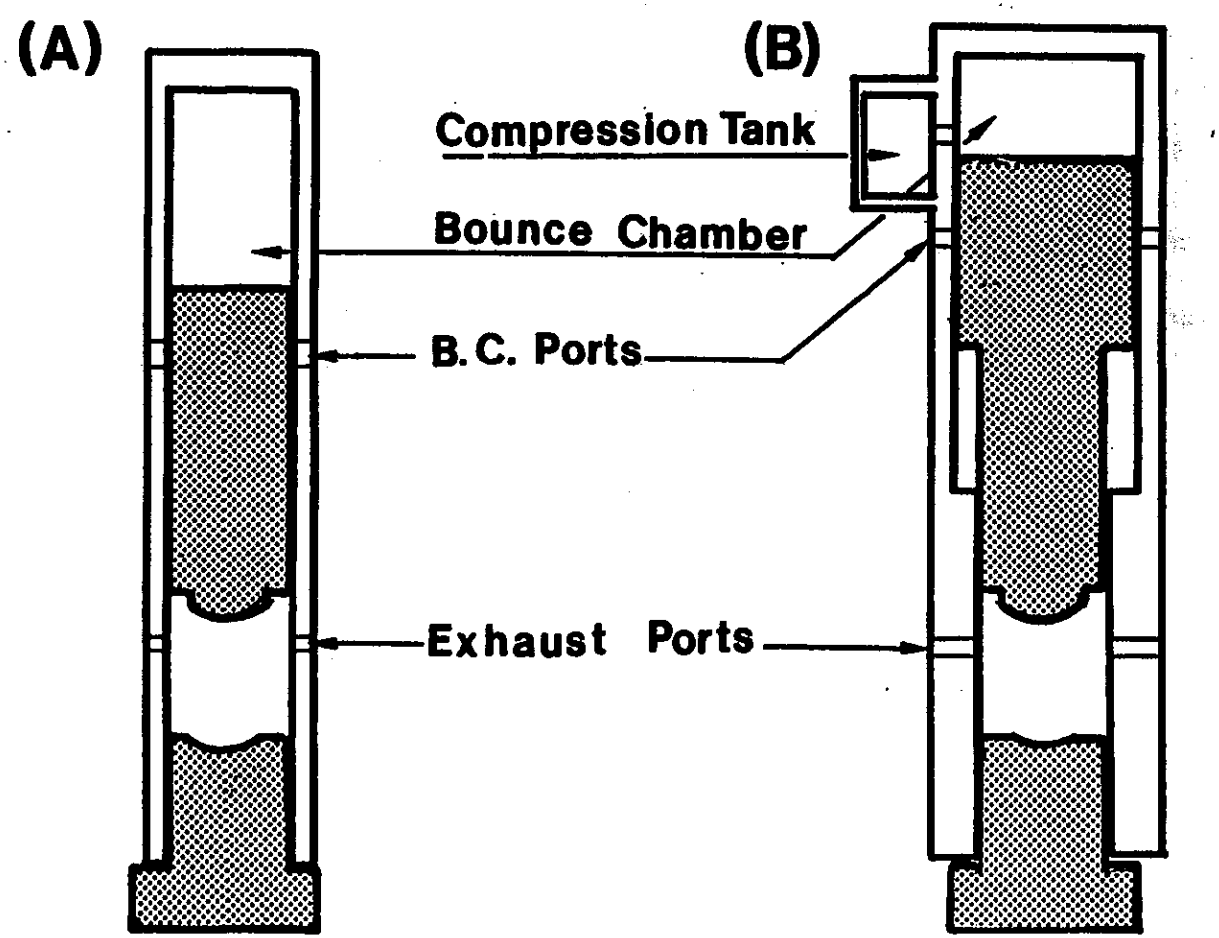

FIGURE 3-7: SCHEMATICS OF CLOSED END DIESEL HAMMERS
(A) UNIFORM (B) NON-UNIFORM RAM

to be reduced such that there is only a very slight lift off or none at all.

Uplift occurs only when the soil resistance forces are sufficiently high. For low resistance forces the stroke will be less than the one for which uplift is imminent.

Another feature of a few closed end hammers (Linkbelt) is an improved scavenging system. This design uses both intake and exhaust ports and an air tank which provides a horizontal air flow through the cylinder when the ram moves downward. It can be expected that the relative amount of unscavenged combustion products present during combustion is smaller than in other hammers.

Another closed end hammer type (BSP) should be discussed. This hammer type employs a vacuum chamber below its ram to increase its operating speed. Two phases of this hammer's operation are shown in Figure 3-8. As can be seen, the hammer is not really closed at the top (although a protective cover is usually present). However, the stroke is limited by the vacuum action under the upper portion of the ram such that it does not become visible during operation. In addition to being faster than an open end hammer this type has the advantage of not lifting off during operation since the vacuum force is always less than the cylinder weight.

3.2.4.1 Hammers with Uniform Rams

The design of these hammers is not very different from the open end hammers. The principal difference is that the ram on its upward travel

ClibPDF - www.fastio.com

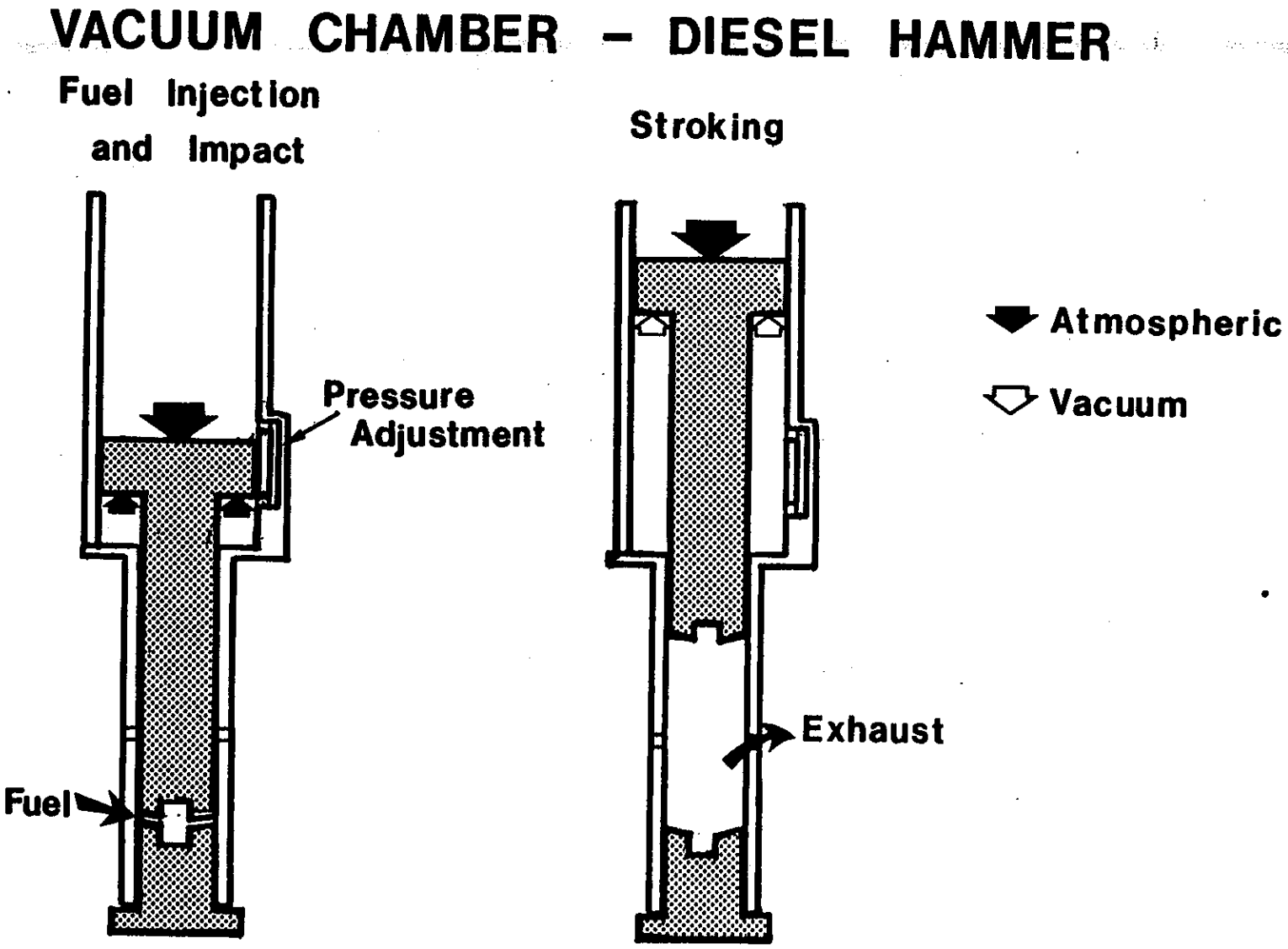

FIGURE 3-8: SCHEMATIC OF A VACUUM CHAMBER DIESEL HAMMER

ClibPDF - www.fastio.com

closes the bounce chamber exhaust ports and, since the cylinder is closed at the top, compresses the air above the ram (Figure 3-7a). Since the bounce chamber is filled with air, compression occurs adiabatically to a chamber pressure:

$$PB = PATM \left(\frac{DEPBB}{DPOS}\right)^{1.4} \qquad (3\text{-}12)$$

where DEPBB is the distance from exhaust ports and DPOS is the distance from the ram top to the bounce chamber top. Of course, for DPOS being greater than DEPBB

$$PB = PATM . \qquad (3\text{-}13)$$

There exists a value of DPOS at which the pressure becomes so large that the cylinder starts to lift up. If the weight of the hammer excluding ram and driving system is given by RWH, then this limiting pressure is given by

$$PLIM = \frac{RWH}{ARAM} + PATM . \qquad (3\text{-}14)$$

From Equation (3-12) one finds the maximum stroke is

$$STRMAX = DBCIB + DEPBB \left(1 - \left(\frac{PATM}{PLIM}\right)^{\frac{1}{1.4}}\right) . \qquad (3\text{-}15)$$

DBCIB is the distance that the ram travels upward before it closes the bounce chamber ports.

3.2.4.2 <u>Hammers with nonuniform rams and compression tanks</u>

Sometimes the top of the ram has a larger cross section (ART) than the

ClibPDF - www.fastio.com

bottom in order to reduce the precompression force for better hammer performance in easy driving. Also, a compression tank may be attached to the bounce chamber. In this way the bounce chamber volume is relatively large until the ram closes the ports of this tank. The remaining volume in the cylinder is called a safety volume. As the ram progresses into it the pressures increase very rapidly and hammer lift off will soon occur.

Because of the existence of a pressure tank of volume VCT, Equation (3-12) has to be revised. The bounce chamber pressure is then:

$$PB = PATM \left(\frac{(DEPBB)(ART) + VCT}{(DPOS)(ART)}\right)^{1.4} \qquad (3\text{-}16)$$

which is valid for DPOS ≥ DSF. (DSF is the distance from the pressure tank port to the bounce chamber top).

The maximum pressure in the compression tank, PCT, is given by substituting DSF for DPOS in Equation (3-16). Defining

$$VBIN = (DEPBB)(ART) \qquad (3\text{-}17a)$$

and

$$VSF = (DSF)(ART) \qquad (3\text{-}17b)$$

one obtains

$$PCT = PATM \left(\frac{VBIN + VCT}{VSF}\right)^{1.4} \qquad (3\text{-}18)$$

and for DPOS < DSF one can now find

$$PB = PCT \left(\frac{DSF}{DPOS}\right)^{1.4} \qquad (3\text{-}19)$$

ClibPDF - www.fastio.com

or

$$STRMAX = DBIB + DEPBB - DSF\left(\frac{PCT}{PLIM}\right)^{1/1.4} \qquad (3\text{-}20a)$$

If the maximum stroke occurs for DPOS > DSF then

$$STRMAX = DBCIB + \frac{VBIN+VCT}{ART}\left(\frac{PATM}{PLIM}\right)^{1/1.4} \qquad (3\text{-}20b)$$

3.2.5 The Vacuum Chamber Hammer

This hammer type utilizes a vacuum rather than compressed air as for other closed end hammers to reduce its stroke and, therefore, increase its blow rate. The essential components and phases of operation are shown in Figure 3-8. Since the vacuum force is limited (maximum: atmospheric pressure, PATM, times the difference in area between ram top and bottom, DELA) uplift cannot occur as long as the cylinder weight exceeds this value. The hammer can therefore be treated as an open ended hammer type as long as the vacuum force is properly considered.

If the distance of the ram above the anvil is DBC, and the pressure in the vacuum chamber starts to decrease when the ram is at a distance DSTART and if DIN = VIN/DELA (with VIN = the volume in the chamber at DBC = DSTART) then the net force, F, on the ram in downward direction is

$$F = PATM\ (DELA)\left(1 - \left(\frac{DIN}{DBC - DSTART + DIN}\right)^{1.4}\right). \qquad (3\text{-}21)$$

Of course, if DBC is less than DSTART (anvil has moved downward) then no vacuum force exists. It should be noted that the cylinder position, DCYL, is considered in the program but not included here for the sake of clarity.

ClibPDF - www.fastio.com

In order to be able to treat the hammer like an open ended one a formula must be derived for the ram velocity at the ports, VFALL.

$$VFALL = \sqrt{2 \frac{G}{W} ((STROKE - DEPIB)(W + PATM(DELA)) + DP)\, EFFICY} \quad (3\text{-}22)$$

where $DP = PATM\ (DELA)\ \frac{DIN^{1.4}}{0.4}\ (DB^{-0.4} - DE^{-0.4})$,

$DE = DEPIB - DSTART + DIN$,

$DB = STROKE - DSTART + DIN$

and W and G are ram weight and gravitational acceleration, respectively.

3.2.6 The Air/Steam Hammer Model

The Air/Steam Hammer is much simpler to model than diesel hammers, first, because it has an external power supply and, second, because it has only a few simple hammer components. The ram usually consists of a compact block with a so-called ram point attached to its bottom. The ram point strikes against the capblock. For this reason, the impact is cushioned by a soft material. This in turn allows the ram flexibility to be neglected.

The ram is raised by externally produced air or steam pressure (Figure 3-9b) acting against a piston, housed in the hammer cylinder, which in turn is connected to the ram by a rod. Once the ram is raised a certain distance a valve is activated and the pressure in the chamber is released. At that time the ram has some upward velocity. Therefore it "coasts" up to the maximum height (stroke) and then falls free to impact on the capblock (Figure 3-9a). Upon impact pressure enters again the cylinder. The hammer described

ClibPDF - www.fastio.com

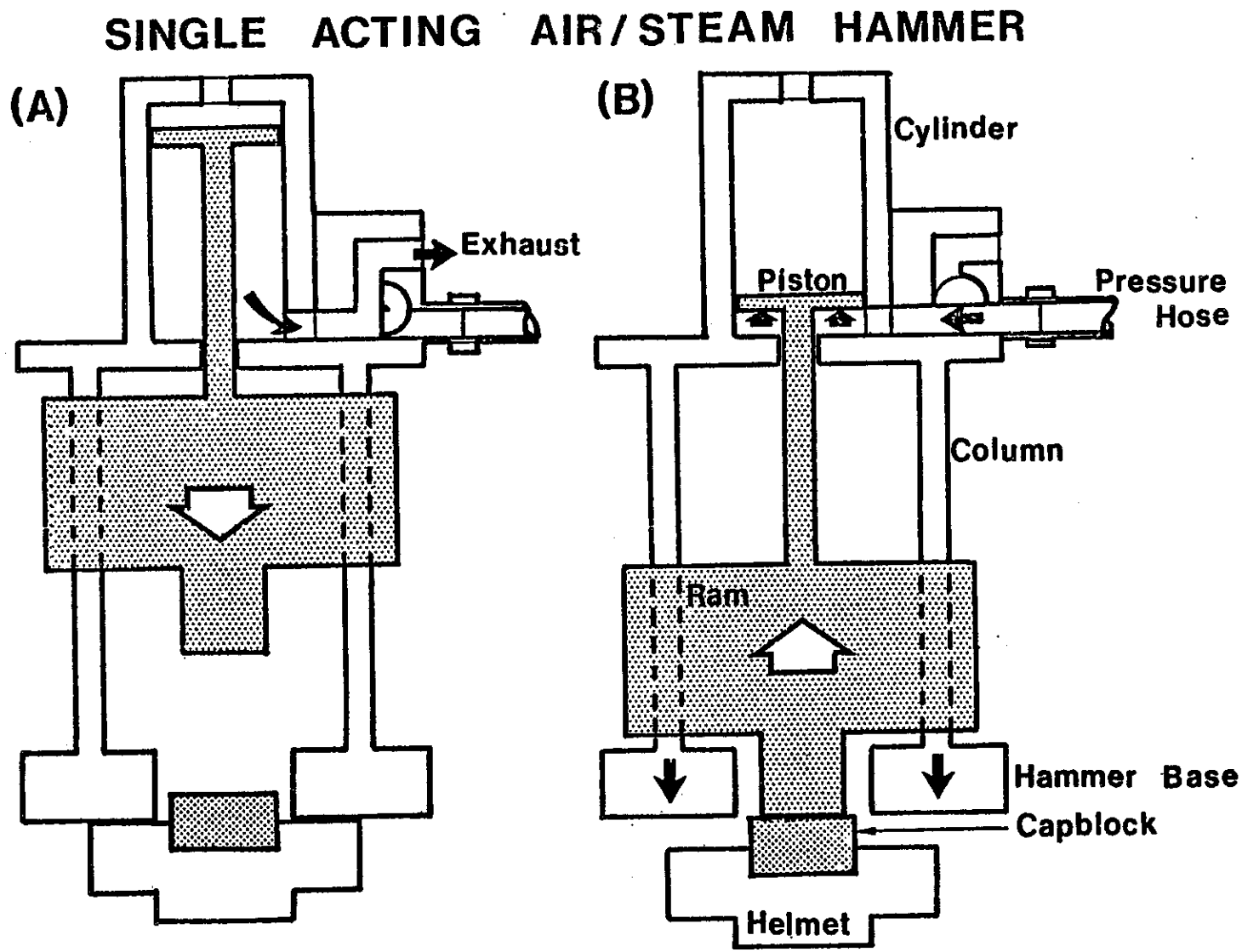

FIGURE 3-9: SIMPLE ACTING AIR/STEAM HAMMER
(A) DURING FALL (B) AFTER IMPACT

ClibPDF - www.fastio.com

above is known as the single acting air/steam hammer.

A double acting hammer is one in which the ram is accelerated during its fall by pressure in addition to gravity. The working principle of one type of double acting hammer, the differential hammer, is illustrated in Figure 3-10.

The pressure applied at the top of the piston acts against the top of the cylinder similar to the bounce chamber pressure in a closed end diesel hammer. Of course, the pressure could lift the hammer assembly, of weight WA to which the cylinder is connected. Thus, maximum hammer output will be achieved when the pressure is kept at its upper limit (PLIM, here gage pressure) at which assembly lift off is incipient.

The maximum energy of a differential acting hammer is

$$EMAX = (W + PLIM(A))\ STRM \qquad (3\text{-}23a)$$

where W is the weight of the ram, A is the effective cylinder area, and STRM is the maximum stroke of the hammer. (Note that the effective cylinder area is equal to that of the smaller (lower) piston). Since

$$A = WA/PLIM \qquad (3\text{-}23b)$$

the potential energy of a hammer driven by an actual pressure PSTEAM is

$$E = (W + PSTEAM\ \frac{WA}{PLIM})\ STRM. \qquad (3\text{-}23c)$$

From this relation an effective stroke, STROKE, is derived that a weight W,

ClibPDF - www.fastio.com

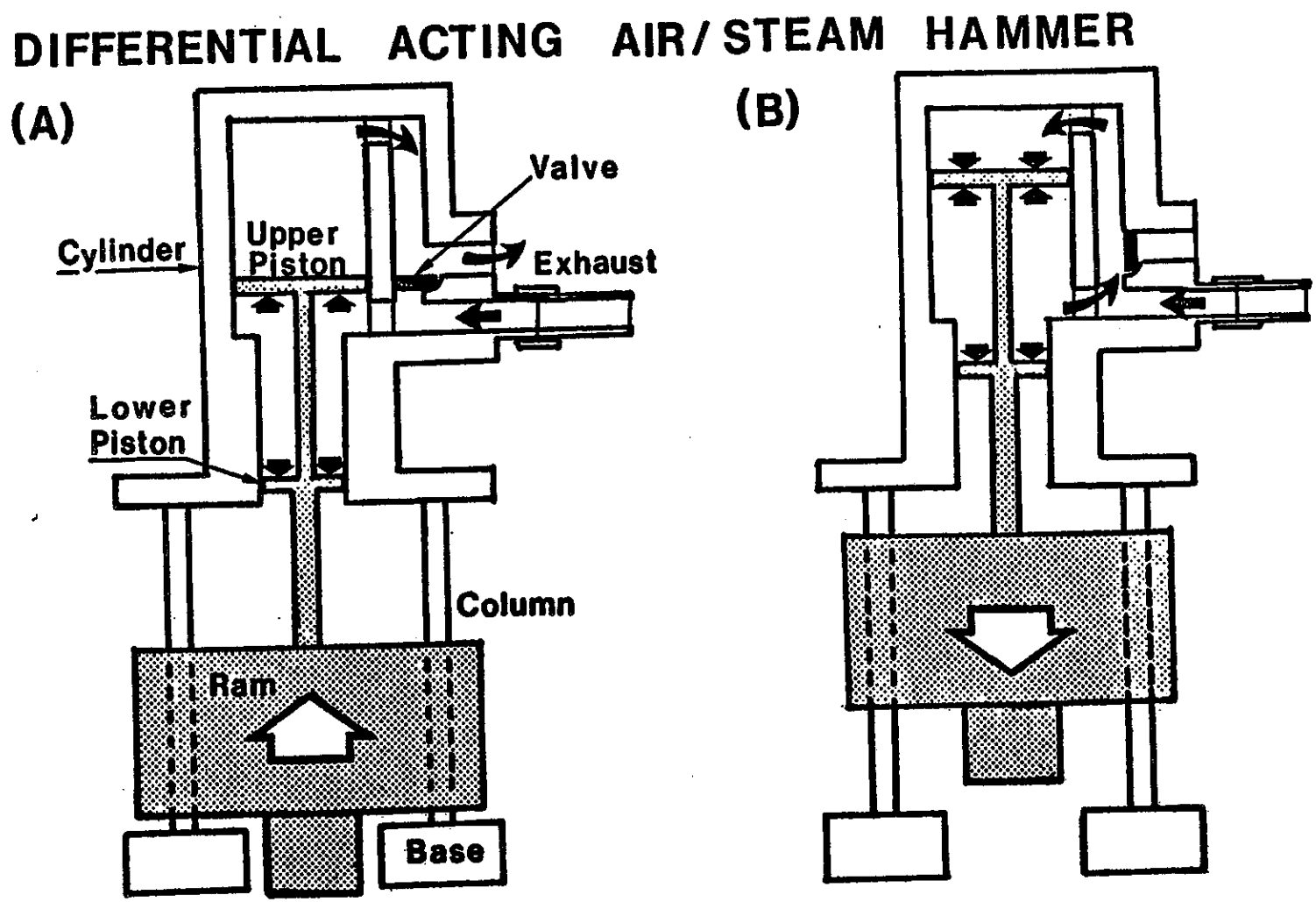

FIGURE 3-10: DIFFERENTIAL ACTING AIR/STEAM HAMMER
(A) AFTER IMPACT (B) DURING FALL

ClibPDF - www.fastio.com

should fall in order to provide a kinetic energy equal to E:

$$\text{STROKE} = \text{STRM}\left(1 + \frac{\text{PSTEAM}}{\text{PLIM}} \frac{\text{WA}}{\text{W}}\right). \qquad (3\text{-}24)$$

Unfortunately, the quantities STRM and PSTEAM are often lower than specified since the ram might not rise high enough or pressure losses occur and other losses might occur during the fall. For this reason it is common to multiply the effective stroke of both single and double acting hammers by an efficiency, EFFICY, which is a number less than or equal to one. The ram impact velocity then becomes:

$$\text{VFALL} = \sqrt{(\text{STROKE})\ (\text{EFFICY})2\text{G}} \qquad (3\text{-}25)$$

(G is the gravitational acceleration).

The mechanical model of the air/steam hammer (Figure 3-11) includes M masses and M-1 stiffnesses to represent the ram. Mass M+1 is the cap mass (capblock plus helmet) and the stiffness M is assigned to the capblock stiffness. In most cases an air/steam hammer is modeled with only one ram mass and no ram stiffness (M = 1). Coefficients of restitution and "DS-values" (see Section 3.2.2) are applicable to the cap cushion, the pile top cushion (if present) and the pile top.

As an addition to this active hammer portion a passive one is considered consisting of MA masses and stiffnesses that represent the hammer assembly. This assembly is assumed to rest on the helmet before impact and to fall freely after impact until an impact of assembly with cap occurs.

ClibPDF - www.fastio.com

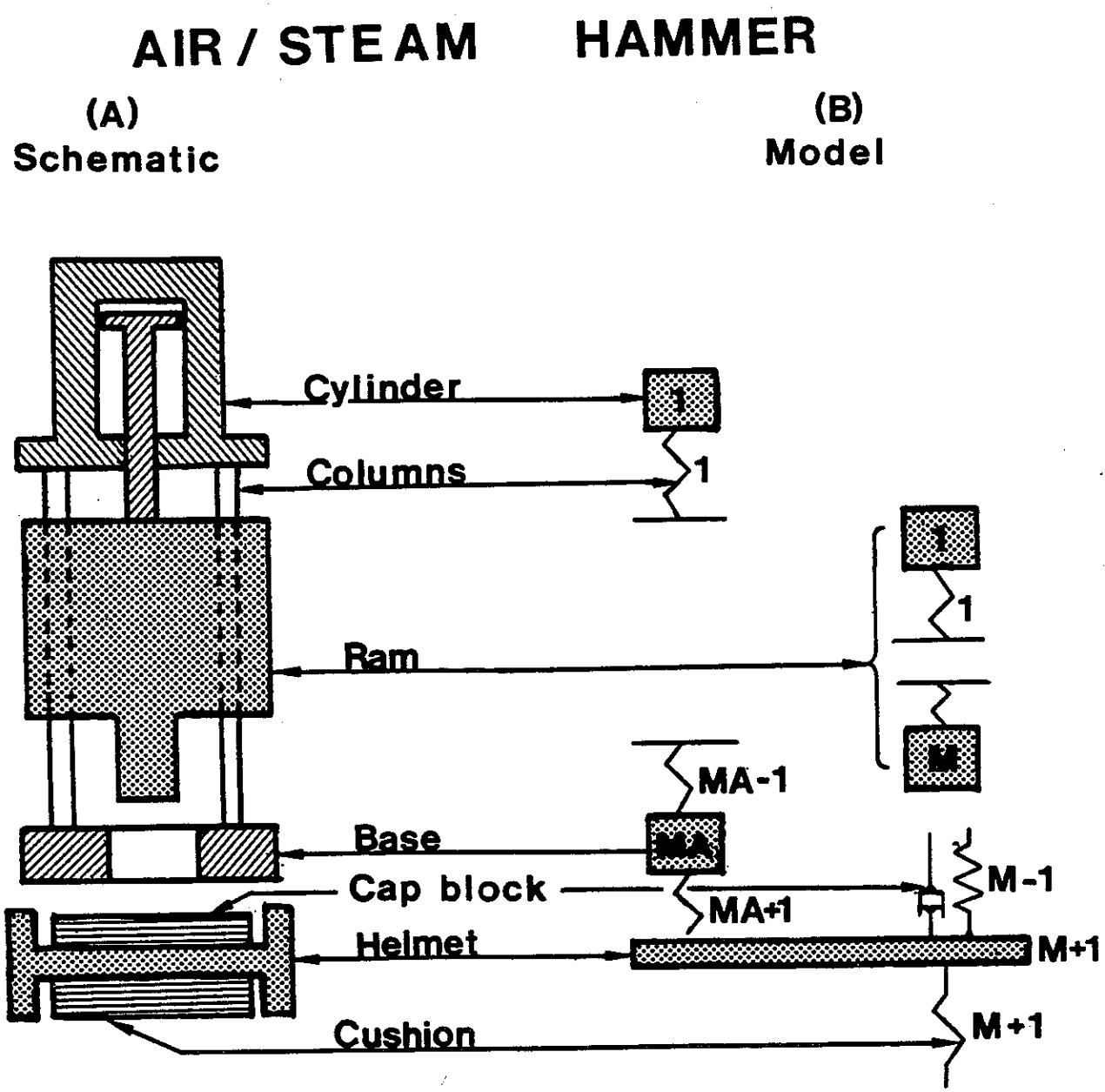

FIGURE 3-11: AIR/STEAM HAMMER (A) SCHEMATIC AND (B) WEAP MODEL

ClibPDF - www.fastio.com

According to Figure 3-11 the model of the assembly will consist of MA masses and MA stiffnesses. Usually, MA equals two. Then the weights correspond to cylinder and base weights and the two stiffnesses should be derived from that of the ram guide bars. Since the impact of the assembly is uncushioned it is recommended that for both springs in this system the same value be used, namely, twice that of all assembly columns. In this way the overall flexibility of the assembly is correctly represented without much sacrifice in accuracy. The flexibilities of both the helmet and lower assembly mass are extremely small and can hardly be modeled as elastic bodies. A coefficient of restitution and a "DS-value" are used in the program to model this assembly drop as realistically as possible.

3.3 Pile

The pile model consists of springs, masses and dashpots (see Figure 3-12). The pile is divided in N segments whose lengths are given by

$$DL = ALPH(I) \quad (XPT) \tag{3-26}$$

where XPT is the total pile length and ALPH(I) is a multiplier which is normalized (by the program) such that:

$$\sum_{I=1}^{N} (ALPH(I)) = 1.0 \tag{3-27}$$

The mass of the I-th segment is

$$PM(I) = \overline{RP} \quad \overline{(AP)} \quad DL \tag{3-28}$$

ClibPDF - www.fastio.com

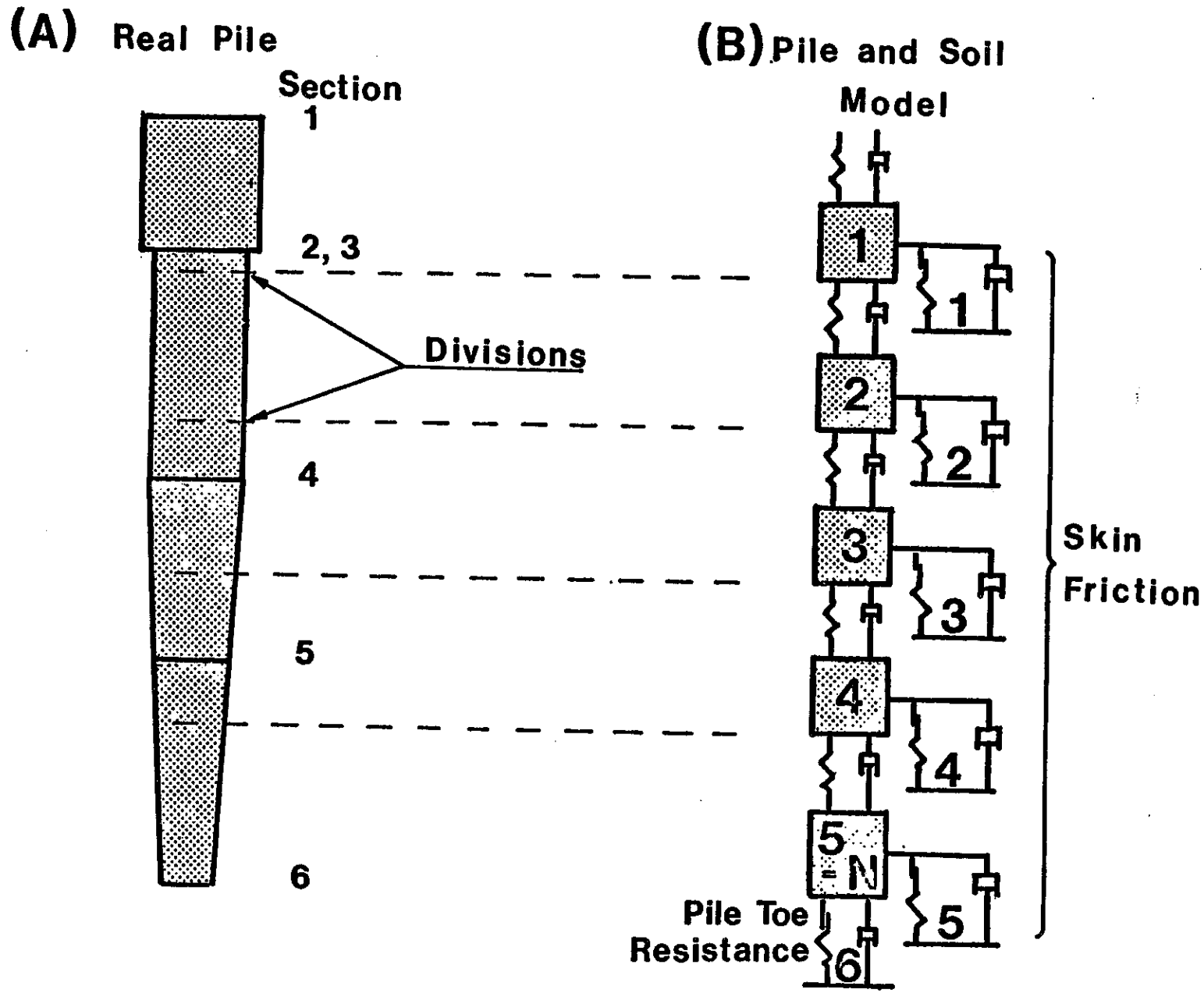

FIGURE 3-1. : (A) SCHEMATIC REPRESENTATION OF PILE AND (B) PILE AND SOIL MODEL

ClibPDF - www.fastio.com

with $\overline{RP}$ being the average mass density of the pile and $\overline{AP}$ the average cross sectional area of the pile. The averages are taken over DL.

Similarly the segment stiffnesses are

$$STP(I) = \frac{\overline{EP}\,(\overline{AP})}{DL} \tag{3-29}$$

where $\overline{EP}$ is the average elastic modulus over the element length. Obviously, multi-material piles can be treated in this fashion.

A third parameter, the <u>pile</u> damping value can be specified for the pile. Since little is known about the correct structural damping model and since this type of damping produces relatively small forces compared to soil damping, an elaborate model does not seem justified. Thus, viscous damping was assumed with parameters:

$$CDP(I) = \frac{2}{100}\ IBD\ \sqrt{STP(I)\ PM(I)} \tag{3-30}$$

with IBD being the damping constant in percent of critical. Note that Equation 3-30 is based on the definition of critical damping of the one degree of freedom oscillator.

The damping force between two segments is then

$$PD(I) = CDP(I)\ (VP(I-1) - VP(I)) \tag{3-31}$$

where VP(I) is the velocity of the I-th segment.

ClibPDF - www.fastio.com

The damping constants IBD are not related to pile length. Thus, if for a particular pile a different number of elements are used with the same damping parameters, then the total damping force is different. This approach is not quite satisfactory and is only tolerated in light of the small effects of pile damping and the limited knowledge of material damping. Further efforts in this area are encouraged.

3.4 Soil

The soil model used offers as an option some differences from the one usually employed. It basically consists of a spring and dashpot (Figure 3-12). The elastic spring yields at a pile segment displacement QS(I) (quake) such that there is no further increase in static resistance with increased displacement (RS(I) = SU(I), SU being the ultimate static resistance at that element). Unloading, i.e. when the pile segment has an upward velocity, follows at a spring rate that is in the usual case equal to that in the loading path.

An option was built into this model allowing the use of a coefficient of restitution, ESOIL, which is employed such that

$$\overline{SOK(I)} = \frac{SOK(I)}{ESOIL^2} \qquad (3\text{-}32)$$

where SOK(I) indicates the soil stiffness at the I-th pile element and where the barred quantity indicates unloading. Note that ESOIL is the same for all pile elements.

In the usual case where the pile experiences an appreciable net set the

ClibPDF - www.fastio.com

energy consumption by the use of a coefficient of restitution is negligible. However, for the very hard driving cases (blow count greater than 120 blows per foot) an energy loss due to an ESOIL - value will improve the validity of the soil model.

The damping model can be chosen according to Smith

$$DAM = J(I)\ VP(I)\ RS(I) \tag{3-33}$$

where DAM is a damping force in kips (kN) and J(I), VP(I) and RS(I) are the damping factor in sec/ft (sec/m), the pile velocity in ft/sec (m/sec) and the static resistance force in kips (kN), respectively; all taken at the same pile segment I.

The second choice is a non-dimensionalized viscous damping for which

$$DAM = JC(I)\ VP(I)\ \sqrt{STP(I)\ PM(I)}. \tag{3-34}$$

Here JC(I) is the Case (Institute of Technology) damping factor of unit dimension. Note that

$$\sqrt{STP(I)\ PM(I)} = EA/c \tag{3-35}$$

(this is also called pile impedance; Young's modulus, E, times cross sectional area, A, divided by wave speed, c; all in the pile). The use of the expression on the left of Equation 3-35 is preferred as it reflects the average properties at an element. Recalling that viscous damping is defined as

$$DAM = JV(I)VP(I) \tag{3-36}$$

ClibPDF - www.fastio.com

with JV(I) being the viscous damping constant it is apparent that

$$JC(I) = \frac{JV(I)}{\sqrt{STP(I)\ PM(I)}} = \frac{JV(I)}{EA/c} \qquad (3\text{-}37)$$

while Smith's damping factor becomes

$$J(I) = \frac{JV(I)}{RS(I)} \qquad (3\text{-}38)$$

The distribution of damping is handled in the following way: For Smith's damping a constant factor is used along the pile skin and another factor is used at the toe. This actually means that the corresponding viscous damping factor varies proportionally to the static resistance distribution along the skin. In order to have a similar situation for the Case damping approach the input consists here also of skin and toe damping factors which are converted to viscous damping factors by virtue of Equation 3-37. The skin damping factor is then distributed to the segments in proportion to the static resistance.

3.5 Numerical Treatment

There are two aspects in the numerical treatment of the analysis that differ substantially from the TTI or Smith's approach. First the integration equations involve also the acceleration terms, and second a so-called predictor-corrector approach is used.

The integration equations are simply (note that subscripts indicating

ClibPDF - www.fastio.com

element numbers are omitted if not necessary for clarity):

$$VN = \frac{1}{2} (AO + AN)\ DT + VO \qquad (3\text{-}39)$$

and

$$DN = \frac{1}{6} (2AO + AN)\ DT^2 + VO(DT) + DO. \qquad (3\text{-}40)$$

In these equations A stands for acceleration, V for velocity, D for displacement, O (old) for the beginning and N (new) for the end of the current time increment, DT.

Starting with the hammer and continuing with the pile a prediction of the values DN and VN is made by integration using Equations 3-39 and 3-40. Since AN is not known it is set to AO. Then the top (FO) and bottom (FU) spring forces at the I-th element can be computed:

$$FO = (DN(I-1) - DN(I))\ ST(I) \qquad (3\text{-}41a)$$

and

$$FU = (DN(I+1) - DN(I))\ ST(I+1) \qquad (3\text{-}41b)$$

(an H or P after DN and ST would indicate hammer or pile, respectively). Force contributions due to pile damping at the I-th segment are:

$$FDO = (VNP(I-1) - VNP(I)) * CDP\ (I) \qquad (3\text{-}42a)$$

and

ClibPDF - www.fastio.com

$$FDU = (VNP(I+1) - VNP(I)) \cdot CDP(I+1). \qquad (3\text{-}42b)$$

Static resistance forces, RES, are computed using the soil stiffness SOK

$$RESN = RESO + (DN-DO)\ SOK \qquad (3\text{-}43a)$$

with

$$|RESN| \leq SU(I) \qquad (3\text{-}43b)$$

and for the toe

$$0 \leq RESN \leq SU(N+1) \qquad (3\text{-}43c)$$

Due to damping resistance

$$DA = (JV)(VNP) \qquad (3\text{-}44a)$$

for Case and

$$DA = (J)(VNP)(RESN) \qquad (3\text{-}44b)$$

for Smith's damping.

Including the gravitational acceleration, G, the new acceleration value can now be found:

$$AN = G + (FO + FU + FDO + FDU - RESN - DA)/PM \qquad (3\text{-}45)$$

(For ram bottom and anvil this equation contains, of course, the gas pressure force too). Integration of AN leads to new VN and DN values.

ClibPDF - www.fastio.com

Once all VN and DN values are corrected the change from the previous quantities is determined and the process is repeated, computing again for all elements the various quantities starting with Equation 3-41a. This process is repeated until both the pile top force and bottom velocity converge. An input directed maximum number of cycles (ITER) is observed.

ClibPDF - www.fastio.com

CHAPTER 4

PROGRAM INPUT INFORMATION

4.1 Introduction

In this chapter the program input information will be described briefly. The input structure was designed so as to minimize the effort required of the engineer in the preparation of data. Therefore, as much routine computation as possible is performed internally. However, in some cases the flexibility of very detailed engineer input is desirable, so options are available which control the form of the input required by the program.

In one particular case, the hammer, it is usually unnecessary for the user to prepare detailed data to describe the hammer since there is a limited number of available hammers. The TTI program has required that each user obtain the hammer details from manufacturers or dealers. A great danger exists that incorrect information is input. In the WEAP program hammer information has been obtained from the manufacturers. Where questions arose the manufacturer was contacted and clarification obtained.

4.2 Open End Diesel Hammer

To call a hammer the user needs only to specify the hammer number (IHAMR) from a list of hammers in the file. There exists an option (IHAMR = 0) that allows the input of all hammer parameters. These parameters are in order:

NAME ..... an alphanumeric string of up to eight characters.

HM(I) .... weight of the I-th ram segment in kips for all I(I=1,M).

STH(I) ... stiffness of the I-th ram segment in kips/inch for I = 1, M-1.

ClibPDF - www.fastio.com

M	the number of ram masses. It can be determined by dividing the ram length by 2.5. M should be greater than or equal to two for all Diesel hammers.
HM(M+1) ...	weight of anvil in kips
STH(M) ...	stiffness of last ram element and anvil combined in kips/inch (see Equation 3-4).
TDEL	combustion delay in seconds (values between 0.0 and 0.002 seconds are normal for regular injection).
VFIN	final volume or combustion chamber volume in cubic inches.
DEPIB	distance between exhaust ports and impact block (anvil) in inches.
ARAM	cross sectional area of cylinder in square inches.
P1, P2,.... P5	combustion pressures for up to five fuel settings in pounds per square inch. Note that only P1 must be given. Default of P1 causes the use of P1 = 1000 psi.
EFFICY ...	a hammer efficiency (see Equation 3-9)
STRM	maximum stroke in inches as specified by the manufacturer. This value will be used as a convergence criterion on the stroke. It is assumed that the stroke cannot exceed this value.
EXPP	exponent for the expanding, combusted gases. A value between 1.2 and 1.4 is reasonable.
POWSCAV ..	should be set to 1 if the scavenging is independent of stroke.
DINJ	distance between ram location at which atomized fuel is injected and anvil in feet. DINJ = 0.0 for regular fuel injection.
TGI	the duration of atomized fuel injection or the duration of ignition in general.
ITYPH	hammer type: here=1.001 for open end diesel.

ClibPDF - www.fastio.com

4.3 Closed End Diesel Hammers

The data needed for the complete description of a closed end or a vacuum chamber (VCH) hammer are (in addition to those for open end hammers) as follows:

ART ..... the cross sectional area of bounce chamber in square feet.

DEPBB .... the distance between the combustion chamber ports and the top of the combustion chamber in feet (not for VCH).

DSF ..... the distance between the pressure tank ports (only if present) and the top of the bounce chamber in feet. For VCH this is the distance that the ram travels upward before the vacuum chamber pressure starts to decrease.

DBBT ..... the distance between the anvil and the top of the combustion chamber minus the ram length in feet (not for VCH). Note that DBBT - DEPBB = DBCIB as used in Equation 3-15.

RWH ..... the hammer assembly weight, i.e. that force which cannot be exceeded by the bounce chamber (gage) pressure times ART (not for VCH).

EXPB ..... the exponent used for calculation of the bounce chamber pressure (usually 1.4).

VCT ..... the volume of the compression tank in cubic feet. For VCH this is the initial vacuum chamber volume (at the time when the pressure starts to decrease).

Note that ITYPH is to be given as 2.001 for all closed end diesel hammers except vacuum chamber hammers which are type ITYPH = 1.001. Note also that STRM is disregarded for ITYPH = 2.001.

4.4 Air Steam Hammers

These hammer types require the following input values:

ClibPDF - www.fastio.com

(a) As for diesel hammers:

NAME

HM(I), I = 1, M

STH(I), I = 1, M-1

M

P1 (Here, maximum (gage) pressure for which uplift just occurs in psi; for double acting air-steam hammers only).

EFFICY

STRM which is here the regular working stroke in inches.

RWH (for double acting hammers only).

ITYPH (here equal to 3.001, i.e. air-steam hammer).

(b) In addition to this data, hammer assembly information is necessary if its effect is to be studied:

AM(I) .... the assembly weights in kips for I = 1, MA.

STA(I) ... the assembly stiffnesses in kips/inch for I = 1, MA.

MA ..... the number of assembly stiffness values. Note that MA = 0 causes the assembly analysis to be ignored.

4.5 Other Hammer Related Input Information

This data is required (often at option) even if the program stored hammer information is used.

IOSTR .... (Ignored for air/steam hammers).

If set equal to 1 it will cause one stroke (either specified or unspecified) to be analyzed. Thus, no iteration

ClibPDF - www.fastio.com

on stroke will result. If equal to 1, the stroke specified in STROKE (see below) or the program assumed stroke (5.0 feet for open end and STRMAX for closed end hammers) is analyzed and iteration on maximum fuel pressure is performed.

If 0 (or not specified) then the maximum fuel pressure (P1, ..., P5 as specified by IFUEL) is used on all iterations on stroke.

Generally speaking, hammers that are operated at a fixed fuel setting should be analyzed with an iteration on stroke. There are hammers, however, (e.g. BSP) which do not have a fixed setting and which, therefore, should be analyzed by assuming a stroke iterating on fuel setting (combustion pressures).

The engineer must be aware that the fixed stroke option may provide unreasonable answers. For example, a stroke specified relatively high together with a low soil resistance may not be achieved in the field.

IFUEL .... (Ignored for air/steam hammers).

If set to 1, 2, ---, 5 the corresponding pressures P1, P2, ---, P5 will be used. Thus, IFUEL amounts to a fuel setting. If the corresponding pressure is zero P1 will be used; if P1 is zero 1000 psi is assumed.

IFUEL may or may not correspond physically to fuel settings

ClibPDF - www.fastio.com

at the hammer. Measurements of combustion pressures at reduced fuel settings are only available for a DELMAG D-30 Hammer. Using the results from this test as a guide proportional pressure reductions were determined for other hammers. Use of the IFUEL value should be restricted to parameter studies. In general, it is advisable to determine first the maximum stroke using IFUEL = 0 or 1. If it is necessary to limit stroke (e.g. stress limitations) then a fixed stroke (IOSTR = -1) analysis can be made for a similar stroke.

It is then, when hammers with variable fuel pumps are used, an easy task to adjust the fuel pressure in the field such that the analyzed stroke is actually obtained.

TDEL ..... Is the combustion delay in seconds. It overrides the value set in the diesel hammer data. If negative (hammers with fuel injection have only positive time delays since here TDEL is the delay after injection) preignition will result. As discussed earlier 0.00 to 0.002 seconds is reasonable.

STROKE ... For diesel hammers: Is a starting value for the ram stroke in feet if IOSTR = 0. It is the stroke analyzed for IOSTR = 1 or -1.

For air/steam hammers this value overrides the hammer information (both program or user supplied).

ClibPDF - www.fastio.com

EFFICY .... Overrides the efficiency supplied in the hammer information (applicable to all hammer types).

PSTEAM .... The actual air/steam pressure used. To be supplied for differential acting hammers only. If not given PSTEAM will be set to P1, i.e. the maximum value.

RWH ..... Overrides the hammer assembly weight supplied in the hammer information. Ignored for open end diesels or single acting air/steam hammers.

4.6 Driving Accessories

The term "Driving Accessories" refers to the capblock, the helmet and a possible pile cushion. There are a variety of such accessories available and standardization is hardly possible. The User's Manuäl contains data for a few frequently encountered systems.

In the case of no capblock the anvil stiffness will be doubled and an equal stiffness assumed between helmet and anvil. This assumption seems justified in light of the uncertainties involved in metal to metal impact. The data to be specified for the accessories is then:

HM(M+2).....Weight of cap (helmet plus capblock including any pile top adapter) in kips.

STH(M+1) ... Stiffness of capblock in kips per inch.

STH(M+2) ... Stiffness of pile cushion in kips per inch.

In addition to the weight and stiffness values, coefficients of restitution should be specified for all non-elastic materials and/or impact interfaces.

ClibPDF - www.fastio.com

Four values are required:

EANV ..... Coefficient of restitution (C.O.R.) of anvil in the case of diesels or that of the capblock for air/steam hammers.

ECAP ..... C.O.R. of capblock (diesel) or assembly (air/steam).

EPT ..... C.O.R. of pile top.

ECUS ..... C.O.R. of pile cushion.

Default (i.e. input not specified) results in all coefficients to be set to 0.85 with the exception that ECUS would be set to 1 if no cushion is present. The User's Manuel contains suggested values. Other recommendations are: for the anvil and for steel pile tops 0.85, for pile tops of concrete 0.7 and timber, 0.5. If a pile cushion is used with ECUS < 1 then greater EPT values should be chosen. Note: actually, EANV is a hammer property and should be stated with the hammer. However, since this value is hardly measurable and can only be judged by comparing analysis results with measurements, some flexibility is given here by providing the opportunity for change.

4.7 Pile

There are several options which govern the input of the pile properties. The two option parameters to be considered are:

NCROSS ... = 0 means uniform pile

>0 means non-uniform pile

and

IPEL ..... = 0 means automatic generation of pile segment parameters

ClibPDF - www.fastio.com

= 1 means automatic generation of pile segment parameters except that the relative element lengths (ALPH(I)) are to be specified.

= 2 means that all parameters are specified as input including the relative element lengths.

N, the number of pile elements to be analyzed must be given for IPEL > 0. (For IPEL = 0, N is determined for a segment length of approximately 5 feet).

For uniform piles (NCROSS = 0) the following data is sufficient:

XPT ..... the total pile length in feet

AP(1) .... the pile top cross sectional area in square inches

EP(1) .... the pile top elastic modulus in kips per square inch

WP(1) .... the pile top specific weight in pounds per cubic feet.

Material properties are contained in the User's Manual.

For non-uniform piles the cross section and the material values must be completely defined. As it is necessary for the computer to interpolate between neighboring defined cross section values this means that discontinuities (sudden changes) have to be defined with two equal depth values the first of which specifies the quantities above the change, and the second one, those below the change. Examples are given in the User's Manual. The program accepts up to nineteen (19) cross sectional values. These are:

XP(I) .... depth at which values are specified in feet

AP(I) .... cross sectional area in square inches at XP(I)

ClibPDF - www.fastio.com

EP(I) .... elastic modulus in kips per square inch at XP(I)

WP(I) .... specific weight in pounds per cubic foot at XP(I)

As a last set of values those of the pile bottom XP(I) = XPT must be given.

The extended input, i.e. the input of STP(I) (pile segment stiffness), PM(I) (pile segment weight) and ALPH(I) (relative segment length values) is described in the User's Manual. Computation of stiffnesses and weights should be done according to Equations 3-28 and 3-29. Note that RP = WP/G with G being the gravitational acceleration (32.2 ft/sec^2 or 9.81 m/sec^2).

Another input allows the specification of maximum tension force, SPLICE(I), in any one pile spring. Note that the pile top has a spring that cannot transmit tension. This means that SPLICE(1) is always set to zero. All other spring tension forces are set to -5000 kips. If at certain elements other values are requested then ISPL should be set to the number of springs involved and for each spring a pair of values:

J, SPLICE(J) ... element number, maximum tension force in kips (tension is negative) be specified.

SPLICE(I) can also be specified as a "slack" value in feet. Slack is a distance which a spring can extend without exhibiting any tension force. If SPLICE(I) is given between -0.5 and 0.0 then it is assumed to indicate a slack. More information regarding this input can be found in the User's Manual.

Finally, the pile material damping parameter IBEDAM (IBD in Section 3.3) should be specified if values greater than 1 (1% of critical) are desired.

ClibPDF - www.fastio.com

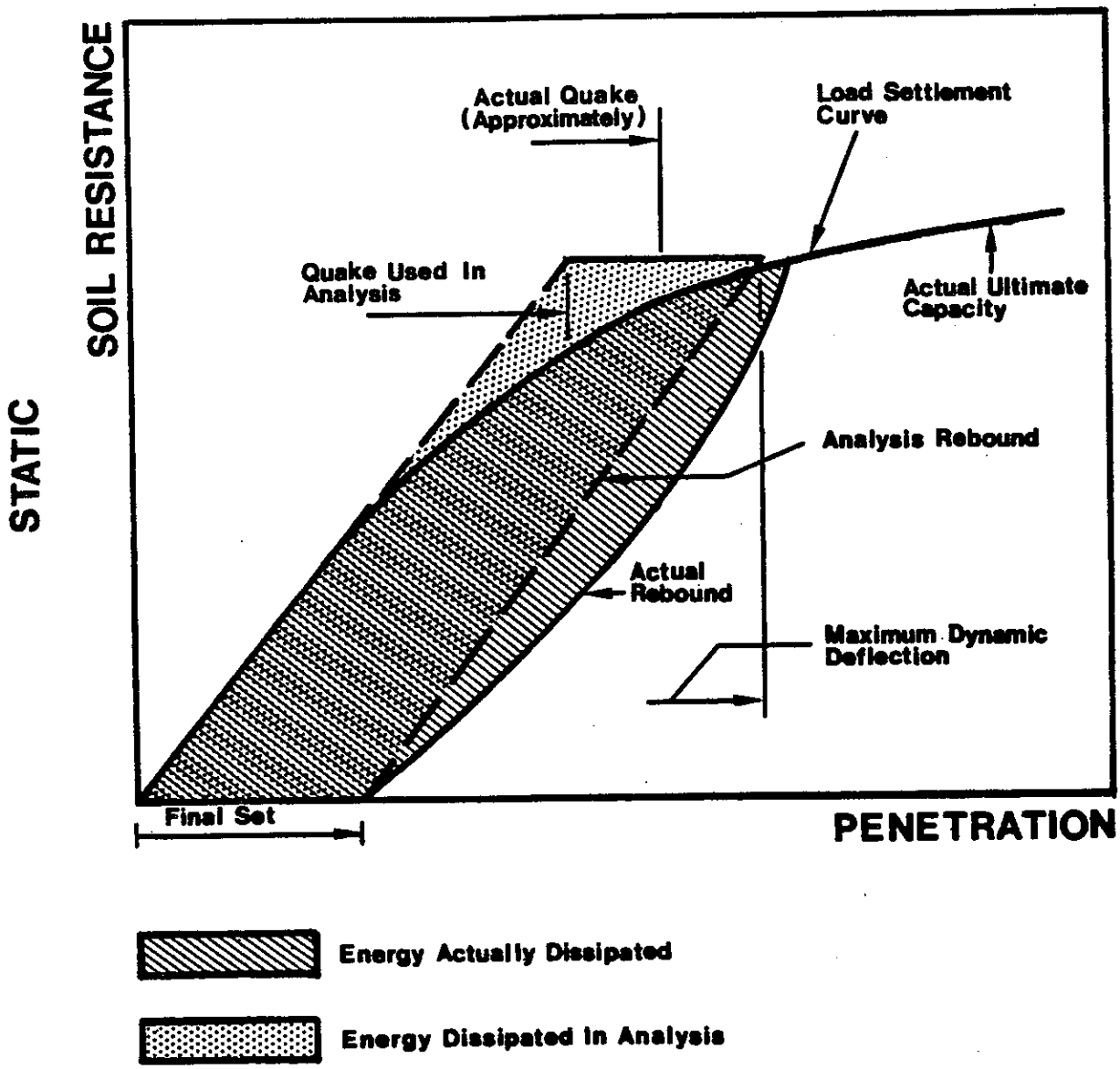

FIGURE 4-1: REAL LOAD DEFLECTION CURVE AND ITS MODEL. IN A CORRECT ANALYSIS QUAKES SMALLER THAN REAL MUST BE USED.

ClibPDF - www.fastio.com

4.8 Soil

Soil data consists of:

quakes,

damping values,

ultimate resistance (optional),

coefficient of restitution of soil and resistance distribution.

Required values are:

QS(1) ... quake at skin in inches (default: 0.1 inches)

QS(N+1).. quake at pile bottom (default: 0.1 inches)

Quakes values were proposed in the literature between 0.1 and 0.5 inches (7). They are usually based on static load test evaluations. However, it should be noted that the assumed elasto-plastic soil resistance law is only an approximation and should allow the pile to obtain a permanent set under a realistic energy consumption (see Figure 4-1 for an example of a reasonable approximation). The questions arising from these approximations together with those of the damping model are the most serious ones with regard to wave equation applications.

Because of these questions it seems unreasonable to use the static quake values as proposed by Coyle etal. (7). It is more likely that values between 0.05 and 0.15 inches give satisfactory results. Note that extremely small values may cause numerical problems.

Damping values impose an even greater problem than quakes because they affect the blow count result to a much larger degree. Recommendations

ClibPDF - www.fastio.com

are given in the User's Manual. Smith's damping values were relatively well proven during several years of use. It is for this reason that Smith's damping should be used whenever no experience with Case Damping exists.

The required damping values are:

SJ(1) .... skin damping constant in s/ft for Smith (ISMITH = 1) damping and dimensionless for Case damping.

SJ(N+1) .. toe damping constant with dimensions as before.

As for pile quantities, all soil parameters QS(I), SJ(I) and SU(I) can be specified for <u>each</u> segment in order to override the automatic conditions. The values are read when the ITYS value is negative.

The total ultimate static resistance value can be specified in three ways:

(a) RULT > 0 in tons leads to the analysis for the one RULT value specified.

(b) RULT = 0 (or blank) causes the computer to determine ultimate resistance values based on the pile impedance (EA/c) and an assumed fraction of impact velocity. There will be at most ten (10) analyses performed. If a blow count has exceeded 1200 blows/foot (100 blows/inch - 40 blows/cm) then the analysis will be halted and the results printed.

(c) RULT < 0 will cause a set of ultimate resistance values (at most 10) to be read and analyzed. These values should be given in an increasing order as the starting values of the

ClibPDF - www.fastio.com

stroke are based on this assumption. Also, the termination condition of (b) hold, again assuming an increasing order of the RULT values.

ESOIL ... is the coefficient of restitution of the soil (default 1.0). If the stroke does not converge for reason of too little energy consumption by the soil (a condition that becomes an unfortunate reality in some cases) then a lower value might be tried. However, values lower than one-half (0.5) cannot be recommended.

The distribution of resistance foces, SU(I) can either be taken from a list of ten (10) types which are built into the program (ITYS) or, if this value is 0 or blank, it should be specified as a series of depth and relative magnitude values:

XP(I), DIS(I) ... I-th depth in feet and I-th magnitude (non-dimensional). As in the case of the pile description, discontinuities in the distribution have to be described with two identical XP(I) values. The last XP(I) value must be equal to the pile length, the first one equal to zero.

The proportion of skin to total resistance has to be specified by IPERCS ... the percentage of skin friction of total RULT. This value can also be specified as a negative number. In this case the skin friction force will be determined from the first RULT value (-IPERCS (RULT)) and will be kept at the same level for further RULT analysis. This means that only a gain of toe bearing is assumed.

4.9 Other Program Options

Other input parameters not yet described must be specified in order to

ClibPDF - www.fastio.com

obtain the desired

(a) Output type and quantity

(b) Analysis type

Output type can be obtained in printed and plotted form. Basically, the higher the IOUT (card 2.000) parameter is specified, the more output is obtained. The IOUT = 0 option causes minimum output which is recommended if more than one RULT value is analyzed (typical production run). IOUT > 9 causes plots to be produced. The use of these options as well as the more extensive print is discussed in detail in the User's Manual.

It should be noted that the program performs several analyses for one RULT value. For this reason all output quantities have to be temporarily stored until it is known that the stroke or maximum combustion pressure has converged. In order to keep the program small enough for implementation on a variety of computers, the output must be limited to certain types (forces or velocities etc.) and to a maximum number of values (number of pile segments, number of time increments).

The magnitude of the time increments has to be chosen less than critical. This critical time increment is the minimum of

$$DTCR = \sqrt{PM(I)/STP(I)} \qquad (4\text{-}1)$$

for all I, or it is the time that the stress wave needs to travel through the shortest element IM

$$DTCR = ALPH(IM)\ (XPT)/c \qquad (4\text{-}2)$$

ClibPDF - www.fastio.com

(if only one material is considered) and the actual time increment either for hammer or pile has to be

$$DT \leq DTCR \tag{4-3}$$

In order to accomplish this a percentage value IPHI (%) can be specified which is defined as

$$IPHI = (DTCR/DT)100 \tag{4-4}$$

This IPHI should be always greater or equal to 100. Default or if IPHI was accidentally set to less than 100 results in IPHI = 140 for diesel and 160 for air/steam hammers. It is reasonable to specify IPHI as large as 200. It should be mentioned here that the program involves checks on DTCR which go beyond Equations 4-1 or 4-2. These checks include the magnitude of damping and static soil resistance.

ClibPDF - www.fastio.com

CHAPTER 5

PROGRAM FLOW

Only a small part of the program is actually a wave equation program. It consists of approximately one-third each input and output coding, one-sixth dynamic analysis and the other sixth, in the case of diesel hammers, of "pseudo-dynamic" and simplified dynamic analyses and general control.

By pseudo-dynamic analysis is meant that the total system is not strictly analyzed. This can be done for the rebound portion once the ram has risen a sufficient distance from the impact block. A simplified dynamic analysis is also used for the precompression period.

The following steps are performed by the program for the open end hammer, standard run,(i.e. fixed fuel, variable stroke).

(a) Read input information

(b) Assemble hammer data

(c) Determine pile segment parameters

(d) Determine soil model parameters

(e) Find stroke (either input or assumed)

(f) Determine ram velocity at exhaust ports

(g) Find initial values just before impact using a simplified dynamic analysis.

(h) Perform a wave analysis until pile rebounds and ram has risen sufficiently.

(i) Find velocity (and therefore stroke) at exhaust ports

ClibPDF - www.fastio.com

(j) For a stroke which is less than 10% different from the assumed one repeat process (h) using the new stroke and modified initial values; for greater differences go to (g). If the stroke was within 5% of the assumed value, print and plot the required output and continue with (h).

(k) If a new ultimate resistance value is to be analyzed, determine new stroke based on previous one and continue at (f).

As an alternative (fixed stroke, variable fuel) step (j) is modified in the following manner: For a rebound stroke that is more than 5% (3% for closed end hammer) different from the assumed stroke the maximum combustion pressure value is changed and the process is continued at step (h). Of course, in step (k) no new stroke is assumed. A block diagram indicating the program flow is shown in Figure 5-1.

The steps taken for the closed end hammer (standard run) differ somewhat from those just discussed. Because of the limitations on the stroke in a closed end hammer and since the throttle setting is reduced when uplift occurs, the process is directed such that, if no other stroke is specified, the maximum stroke (Equations 15 or 20) is used for a first analysis together with the maximum fuel setting. If the soil resistance is relatively small, then a rebound stroke will result. In this case iteration is performed on stroke. For higher rebound strokes uplift would occur and, therefore, the fuel setting has to be reduced. Since the question of fuel con-

ClibPDF - www.fastio.com

ClibPDF - www.fastio.com

Block Diagram Of Program Flow

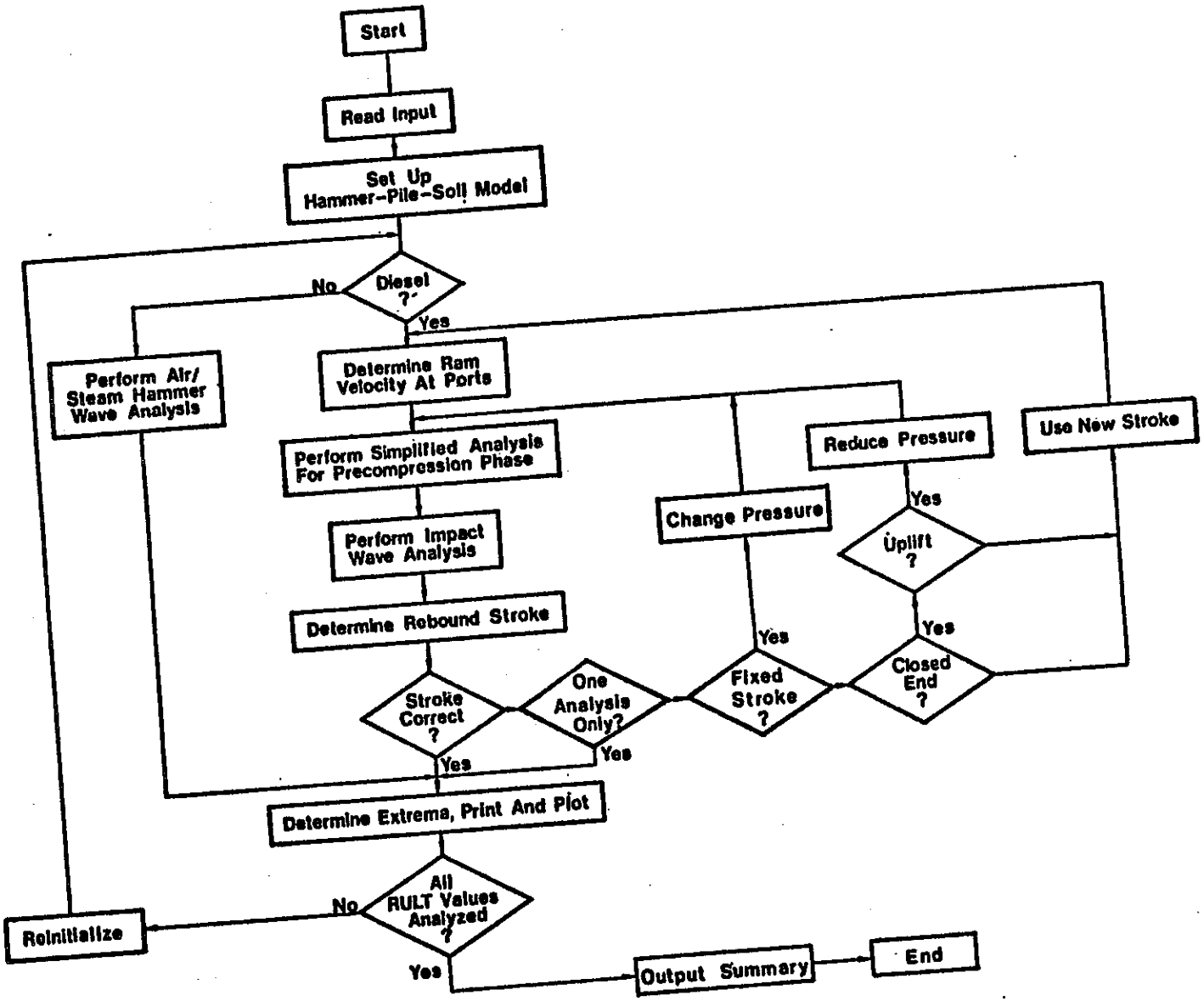

FIGURE 5-1: BLOCK DIAGRAM OF PROGRAM FLOW

sumption is not of importance and since the injection pumps usually employ continuous rather than discrete settings, an arbitrary reduction of 10% of maximum combustion pressure is used. This process is also repeated iteratively.

For closed end hammers (standard run) the program control always causes a decrease in hammer energy supplied and an increase in blow count. In one case this occurs due to a reduced effectiveness of the hammer blow (smaller impact velocity) and in the other case due to a reduced combustion pressure. As the latter effect is probably relatively small, the step size of 10% in pressure reduction seems to be sufficiently accurate.

In the open end program, iterating on stroke, the initial value for stroke is either as given by the user or taken as five feet. If a second RULT (ultimate resistance) value is used (greater than the previous one), then a stroke 20% higher than the previous result is tried. For a third or further RULT value, an extrapolation over the earlier strokes is employed. If the iterations are done on combustion pressure then the pressure from the previous analysis is starting value for the new RULT value.

A similar process is used for the closed end program except in a case where the previous result was the maximum stroke at a reduced fuel setting. In this case the maximum stroke is again assumed together with a throttle setting that is increased by one step. It should be noted that the program thereafter <u>does not increase fuel settings</u>. Thus, RULT values specified in decreasing order could lead to erroneous results.

ClibPDF - www.fastio.com

The program flow of the air/steam hammer analysis is straight forward. Initial values need not to be determined and the stroke is assumed fixed. A greater energy output for higher soil resistance values has been observed, but no attempt was made here to include the effect of variable stroke.

ClibPDF - www.fastio.com

CHAPTER 6

PROGRAM PERFORMANCE

6.1 Introduction

Both the program and the hammer data were extensively tested against measurements. Measurements consisted of pile-top force and velocity and, in two cases, combustion-chamber pressure records. In addition, blow count and stroke were recorded in many cases. The program testing often proved to be difficult since all of the relevant information was not always available. The information required consisted of three different groups.

(1) Driving system data (helmet weight, capblock and cushion stiffness plus all four coefficients of restitution). While the helmet weight was usually accurately known, stiffnesses and coefficients of restitution were either guessed or chosen from a large range of possible values.

(2) Thermodynamic data (combustion delay, combustion pressure, expansion coefficient). The combustion delay was fixed at two milliseconds for all hammers with regular fuel injection. It was determined for atomized injection by parameter studies. Combustion pressures were measured in some cases and determined from stroke and/or force measurements in other cases. In order to do this properly, the expansion coefficient was fixed at 1.3.

(3) Soil data (skin and toe quake, skin and toe damping and the distribution of the resistance forces). The quakes were mostly chosen at 0.1 inches. However, there were a few exceptional cases where larger values had to be chosen to achieve satisfactory agreement between computed and measured

ClibPDF - www.fastio.com

values. Damping values were difficult to determine in that they directly affected the stroke and, therefore, the pile top stress and velocity at impact and the blow count. The distribution of the resistance forces affected the shape of force and velocity curves.

Counting the resistance distribution as only one unknown (although it involves all elements) the above list indicates that often as many as 14 different parameters had to be determined for each test case.

Parameter studies performed by the TTI researchers (6) were basically aimed at matching the predicted with the observed blow count. In the current study, however, the attempt was also made to match force, velocity, pressure and stroke. The parameters given in the literature were often found to be insufficient. The current results shed some light on the quality of the predictions of pile force as well as blow count that may be achieved. Since the information regarding hammer performance in the field was often limited, the answers obtained give an idea of the accuracy which can be expected when the program is used. Thus, the comparisons discussed below can be regarded as an assessment of expected program performance. Many of the problems which have been reported for wave equation programs may be partially the result of excessive expectations.

6.2 Data Selection

A vast amount of dynamic and static data was gathered during the course of the Case Western Reserve University piling research projects. In addition, the consulting activity of the authors and the work of other agencies which

ClibPDF - www.fastio.com

also use the Case Method of pile testing have contributed to the data that was available for pile testing.

The results of 16 different pile analyses are presented in this report. The attempt was made to cover a large number of different hammers and pile types. Names of test piles, references and other basic information are given in Table 1.

There are a relatively large number of DELMAG hammers among the hammer types tested. The reason is that a substantial amount of testing, including combustion pressure and stroke measurements, was conducted on these hammers. Stroke is an especially important quantity in this work and it must be emphasized in program testing.

Only one concrete pile is represented in the data. No timber pile data was included. Both concrete and timber introduce additional uncertainties into the evaluation of the program, mainly because of the unknown conditions at the pile top (pile cushion of conrete piles and pile top quality of timber piles).

6.3 Representation of Results

Figures 6-1 through 6-16 contain comparisons of computed with measured forces, velocities and combustion pressures all as a function of time. Velocity comparisons of this kind are certainly a first in Wave Equation test runs, and the large amount of force vs. time curve comparisons is unequalled. For plotting, the curves were shifted in time such that the impact time was in agreement. In addition, the measured forces were shifted vertically such

ClibPDF - www.fastio.com

TABLE 1: DESCRIPTION OF TEST DATA

Pile No.	Name	Source	Type	Length feet	Hammer	Type
1	FEC 72	C[1]	HBP	40	Delmag D12	OED
2	FEC 72	C	HBP	75	Delmag D12	OED
3	FEC 75	C	HBP	40	Delmag D12	OED
4	Purdue	(10)[2]	HBP	50	Delmag D12	OED
5	DTP 3	(11)	18x18 PC	60	Delmag D22	OED
6	FEC 71	C	HBP	70	Delmag D30	OED
7	Bismark	C	HBP	160	Kobe K22	OED
8	GRTP1	C	HBP	60	Kobe K22	OED
9	K25 VP	(12)	HBP	30	Kobe K25	OED
10	Georgia	(15)	Pipe	40	MKT DE30	OED
11	B-N	S[3]	HBP	119	MKT DA35B	CED
12	CR 4	(13)	Pipe	90	LB 440	CED
13	DTP 33	C	Pipe	41	LB 660	CED
14	Phila 78	(14)	Pipe	43	Vulcan 01	A/S
15	VO8VP	(12)	HBP	30	Vulcan 08	A/S
16	VO8VP	(12)	HBP	30	Vulcan 08	A/S
17	LaVO16	S[4]	Pipe	200	Vulcan 016	A/S

[1]Records from author's consulting practice.
[2]Numbers in parentheses pertain to references at end of text.
[3]Special records, were obtained from New York Department of Transportation
[4]Special records, were obtained from Soil Exploration Company.

ClibPDF - www.fastio.com

that the computed and measured precompression forces agreed. This shift was necessary since the precompression force was often subtracted from the measured force curves because of its static nature.

Almost all figures contain two time scales, milliseconds and L/c units. The L/c units are often helpful in recognizing characteristic effects in the stress waves. One figure (6-16) is also included which shows the automatically plotted three dimensional representation of force vs. pile length and time. These plots are instructive where wave propagation considerations are concerned but of less use in the program testing effort.

The figures always show that portion of the record that was analyzed by the accurate analysis portion (excluding the simplified precompression and expansion phases). This produces plots which are spread over time such that the higher frequency components of the curves become apparent.

6.4 Results

Table 2 contains both observed and computed values of the program results, RULT (total static pile bearing capacity) in tons, blow count in blows per foot and stroke (or an equivalent quantity for closed end hammers). In fact, RULT was determined using either the Case Method (1), the CAse Pile Wave Analysis Program (1), or a static load test. Unfortunately, the static load test was usually not performed when stroke measurements were taken. However, it is felt that so many test cases were solved that sufficient confidence in the program is obtained.

ClibPDF - www.fastio.com

TABLE 2: COMPARISON OF COMPUTED WITH OBSERVED QUANTITIES FOR TESTED DATA

Pile No.	Bearing Capacity tons	Measured Blow Count bl/ft	Measured Stroke ft	Predicted Blow Count bl/ft	Predicted Stroke ft
1	16[C]	6	4.0±.2	9	4.0
2	70[A]	27	6.0±.3	28	5.6
3	60[C]	24	5.4±.1	26	5.4
4	83[L]	40	5.5±.1	36	5.6
5	10[A]	12	4.0±.1	8	4.1
6	125[A]	N/A	N/A	21	5.5
7	200[L]	500	7 (1 plug)	102(150)	6.6(5.5[P])
8	120[A]	41	6 (1 plug)	37	5.5[P]
9	300[C]	120	8.0±.3	151	8.0
10	130[L]	107	N/A	114	8.7
11	31[A]	25	N/A	19	4.0
12	180[L]	R*	Maximum	R	Maximum
13	350[A]	R	Maximum	R	Maximum
14	75[L]	43	Normal	44	—
15	8[L]	6	Normal	7	—
16	260[C]	184	Normal	R	—
17	275[A]	55	Normal	50	—

[P]Using Preignition and reduced fuel pressure

[C]Case Method

[A]CAPWAP Analysis

[L]Load Test

*Refusal ... no noticeable set

ClibPDF - www.fastio.com

Pile No. 1

This pile was driven for a hammer performance test. Combustion chamber pressures and stroke were measured in addition to both pile top acceleration and force. Using the Case Method static capacity prediction as the RULT value a WEAP run was made. The resulting pile top force and combustion pressure are shown together with the measured quantities in Figure 6-1. Maximum force is underpredicted by about 8%. The curve behavior follows the measured curve closedly except that it is somewhat smoother. It should be mentioned that the record portion after time 2L/c after impact is mainly governed by the soil model and is only, to a smaller degree, influenced by the hammer model.

The pressure curves show basically the same behavior except that the measured one is somewhat higher in the beginning and lower later on. Note, however, that the plot is a pressure vs. time plot and that minute changes in ram position appreciably alter the pressure behavior. Since the stroke was determined correctly one can consider the overall pressure behavior to be sufficiently accurate. The force effect on the pile from pressure differences is rather small (100 psi pressure correspond to about 10 kips force).

Pile No. 2

This pile was tested under similar conditions to Pile No. 1. The difference was that a heavy plate was added at the toe. This additional mass accounts for the third force peak (Figure 6-2). This force curve was very well predicted by the program. (Better than 5% agreement for the maximum).

ClibPDF - www.fastio.com

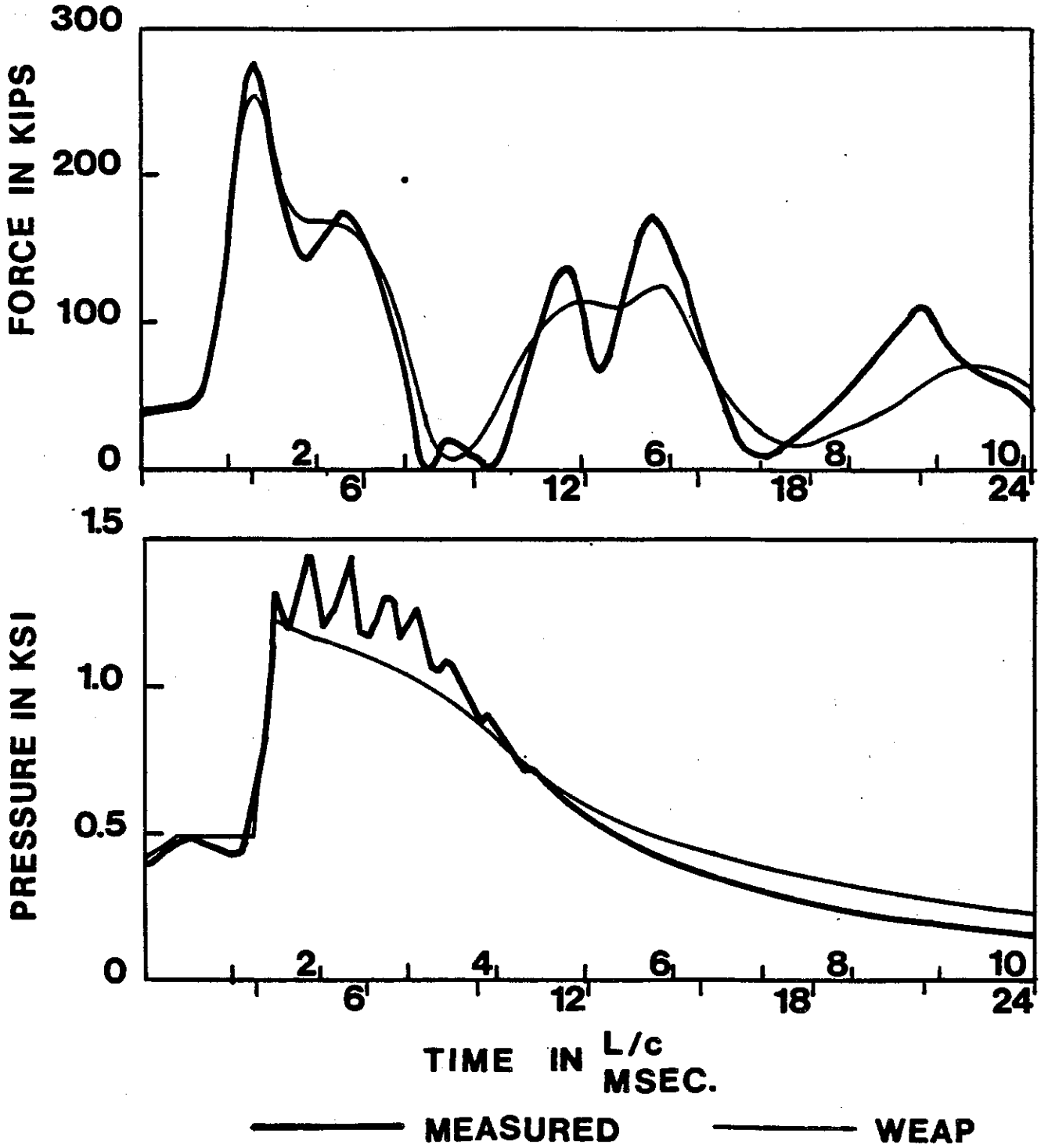

FIGURE 6-1: COMPARISON OF PREDICTED WITH MEASURED PILE TOP FORCES AND COMBUSTION PRESSURES FOR PILE NO.1.

ClibPDF - www.fastio.com

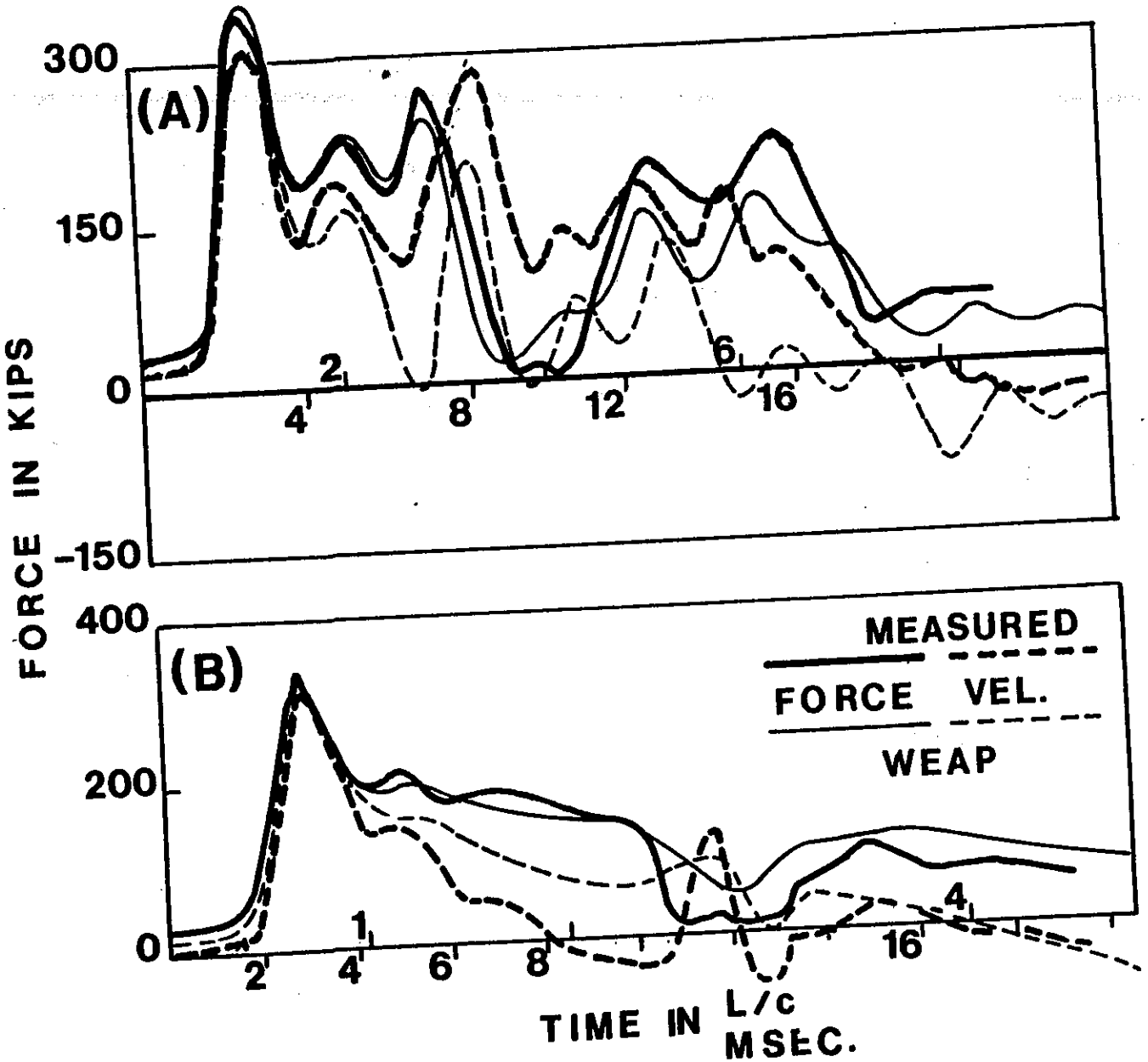

FIGURE 6.-2: COMPARISON OF PREDICTED WITH MEASURED PILE TOP FORCE AND VELOCITY FOR (A) PILE NO. 2 AND (B) PILE NO. 3

ClibPDF - www.fastio.com

The velocity curve (note that velocity curves are plotted after multiplication by the proportionality factor EP(AP)/c) however, though similar in character, deviates before time 2L/c after impact. This deviation is not considered critical since the blow count was determined rather accurately. Also, the calculated stroke was found to be in good agreement with the measured one.

Pile No. 3

This pile was an extension of Pile No. 1. Again force, (Figure 6-2b) stroke and blow count agreement is very good. It is interesting to note that the force shows a rather smooth behavior while the velocity displays a peak at the time of the wave return (10 milliseconds). The maximum force predicted showed an agreement within 5%.

Pile No. 4

Another well-controlled hammer test was performed on the campus of Purdue University on the occasion of the ASCE Specialty Conference in 1972 (see Reference 10). The force and velocity match of Figure 6-3 is quite good (especially at the time of wave return). The maximum force was overpredicted by 11% and the blow count was underpredicted (36 vs. 40 measured). It may be that a force transducer reduced the force peak to some degree. This transducer was inserted between hammer and pile top and utilized steel plates at top and bottom for attachment. The weight of these plates was not modeled and the additional contact area was not considered in the analysis.

ClibPDF - www.fastio.com

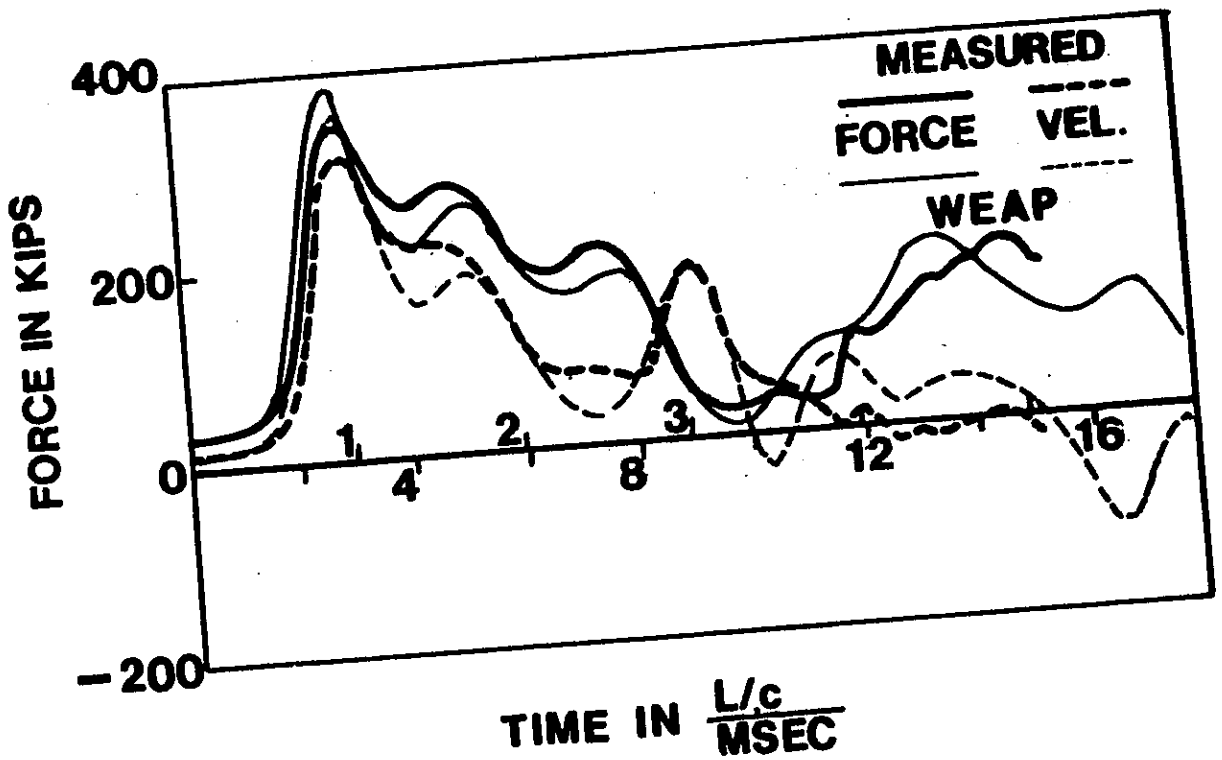

FIGURE 6-3: FORCE AND VELOCITY MATCH FOR PILE NO. 4 (PURDUE)

ClibPDF - www.fastio.com

Under these circumstances the results cannot be expected to be extremely accurate.

Pile No. 5

This pile was of concrete and was tested within a special research project of Case Western Reserve University (11). In order to evaluate whether or not the "easy driving case" can be modeled correctly, an early record was selected with a resistance approximately equal the hammer plus pile weight. This case represents the worst condition regarding tensile stresses. Figure 6-4 shows a very good agreement for the force (8%) considering the uncertainties of cushion properties. The measured velocity shows a higher peak at the time of the wave return which is, perhaps, due to an improper damping assumption. However, for soil resistance values as low as the one used here, a much better agreement seems to be a matter of luck.

Pile No. 6

Another special hammer performance test, this time a DELMAG D-30 hammer, was used for comparison. As can be seen in Figure 6-5 all quantities agree very well, with a maximum force difference that is negligibly small. The computed pressures are somewhat low but for the reasons given for Pile No. 1. These differences are of relatively little concern.

ClibPDF - www.fastio.com

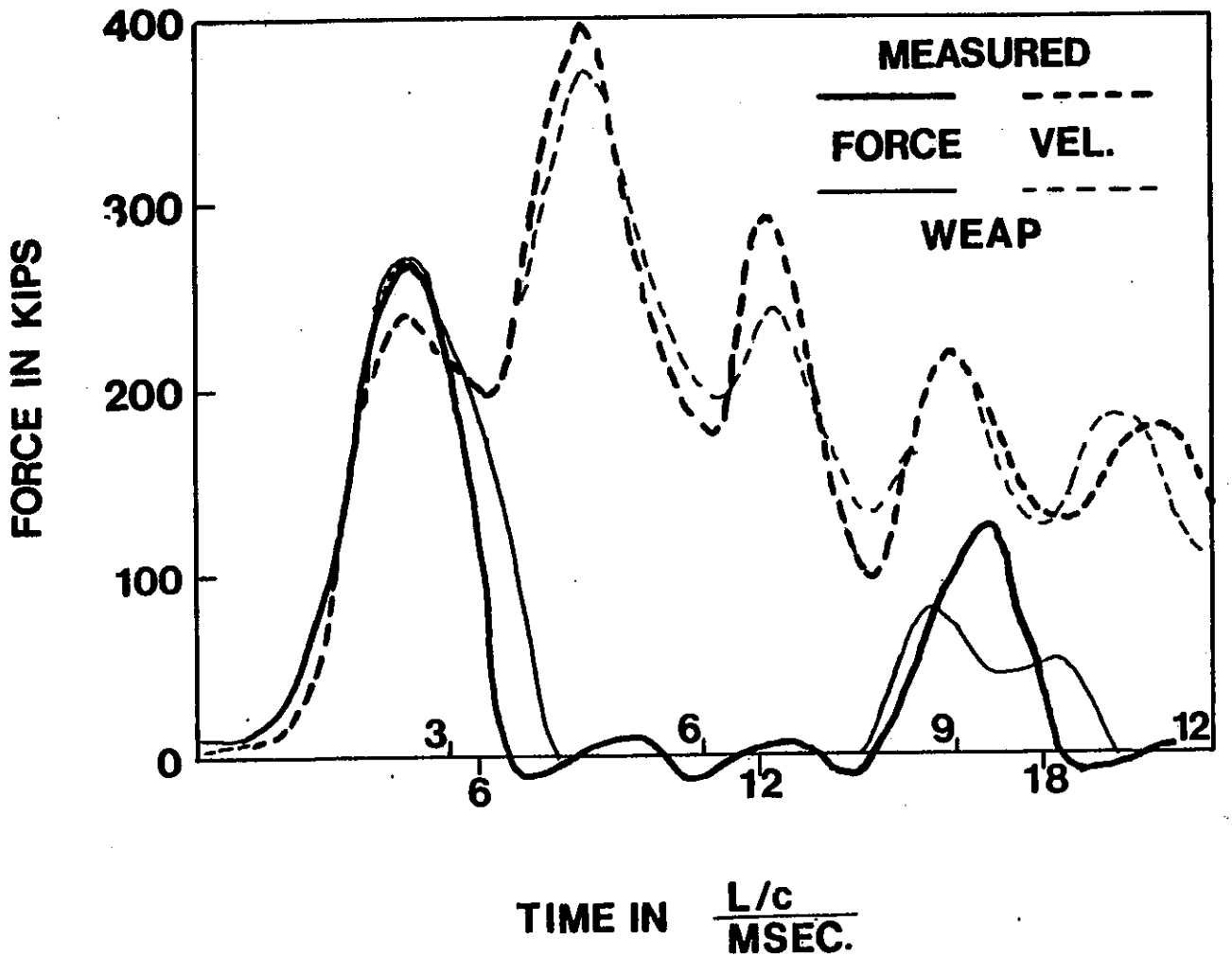

FIGURE 6-4: FORCE AND VELOCITY MATCH FOR PILE NO. 5
(MIAMI DTP 3)

ClibPDF - www.fastio.com

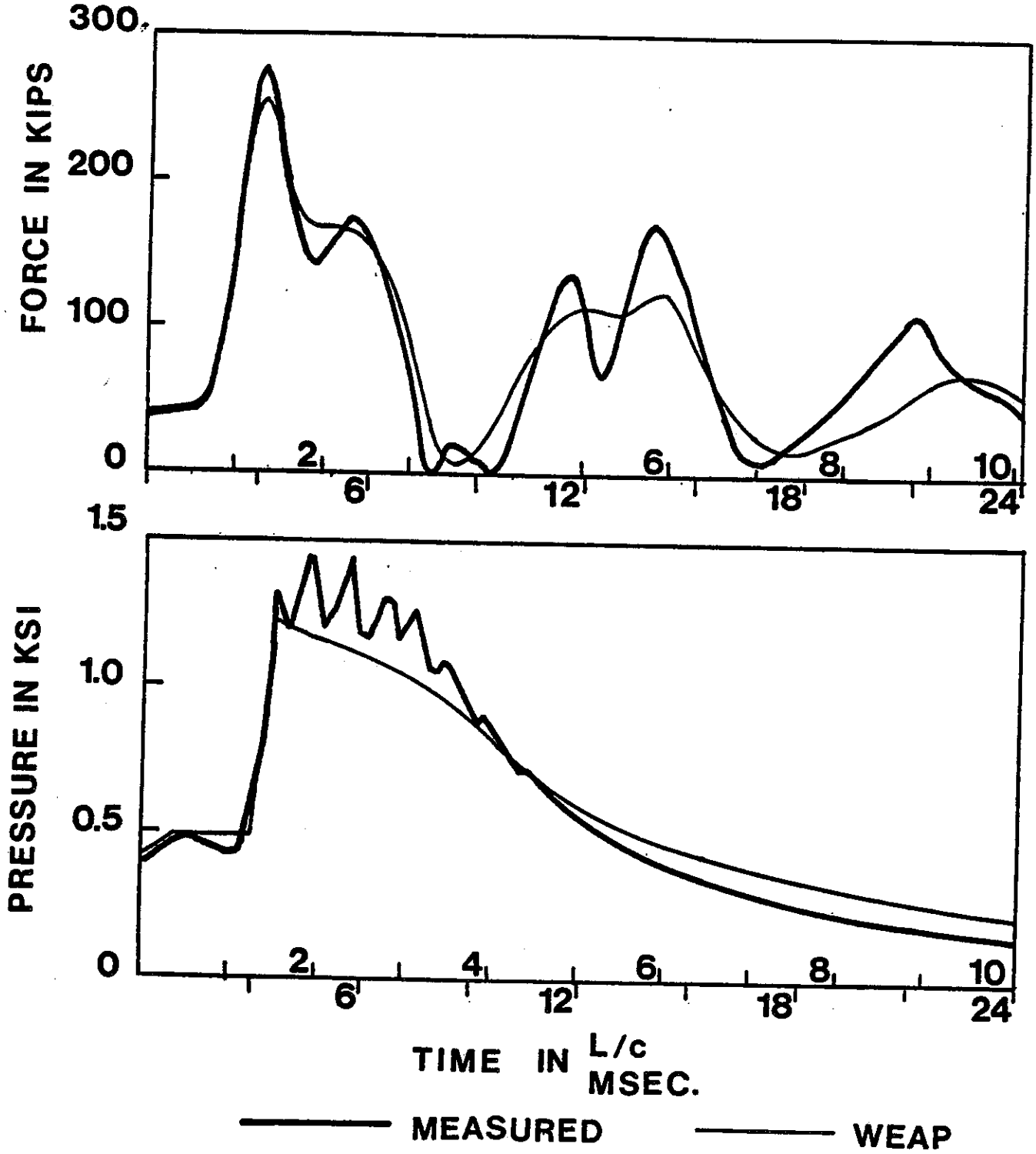

FIGURE 6-5: FORCE, VELOCITY AND PRESSURE MATCH FOR PILE NO. 6

ClibPDF - www.fastio.com

Pile No. 7

This case was selected for two reasons. First, it was a pile driven by a Kobe K22 hammer and second, an exhaust plug was installed into the hammer in order to increase the stroke. The plug produces slower exhausting and, therefore, adds to the pressure in the cylinder after the ram has cleared the ports.

The results shown in Figure 6-6a were produced by a "regular" analysis, i.e. assuming normal hammer performance. It can be seen that the stroke was slightly underpredicted while the force was too high by 18%. Also, the blow count was much smaller than recorded (102 vs. approximately 500). It can also be observed that the measured force increased during impact at a much lower rate.

It was concluded that the hammer both preignited and had a reduced combustion pressure due to poor scavenging. Reanalyzing with a time delay of -0.001 (1 millisecond preignition) and reduced fuel setting (IFUEL = 3) produced the force match of Figure 6-6b. This match is vastly improved and so is the blow count. Since the condition of a plug in the ports cannot be modeled by the program, it is not surprising that the stroke was now smaller than observed (5.5 feet). It can be argued that the effective stroke was indeed about 5.5 feet which indicates a hammer efficiency of 79%.

It is interesting to note that a second plug increased the actual stroke by another 1.5 feet.

ClibPDF - www.fastio.com

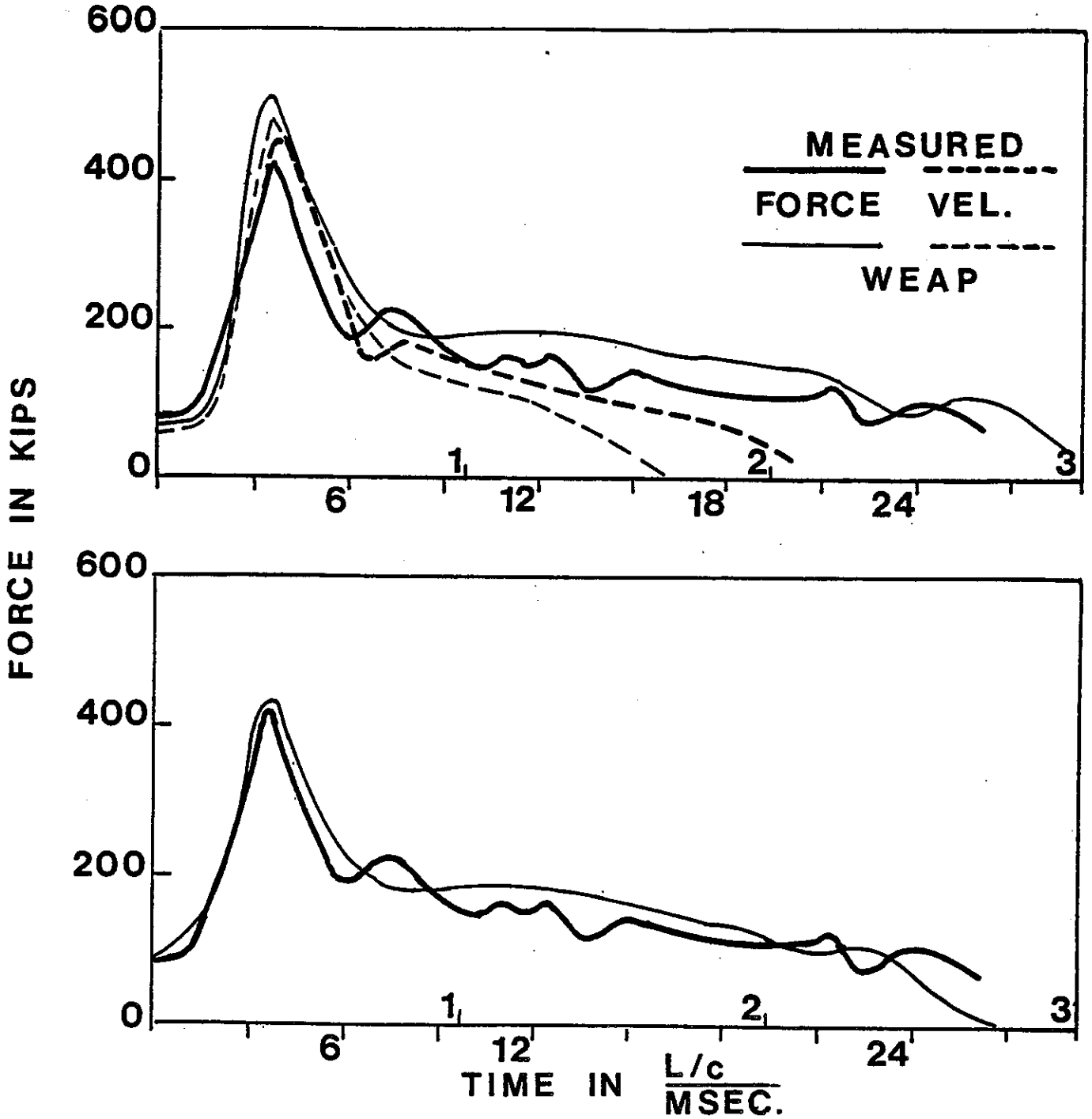

FIGURE 6-6: FORCE AND VELOCITY MATCH FOR PILE NO. 7
(A) NORMAL PROGRAM PERFORMANCE, (B)
USING PREIGNITION AND REDUCED FUEL SETTING

ClibPDF - www.fastio.com

Pile No. 8

The data on this pile was used for testing to check a second time on the performance of the K22 with one exhaust port plugged. Using practically the same assumptions as for Pile No. 6 the match of Figure 6-7 was obtained.

The match shows a 9% overprediction in force and a deviation in behavior after the wave returns. Note that the velocity did correlate very well at impact. The later deviation in force and velocity is probably due to an incorrect soil quake (the full resistance acts too early). However, in light of the assumptions necessary to model this hammer, the agreement can be considered sufficient.

Pile No. 9

The match of force and velocity shown in Figure 6-8 was obtained for an H pile driven by a Kobe K25 hammer to rock. Agreement is very good considering that yielding occurred and the pile actually buckled at the pile top.

The measured forces appear to be higher by 17%. However, since strains in the pile were measured, these forces were actually lower and should not have been computed by using a constant elastic modulus throughout the record. The program properly determined that yielding occurred. Blow count and stroke results are very good.

ClibPDF - www.fastio.com

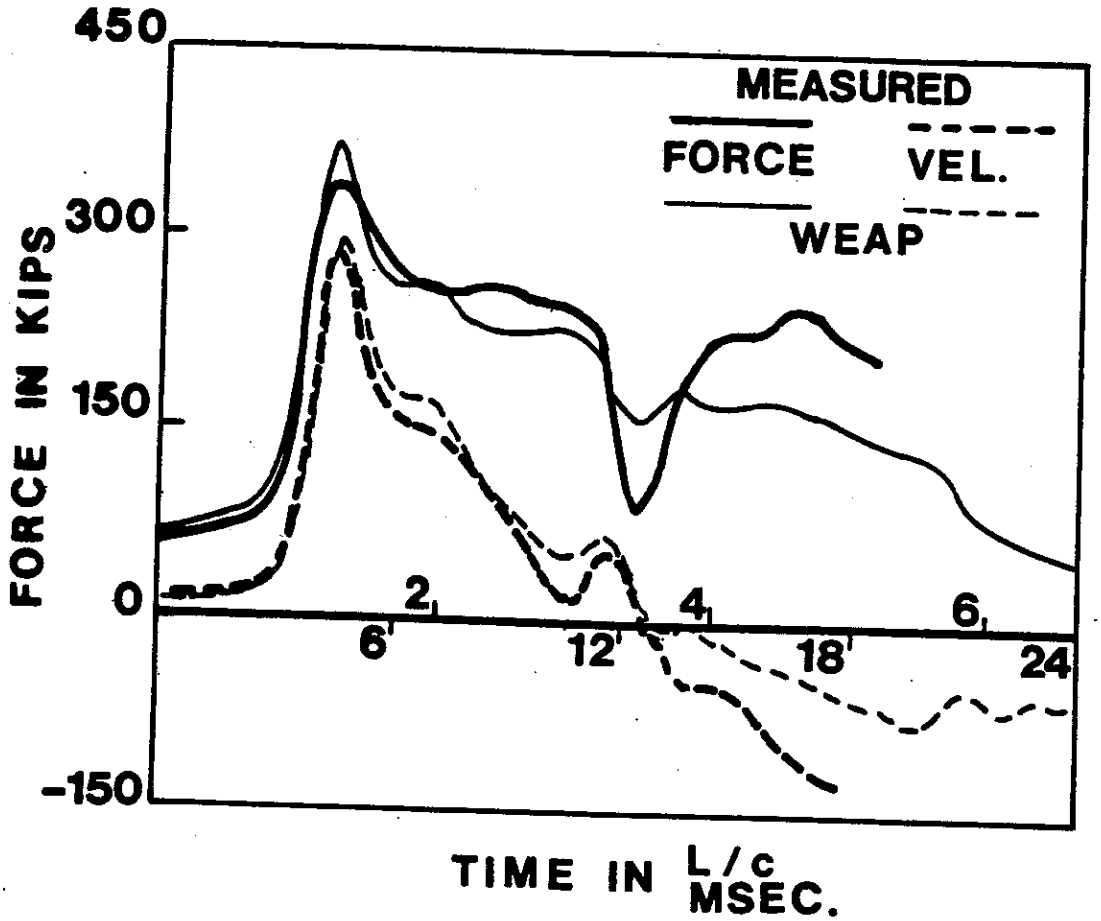

FIGURE 6-7: FORCE AND VELOCITY MATCH FOR PILE NO. 8 USING PREIGNITION AND REDUCED FUEL SETTING

ClibPDF - www.fastio.com

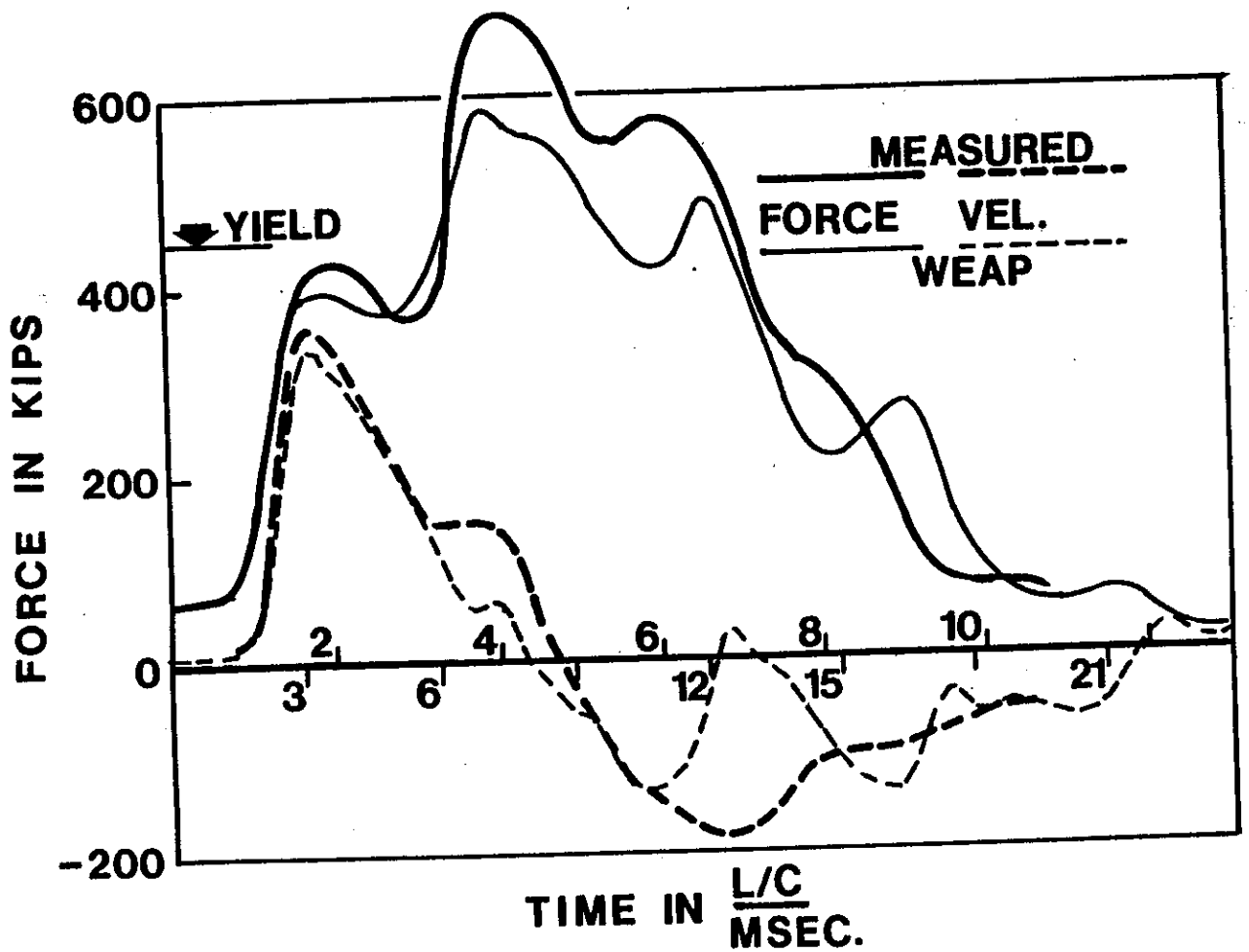

FIGURE 6-8: FORCE AND VELOCITY MATCH FOR PILE NO. 9

ClibPDF - www.fastio.com

Pile No. 10

This pile was driven and tested as a part of the Case Western Reserve University research project (15). It was selected for analysis because it represented an open end MKT hammer (DE30). Although stroke measurements were not undertaken, it is felt that the results indicate a good agreement (blow count 114 predicted vs. 130 measured).

Figure 6-9 shows the match. The maximum force value was determined very accurately. The deviation of force after the impact peak must be due to some resistance near the top since it does not have an equivalent in the velocity curve.

The velocity match is poor at the time of wave return in a manner similarly observed for earlier piles (e.g. No's 3 and 4). This effect is not fully understood and strangely enough, it only occurs if the force valley at time 2L/c after impact is properly matched (Figure 6-6). The authors believe that this high velocity return is due to an improper model of the soil below the pile tip. This problem of a proper soil model has not been solved and should receive attention in further research activities.

Pile No. 11

The measurements on this pile were obtained by the New York Department of Transportation and are the only ones available for a closed end MKT hammer. The match shown in Figure 6-10 is good with regard to both impact and the time of wave return. Between these two times, however, the predicted force and velocity are both higher than measured. This error may

ClibPDF - www.fastio.com

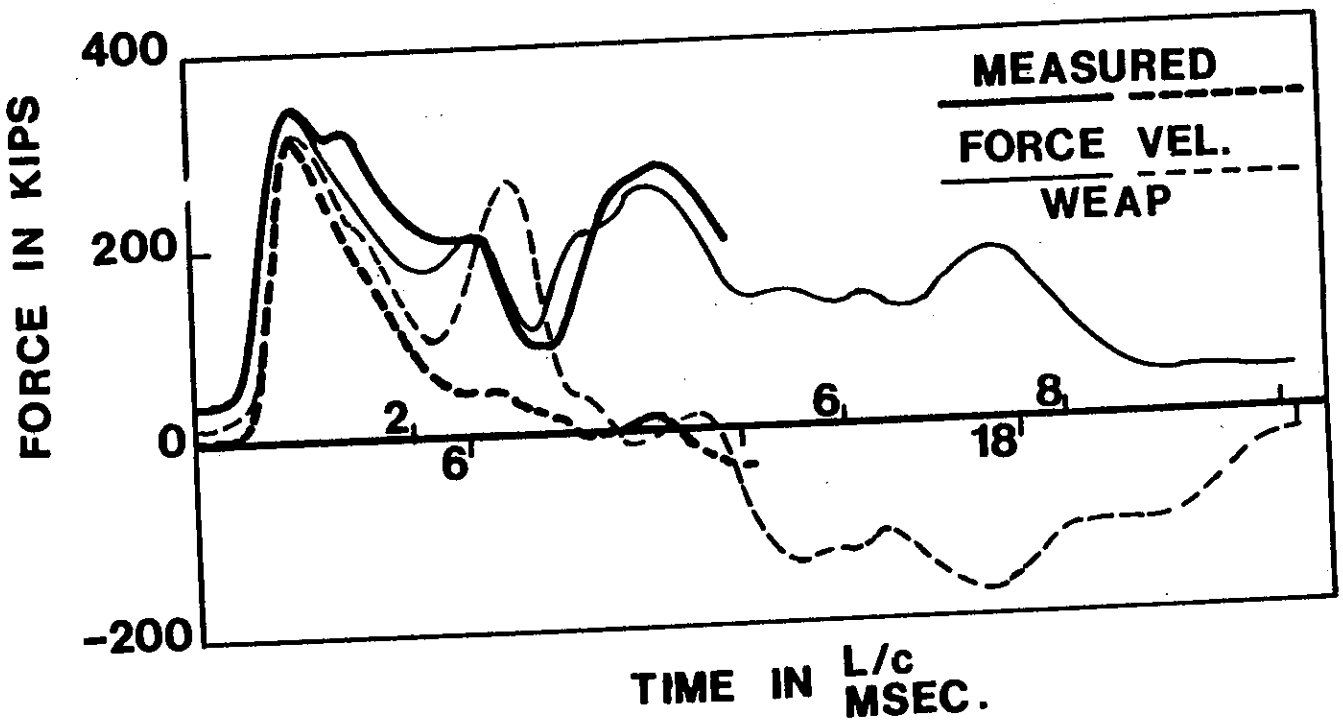

FIGURE 6-9: FORCE AND VELOCITY MATCH FOR PILE NO. 10 (GEORGIA)

ClibPDF - www.fastio.com

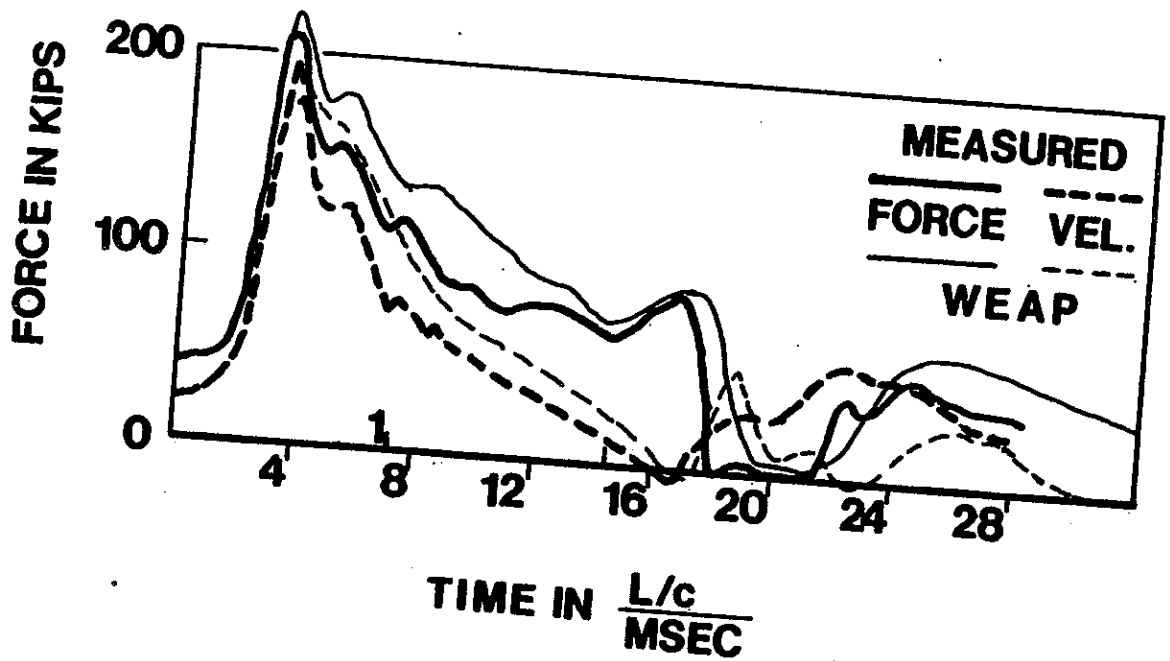

FIGURE 6-10: FORCE AND VELOCITY MATCH FOR PILE NO. 11

ClibPDF - www.fastio.com

be due to a low combustion pressure. (Perhaps because it was in early driving and the hammer did not ignite properly). The fact that the blow count was actually higher (25) than computed (19) supports this explanation.

Pile No. 12

This load test pile was restruck, after a waiting period, by a Link Belt 440 hammer. The hammer lifted off and no penetration of the pile was achieved. Both observations were correctly predicted by the program. The maximum stress prediction was within 5%. The velocity match (Figure 6-11) is in this case somewhat better than the force match. Both matches are poor, probably because of inaccurate skin resistance distribution and ignition timing. The latter event is not as well defined for atomized fuel injection as for those hammers which use the impact for atomization.

Pile No. 13

A Link Belt 660 hammer record is shown in Figure 6-12. The match is very good. (Maximum force match within 8%). As in the case of Pile No. 12, no set was observed and the hammer had to be throttled back in order to avoid lift-off.

Pile No. 14

A rather poor match (21% error in maximum force prediction) is shown in Figure 6-13 for a load test pile from the Case research program (14). The hammer was a Vulcan No. 1, powered by compressed air. Unfortunately, capblock

ClibPDF - www.fastio.com

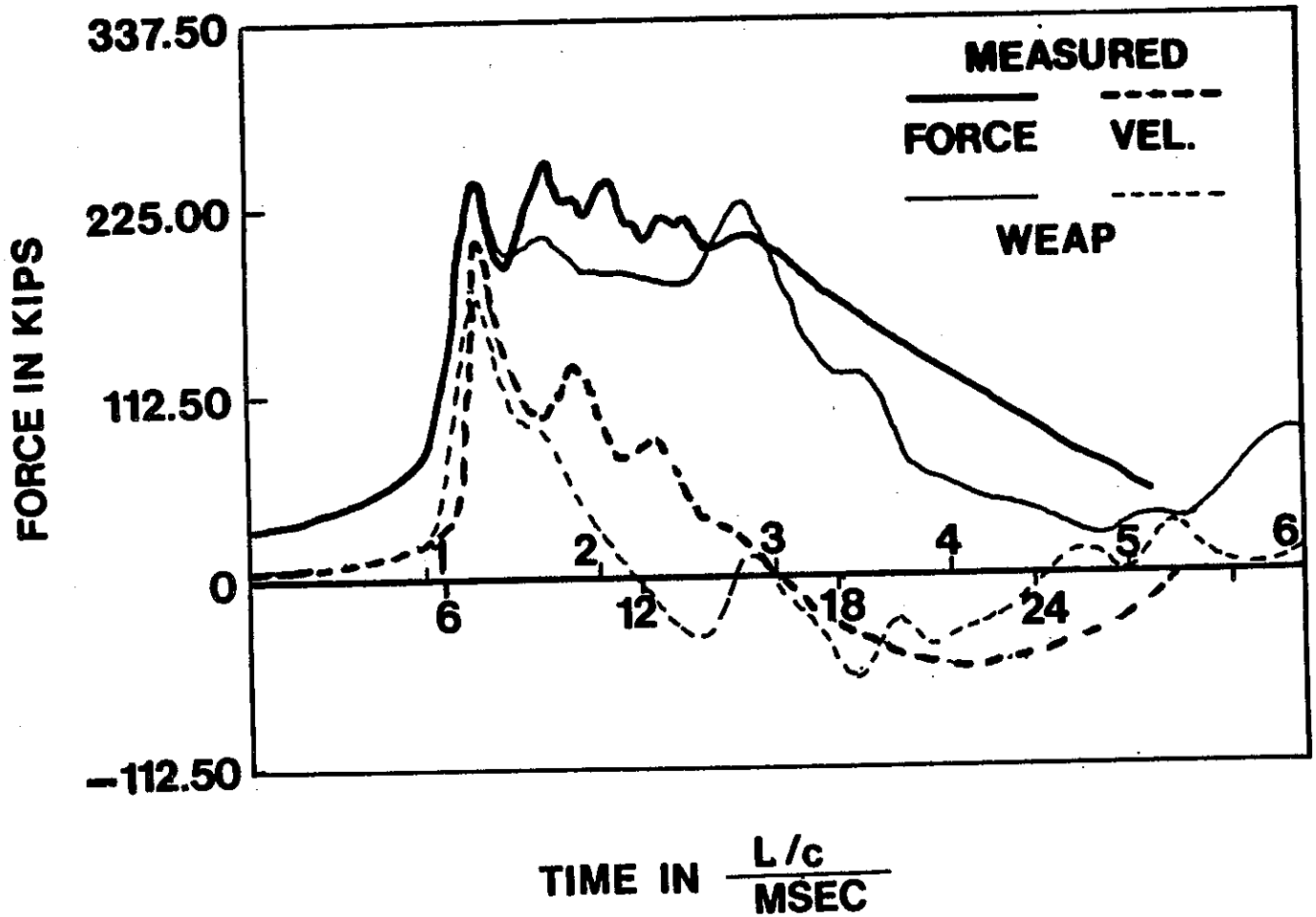

FIGURE 6-11: FORCE AND VELOCITY MATCH FOR PILE NO. 12 (CUYAHOGA RIVER)

ClibPDF - www.fastio.com

ClibPDF - www.fastio.com

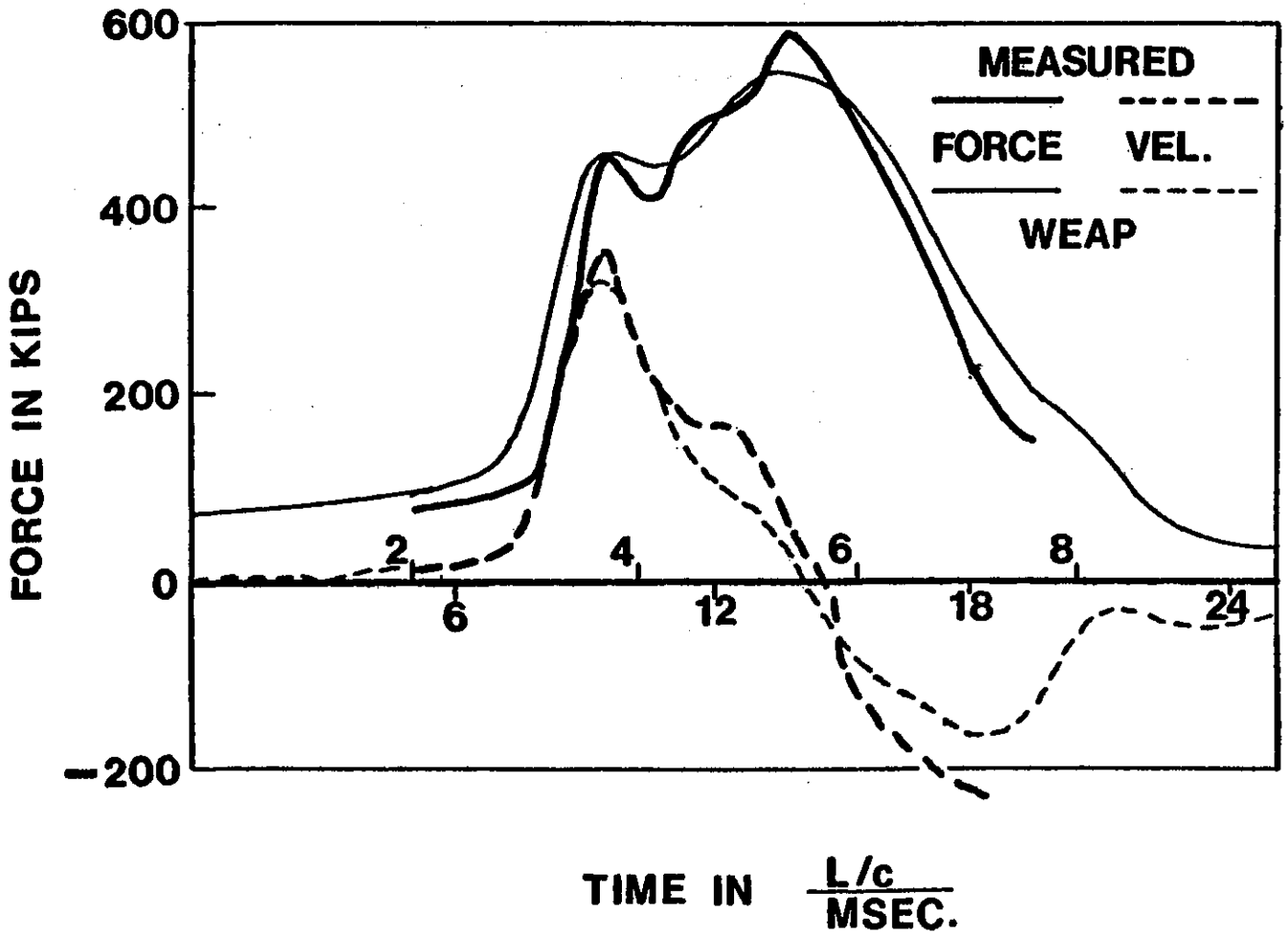

FIGURE 6-1. : FORCE AND VELOCITY MATCH FOR PILE NO. 13

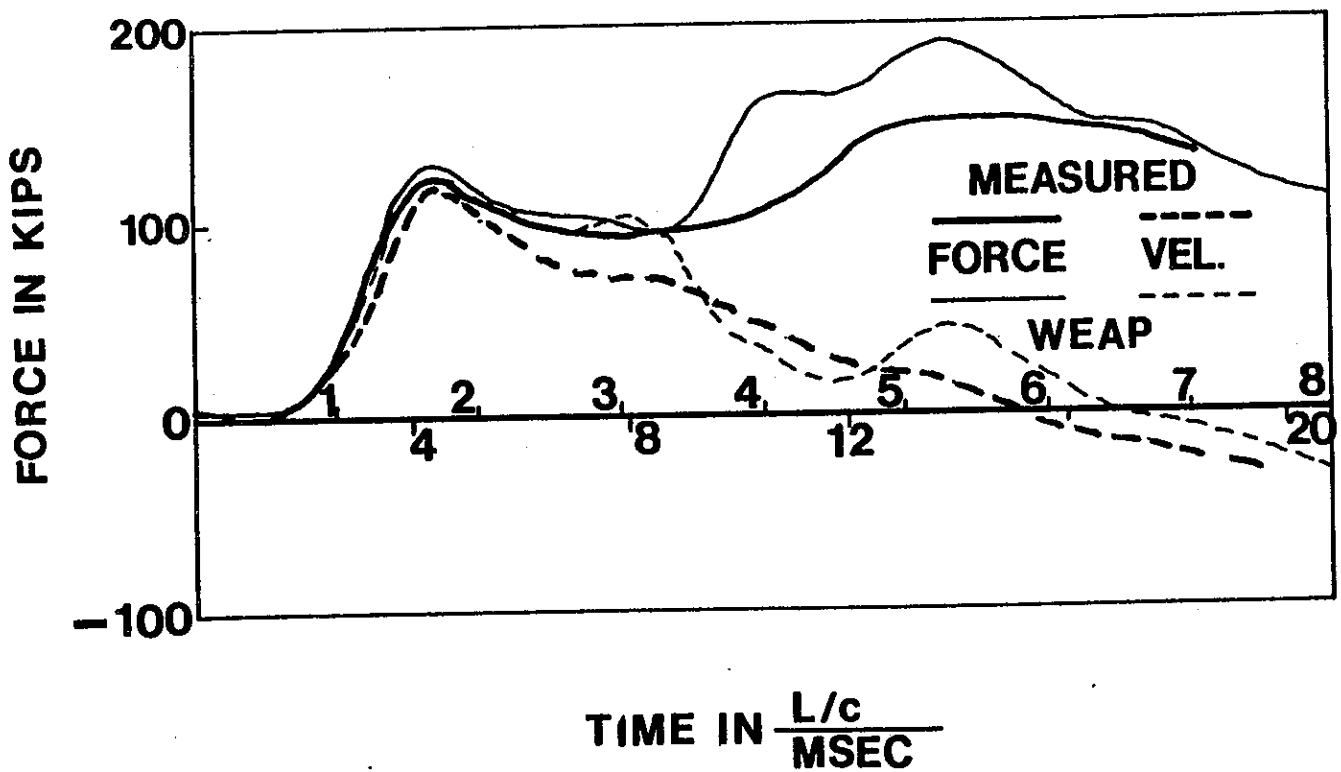

FIGURE 6-13: FORCE AND VELOCITY MATCH FOR PILE NO. 14 (PHILADELPHIA)

ClibPDF - www.fastio.com

and helmet properties were not recorded. The blow count was predicted very accurately.

Piles No. 15 and 16

Both records (Figures 6-14 and 6-15) were actually recorded on the same pile using an air powered Vulcan 08 hammer. The pile was driven at the same site as Pile No. 9, Reference 12.

Both Figure 6-14 which was recorded in easy driving (the capacity of the pile was determined by a pull out test) and Figure 6-15 (which was one of the first records after the pile hit rock) show a very good match. The blow count was accurately determined for the easy driving case; refusal was indicated for hard driving. Note that the measured blow count of 184 is essentially refusal.

Pile No. 17

This was a rather long pile driven by a Vulcan 016 hammer and analysis shows that the assembly drop effect can be predicted rather accurately. Figure 6-16 contains two plots that were obtained on this WEAP run. The lower one is a three dimensional plot of force vs. pile length and time.

Note that the assembly drop creates a wave similar to the impact wave although of lower magnitude.

ClibPDF - www.fastio.com

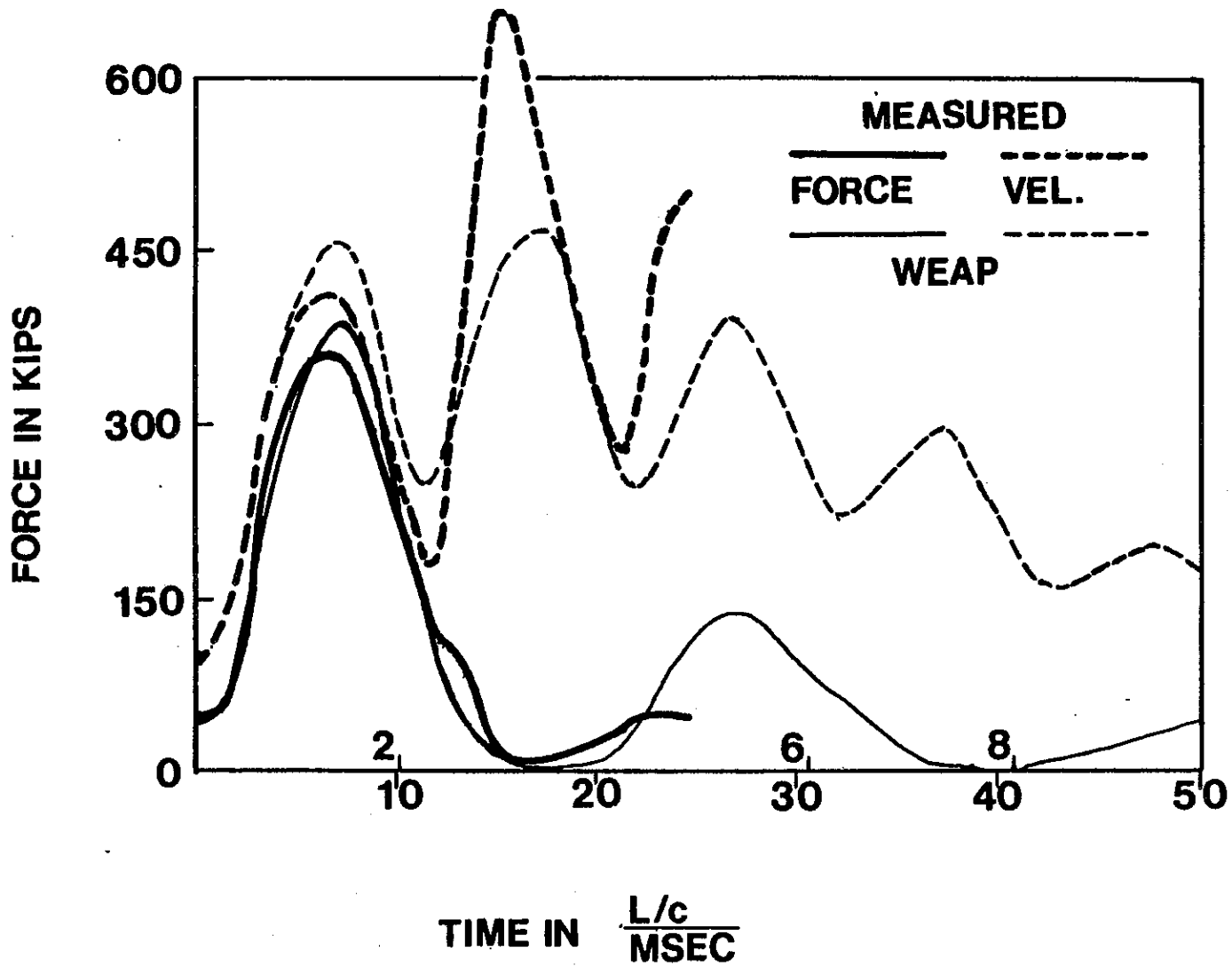

FIGURE 6-14: FORCE AND VELOCITY MATCH FOR PILE NO. 15

ClibPDF - www.fastio.com

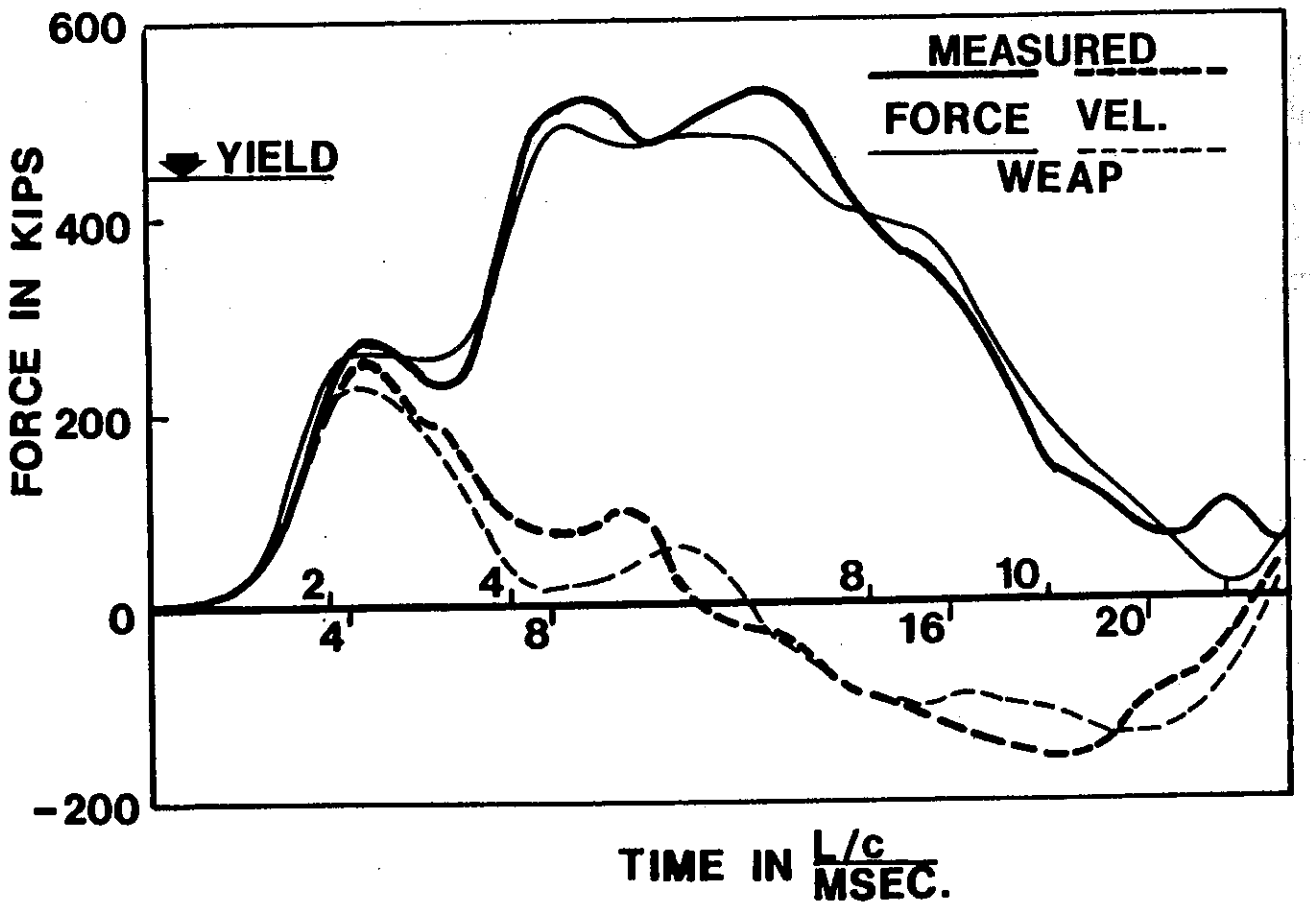

FIGURE 6-15: FORCE AND VELOCITY MATCH FOR PILE NO. 16

ClibPDF - www.fastio.com

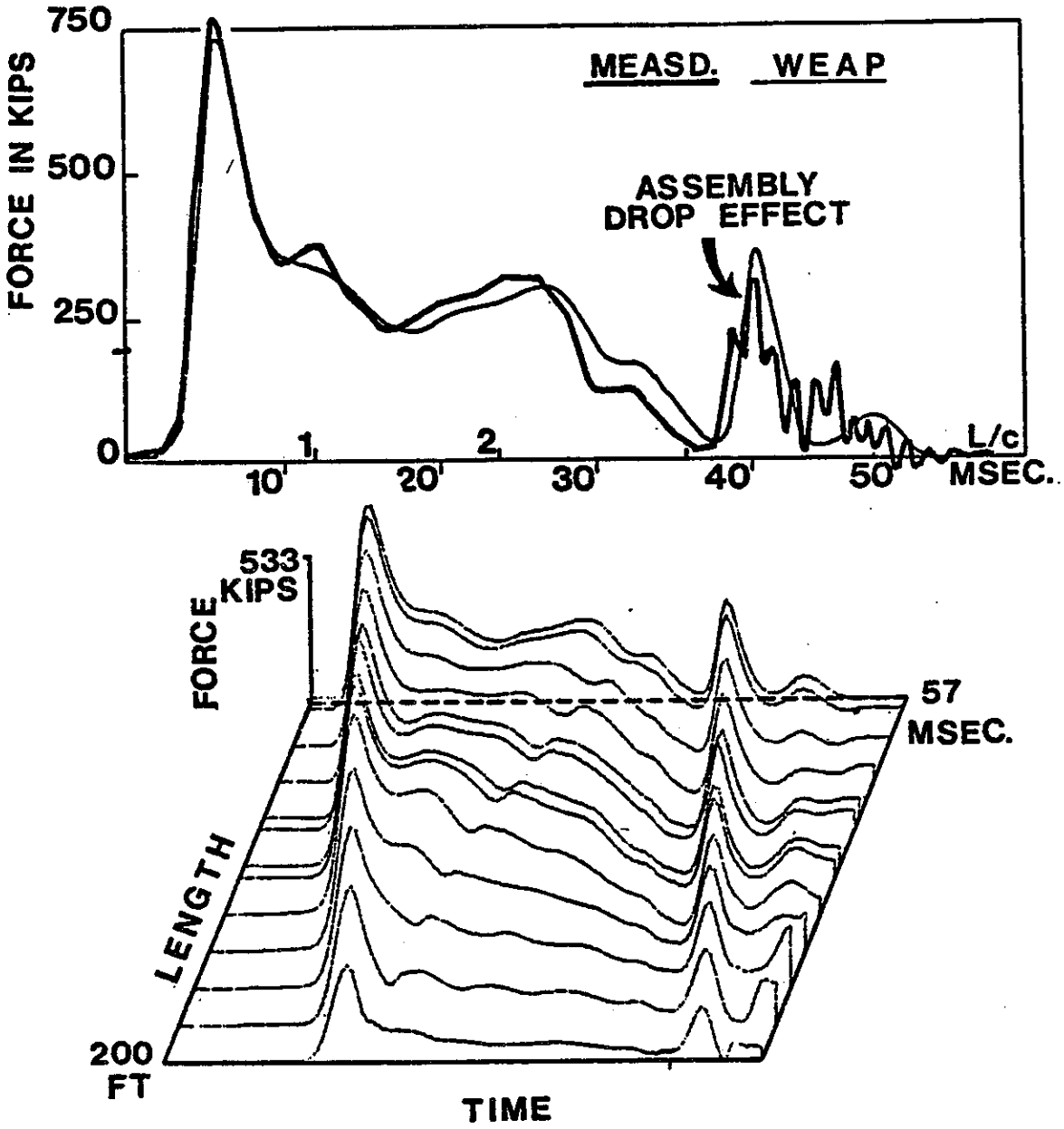

FIGURE 6-16: FORCE MATCH AND THREE DIMENSIONAL FORCE PLOT FOR PILE NO. 17

ClibPDF - www.fastio.com

CHAPTER 7

CONCLUSIONS AND RECOMMENDATIONS

The foregoing results and the experience obtained with the program to date support the following conclusions:

(1) The program can be used very easily for most of commonly encountered dynamic pile analyses.

(2) Stress predictions will be good (less than 10% error) if the components of the driving system are well modeled and if the hammer performs normally. The extensive study of program performance versus actual measurements has proven this point. However, it is only when measurements are available that one can be confident of the modeling if the system is at all unusual.

(3) Blow count (or bearing capacity) predictions were within 10% for most of the cases tested. Exceptions were Piles No. 7, 9, and 16 which had blow counts greater than 120 blows per foot. Blow counts becoming greater than this value result in a very small increase in capacity and are often referred to as "at refusal."

It should be mentioned that small penetrations, less than 0.1 inch per blow, may be associated with higher capacities than predicted by the wave equation. One reason is the assumption of an elasto-plastic static soil resistance. The ultimate resistance is not activated but a final set is obtained because of the nonlinear soil behavior.

(4) Stress and blow count are both dependent on stroke. The stroke,

ClibPDF - www.fastio.com

on the other hand, was well-determined by the program for all those cases in which the hammer performed properly. Improper conditions were found with a hammer whose exhaust ports were partially plugged. Other problems that may be encountered are preignition or low fuel throttle settings.

Since low fuel throttle settings produce low strokes, their effect is readily recognized in the field. Preignition, on the other hand, produces an ineffective blow at a high stroke and is, therefore, dangerous. It can only be recognized by the examination of field measurements.

The use of the program can help in construction control to avoid problems resulting from such abnormal hammer conditions. The engineer has to evaluate pile driving performance using all analysis results (stroke or bounce chamber pressure, blow count and stresses) simultaneously.

(5) The program is well-suited to solve the driveability problem since it uses the actual hammer potential for a given soil condition. Of course, the program does not solve the principal problem of determination of soil bearing capacity.

(6) The program can be used to establish driving criteria in the conventional way except that it will provide a certain stroke value together with stress and blow count. The stroke should be verified in the field.

(7) The program can be used in the investigation of tension stresses in a pile. These stresses can be predicted accurately by the program if the soil resistance distribution and the driving system properties are accurately known. Further work is required to understand dynamic soil performance.

ClibPDF - www.fastio.com

APPENDIX A

COMBUSTION CALCULATIONS USING COMBUSTION CHARTS

A.1 General Remarks

A variety of combustion charts exist which simplify combustion calculations. Among the charts are those of Hotel, Williams and Sattersfield (8), and Newhall and Starkman (9). Unfortunately, these charts are usually devised for four cycle engines or they only consider the combustion of isooctane. Thus, some errors are made in using these charts. However, the uncertainties in basic assumptions usually introduce greater errors than those caused by the use of the charts.

One important question is the degree to which scavenging occurs. Suppose, that the stroke is five times the distance from the exhaust ports to the impact block. Now if the piston has reached the top dead center the gases in the cylinder consist in the worst case of 20% burned products and 80% fresh air. Depending on the geometry of the exhaust ports the down stroke of the piston might either cause all fresh air, all burned products or a fraction of air and fresh products to be exhausted. Thus, the ratio of burned products to fresh air, f, might be anywhere between 0 and 100%.

For the following sample calculation the charts of (9) were used. These charts were set up for isooctane combustion but since the H/C ratio of this fuel is similar to that of diesel fuel, the results should not be affected seriously.

ClibPDF - www.fastio.com

"The Unburned Compression Chart" i.e. the charts that are valid for the compression phase, in (9) were prepared assuming an air-fuel mixture. In the case of diesel hammers, however, pure air (or a mixture of air and combustion products) is compressed. For this reason the unburned charts are not used but rather the results from measurements.

The burned product to fresh air ratio, f, will be assumed at 20% (a very high value compared with the usual engine cycles) together with a constant volume combustion. The latter assumption is justified because the combustion occurs at a very high rate (as evidenced by Figure 6) and because the volume is at the minimum during combustion. This is also apparent from the measurements as the precompression force stays constant during the combustion delay.

Another error is introduced by using the chemical energy value, U_c, as given in (6). This effect can be considered negligible, too.

A.2 Sample Calculation

As an example, consider a DELMAG D-12 hammer with a compression ratio, C.R., of 1:13.5, a fuel charge of 0.00463 lbs. (2.1 grams) per blow and an initial volume of 1308 cubic inches (2.14 cubic decimeters) of air. Assuming an initial temperature of 537°R (25°C) the volume of one pound of air (454 grams) is 13.53 cubic feet (383.1 cubic decimeter). The air to fuel ratio is, therefore

$$A/F = \frac{\frac{1308}{1728(13.53)}}{0.00463} = 12.1$$

ClibPDF - www.fastio.com

The chemically correct mixture has an air/fuel ratio of 15.0 for Diesel fuel (based on the combustion of 1 mol $C_{12}H_{26}$ with 18.50 mols of O_2 and (18.5)(3.773) moles of N_2).

Thus the mixture is $100\,\frac{15-12.1}{12.1} = 24\%$ fuel rich. The charts for a 20% fuel rich mixture will be used.

(a) Compression cycle

The measured pressure at impact was on the average 500 psi (34.5 bar). Assuming the pressure volume relation to follow

$$p = p_{atm}\left(\frac{V_{atm}}{V}\right)^{exp} = p_{atm}\,(C.R.)^{exp}$$

with p_{atm} and V_{atm} being the atmospheric pressure and the corresponding volume respectively, one obtains for the unknown exponent

$$exp = \frac{p}{p_{atm}}\,\frac{1}{C.R.} = \frac{500}{14.7}\,\frac{1}{13.5} = 1.36$$

(instead of 1.4 as for the adiabatic and pure air process).

The precompression temperature can then be determined from

$$T = 537\left(\frac{500}{14.7}\right)^{1-\frac{1}{1.36}} = 1366 \quad °R$$

$$(T = 759\ °K)$$

The internal energy for this temperature is taken from Chart 6. Thus, using the $\phi = 1.2$ curve, one obtains approximately

ClibPDF - www.fastio.com

$$U_2 = 185 \text{ BTU } (195 \text{ kilo Joule})$$

(b) Combustion

Going to Chart 3 and using $f = 0.2$ the chemical energy becomes

$$U_c = 0.8\ (-60.88) + 0.2\ (-1379) = -324 \text{ BTU } (-341 \text{ kJ})$$

Thus

$$U_3 = 185 - 324 = -139 \text{ BTU } (-146 \text{ kJ})$$

The volume V_3 is the compressed volume which according to the legend of Chart 5 and using $K_\phi = 1.2 = 0.3778$ becomes

$$V_3 = 0.3778\ \frac{1366}{500} = 1.03 \text{ ft}^3$$
$$(29.17 \text{ dm}^3)$$

and from Chart 3, approximately:

$$p_3 = 1800 \text{ psi } (124 \text{ bar})$$
$$T_3 = 4750\ ^\circ\text{R } (2639\ ^\circ\text{K})$$
$$S_3 = 2.205 \text{ BTU}/^\circ\text{R } (4.19 \text{ kJ}/^\circ\text{c})$$

(c) Expansion

The final volume of expansion is

$$V_4 = 1.03\ (13.5) = 13.9 \text{ ft}^3\ (393 \text{ dm}^3)$$

ClibPDF - www.fastio.com

and with S_4 = 2.205 BTU/°R (4.19 kJ/°c)

one obtains

$$p_4 = 70 \text{ psi } (4.83 \text{ bar})$$

$$T_4 = 2420 \text{ °R } (1344 \text{ °K})$$

$$U_4 = -830 \text{ BTU } (788 \text{ kJ})$$

(d) Work

Expansion: $W_e = U_3 - U_4 = -139 - (-830)$

$$W_e = 691 \text{ BTU } (729 \text{ kJ})$$

Compression: $W_c = U_2 - U_1 = 185 - 0$

$$W_c = 185 \text{ BTU } (195 \text{ kJ})$$

Net Work: $W_n = 691 - 185 = 506 \text{ BTU } (534 \text{ kJ})$

Thermal Efficiency

$$\eta_{th} = \frac{W_n}{(\text{LHV})(\text{Fuel weight})} = \frac{506}{(19{,}240)(0.056)} = 47\%$$

(Using the weight of diesel fuel per cycle).

A.3 Discussion

The fuel energy per blow converted to work is theoretically

$$W_t = 0.47\ (19240)(0.00463) =$$

$$41.9 \text{ BTU } (44 \text{ kJ})$$

or

$$W_t = 41.9\ (0.778) = 32.6 \text{ k-ft}$$

ClibPDF - www.fastio.com

Note that this corresponds to a stroke of

$$\text{Stroke} = \frac{32.6}{2.75} = 11.9 \text{ ft } (3.63 \text{ m})$$

and that the hammer is rated at 22.5 k-ft (30.5 kJ) for an 8.2 ft (2.50 m) stroke. Such a stroke is more than the maximum possible one of 10.8 ft (3.30 m). In general, only a small portion of the rated energy is actually consumed and it is therefore estimated that the computed energies are approximately 50% too high. This argument is confirmed by the fact that the combustion pressure was computed much higher than measured.

For this reason it was decided to use the measured combustion pressure as a starting value for the expansion process which was then modeled isentropically using an expansion exponent that is given by the combustion chart. In the current case (D-12, 20% fuel rich) one obtains

$$\exp = \frac{1800}{70} \frac{1}{C.R.} = 1.25$$

In order to account for some additional losses during the expansion process, the exponent was chosen as 1.3. As a further argument against pressure calculations based on combustion theory, it should be mentioned that the strokes predicted by the present wave analysis, using the model just described, are in very good agreement with those observed. A limited pressure diesel cycle with measured pressures but a theoretical pressure volume relation would

ClibPDF - www.fastio.com

also produce a much larger net work and cannot be considered a satisfactory approach (see also Figure A1 for a comparison of computed with measured work).

Calculations were also performed in which the combustion product to air ratio, f, was determined assuming a maximum combustion pressure of 1600 psi. The result was f = 0.48.

The reason for the differences between theory and measurement probably lie in the inefficient way fuel is mixed with the air. The atomized injection hammers are actually using much lower fuel/air ratios.

ClibPDF - www.fastio.com

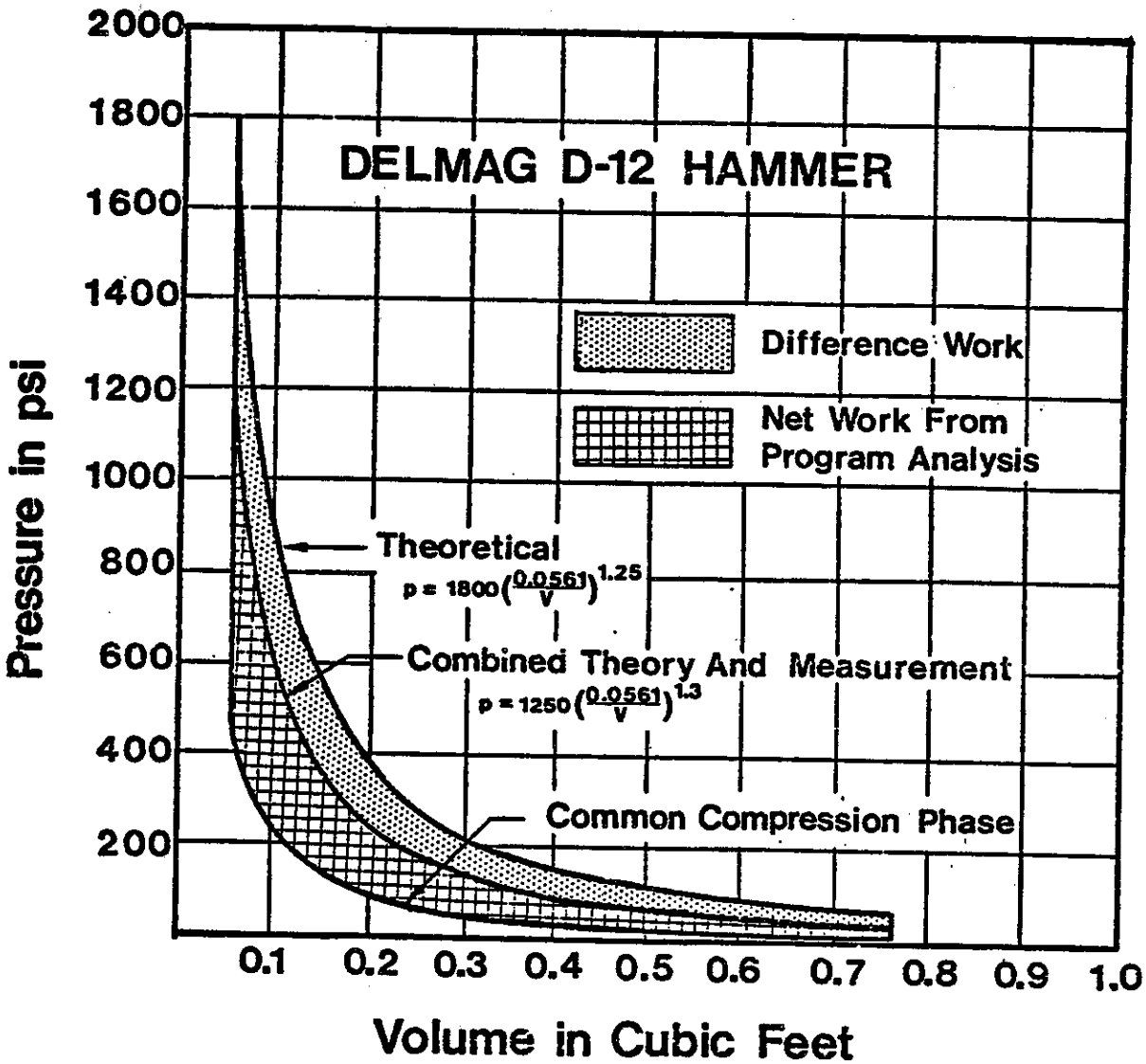

FIGURE A1: COMPARISON OF COMPUTER WITH MEASURED COMBUSTION AND EXPANSION CYCLE.

ClibPDF - www.fastio.com

REFERENCES

1. Goble, G. G., Likins, G. E., and Rausche, F., "Bearing Capacity of Piles from Dynamic Measurements", Final Report, Department of Civil Engineering, Case Western Reserve University, Cleveland, Ohio, March 1975.

2. Smith, E. A. L., "Pile Driving Impact", Proceedings, Industrial Computation Seminar, September 1950, International Business Machines Corp., New York, N.Y., 1951, p. 44.

3. Smith, E. A. L., "Pile Driving Analysis by the Wave Equation", Proc. ASCE, August 1960.

4. Forehand, P. W., and Reese, J. L., "Prediction of Pile Capacity by the Wave Equation", Journal of the Soil Mechanics and Foundations Division, ASCE, Paper 3820, SM2, March 1964.

5. Samson, C. H., Hirsch, T. J., Jr., and Lowery, L. L., "Computer Study for Dynamic Behavior of Piling", Journal of the Structural Division, ASCE, Vol. 89, No. ST4, Proc. Paper 3608, August 1963.

6. Lowery, L. L., Hirsch, T. J., Jr., and Samson, C. H., "Pile Driving Analysis — Simulation of Hammers, Cushions, Piles and Soils", Research Report 33-9, Texas Transportation Institute, August 1967.

7. Coyle, H. M., Bartoskewitz, R. E., and Berger, W. J., "Bearing Capacity Prediction by Wave Equation Analysis — State of the Art", Texas Transportation Institute, Research Report 125-8, August 1973.

8. Hottel, H. C., Williams, G. C., and Satterfield, C. N., "Thermodynamic Charts for Combustion Pressures", New York, N. Y., J. Wiley, 1949.

9. Newhall, A. K., and Starkman, E. S., "Thermodynamic Properties of Octane and Air for Engine Performance Calculations", SAE Technical Progress Series, No. 7, 1963

10. Goble, G. G., Kovacs, W. D., and Rausche, F., "Field Demonstration: Response of Instrumented Piles to Driving and Load Testing", Proceedings of the Specialty Conference on Performance of Earth and Earth-Supported Structures, Volume III, Purdue University, Lafayette, Indiana, June 1972.

11. Goble, G. G., Fricke, K. E., Likins, G. E., Jr., "A Static and Dynamic Pile Test in Dade County, Florida", Department of Solid Mechanics, Structures and Mechanical Design, Case Western Reserve University, Cleveland, Ohio, March 1974

ClibPDF - www.fastio.com

12. Case Western Reserve University, Pile Research Project, "H-Piles Driven to Rock", data obtained Summer 1975, to be published.

13. Goble, G. G., and Rausche, F., "Static and Dynamic Tests in the Cuyahoga River Valley", Interim Report, Department of Solid Mechanics, Structures and Mechanical Design, Case Western Reserve University, Cleveland, Ohio, June 1973.

14. Goble, G. G., and Rausche, F., "Static and Dynamic Tests on Two Pipe Piles in Philadelphia, Pennsylvania", Division of Solid Mechanics, Structures and Mechanical Design, Case Western Reserve University, Cleveland, Ohio, January 1972.

15. Goble, G. G., and Likins, G. E., Jr., "Predicting the Bearing Capacity of a Pile from Dynamic Measurements in Tarver, Georgia", Department of Solid Mechanics, Structures and Mechanical Design, Case Western Reserve University, Cleveland, Ohio, February 1974.

ClibPDF - www.fastio.com

SI CONVERSION FACTORS

To Convert	To	Multiply By
pounds (lbm)	kilograms (kg)	0.4536
pounds (lbf)	Newtons (N)	4.448
kips (1000 lbf)	kilo Newtons (kN)	4.448
inches (in)	meters (m)	0.0254
feet (ft)	meters (m)	0.3048
foot-pounds (ft-lbf)	joules (J)	1.356
pounds/foot (lbm/ft)	kilogram/meter (kg/m)	1.488
pounds/inch^2 (psi)	Pascal (P)	6894
kips/inch^2 (ksi)	Mega Pascal (MP)	6.894
kips/foot^2 (ksf)	kilo Pascal (kP)	47.88
pounds/foot^3 (pcf)	kilogram/meter^3 (kg/m^3)	16.02
seconds/foot (s/ft)	seconds/meter (s/m)	3.281

IMPORTANT CONSTANTS

Name	Symbol	English	SI
Earth gravitational acceleration	g	32.2 ft/s^2	9.81 m/s^2
Water specific weight	γ_w	62.4 pcf	1000 kg/m^3
Steel specific weight	γ_s	492 pcf	7880 kg/m^3
Steel elastic modulus	E_s	30000 ksi	207000 MP

☆U.S. GOVERNMENT PRINTING OFFICE: 1981—341-428:1080

ClibPDF - www.fastio.com